SAND2022-14729C

Sandia National Laboratories

New Salt Constitutive Model Status

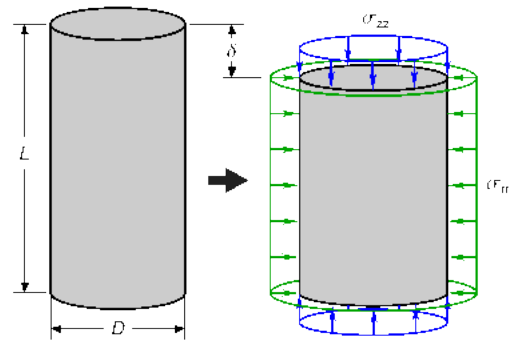

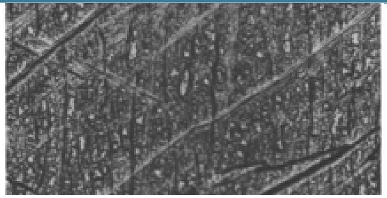

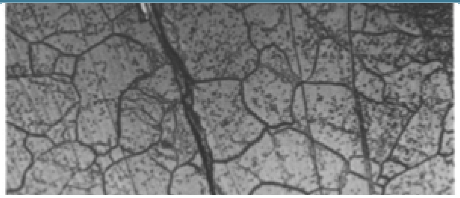

Benjamin Reedlunn

Materials and Failure Modeling Department

WIPP Rock Mechanics Technical Exchange

October 27th, 2022

U.S. DEPARTMENT OF ENERGY NNSA

Sandia National Laboratories is a multi-mission laboratory managed and operated by National Technology and Engineering Solutions of Sandia, LLC., a wholly owned subsidiary of Honeywell International, Inc., for the U.S. Department of Energy's National Nuclear Security Administration under contract DE-NA-0003525. This research is funded by WIPP programs administered by the Office of Environmental Management (EM) of the U.S. Department of Energy.

SAND2022-XXXXX

Sandia National Laboratories is a multimission laboratory managed and operated by National Technology & Engineering Solutions of Sandia, LLC, a wholly owned subsidiary of Honeywell International Inc., for the U.S. Department of Energy's National Nuclear Security Administration under contract DE-NA0003525.

Outline

1. Motivation
2. Model Overview
3. Calibrations
4. Non-Monotonic Loading
5. Summary

Motivation

Motivation

Munson-Dawson model

1. Advantages
   1. Well-known
   2. Easy to calibrate against constant stress tests
   3. Captures most low and medium stress behavior
2. Small Disadvantages
   1. Highly phenomenological
      1. $\dot{\varepsilon}^{vp} = \dot{\varepsilon}^{tr} + \dot{\varepsilon}^{ss}$
   2. Cannot be fit into framework of Rational Thermodynamics
3. Larger Disadvantages Relevant to Empty Areas at WIPP
   1. Does not include damage and healing
   2. Cannot capture high strain rate (high stress) behavior
   3. Cannot capture re-hardening during non-monotonic loading

Damaged, High Strain Rate, Behavior

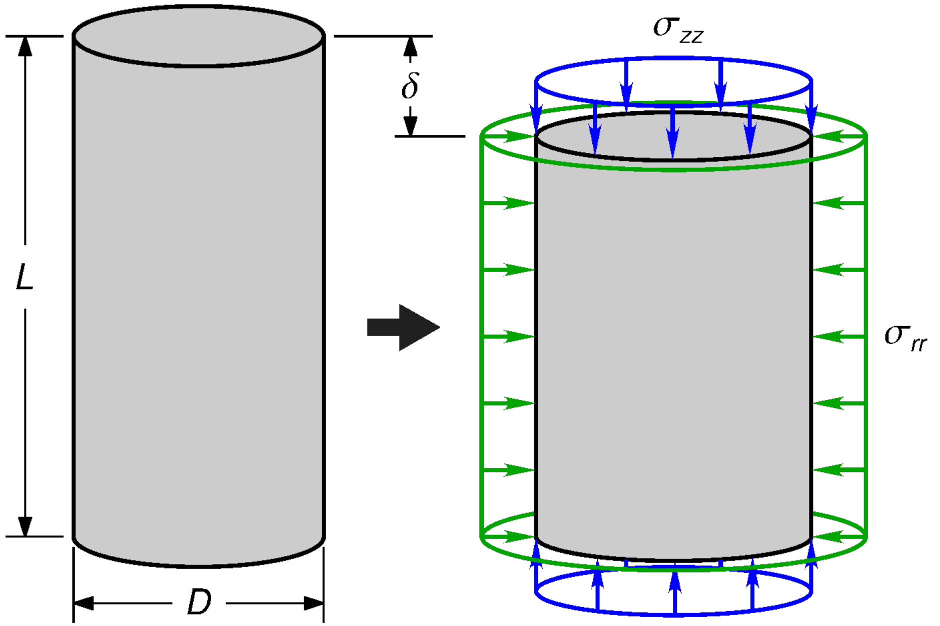

$$\frac{L}{D} = 2$$

$$\varepsilon_{zz} = \ln\left(1 + \frac{\delta}{L}\right)$$

$$\tilde{\sigma} = |\sigma_{zz} - \sigma_{rr}|$$

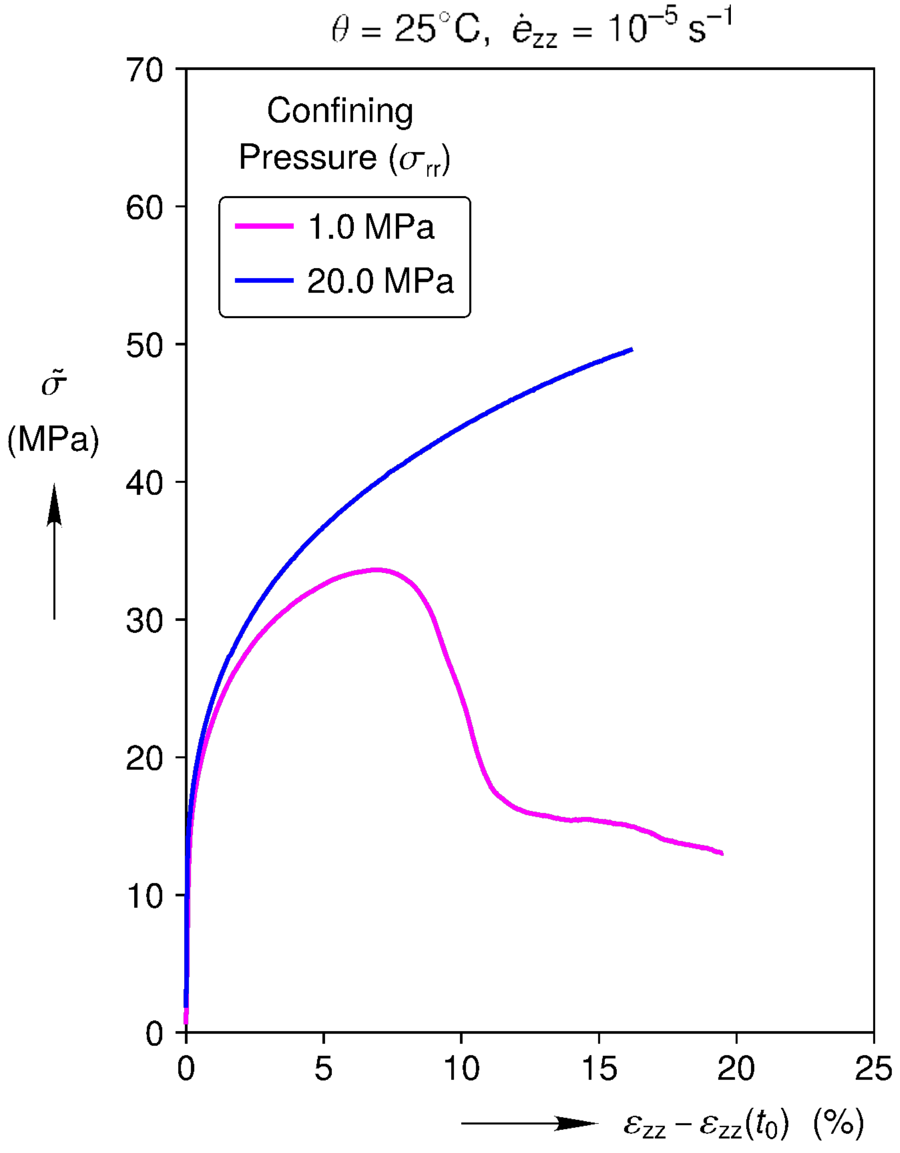

Experimental measurements from: Salzer et al. (2015) and Düsterloh et al. (2015).

Damaged, High Strain Rate, Behavior

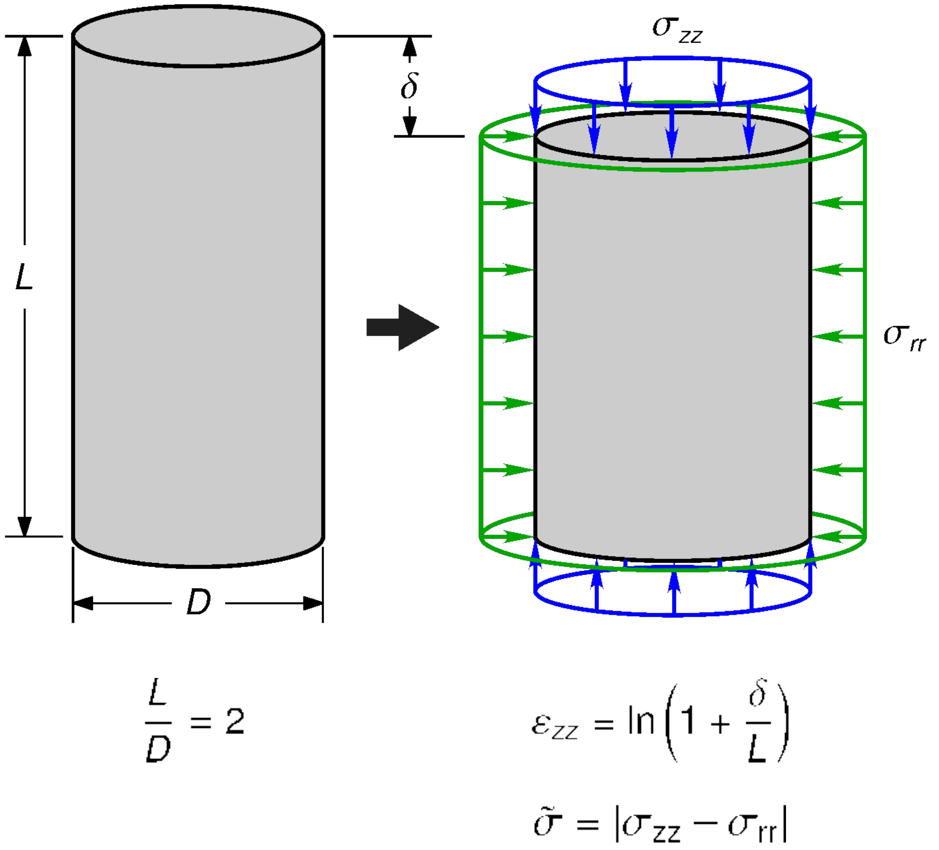

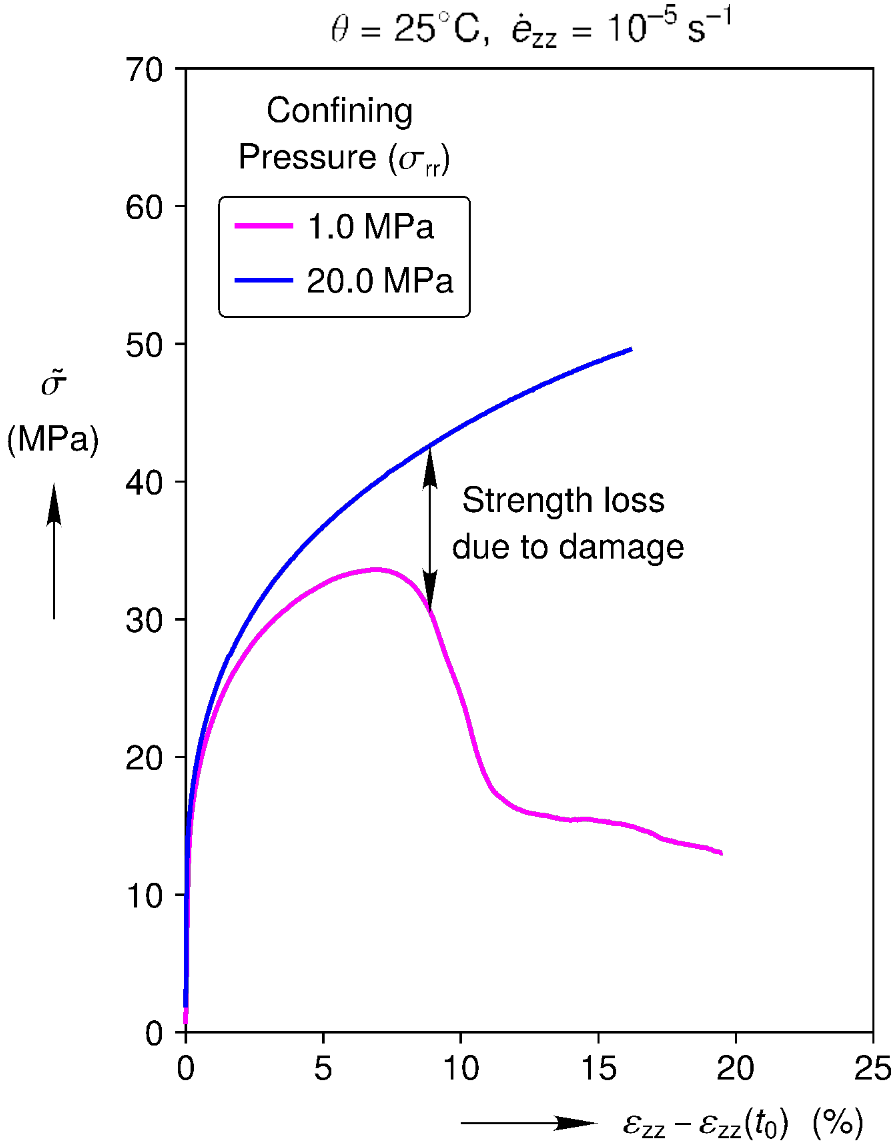

Experimental measurements from: Salzer et al. (2015) and Düsterloh et al. (2015).

Damage-Free, High Strain Rate, Behavior

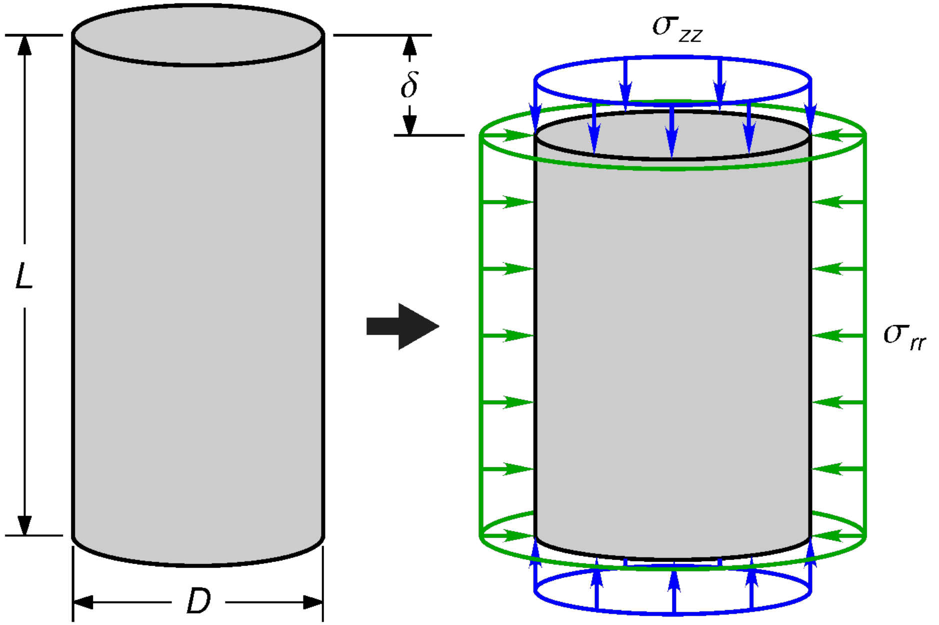

$$\frac{L}{D} = 2$$

$$\varepsilon_{zz} = \ln\left(1 + \frac{\delta}{L}\right)$$

$$\tilde{\sigma} = |\sigma_{zz} - \sigma_{rr}|$$

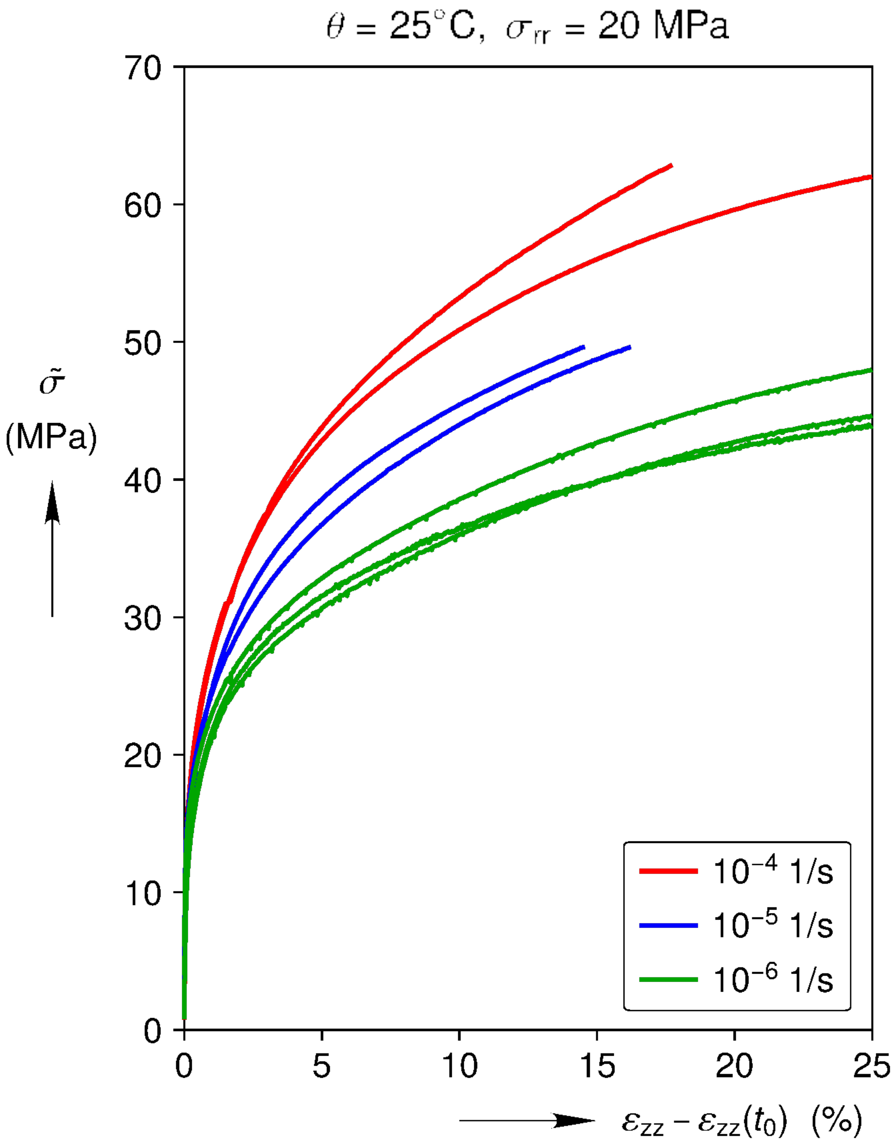

Experimental measurements from: Salzer et al. (2015) and Düsterloh et al. (2015).

Damage-Free, High Strain Rate, Munson-Dawson Predictions

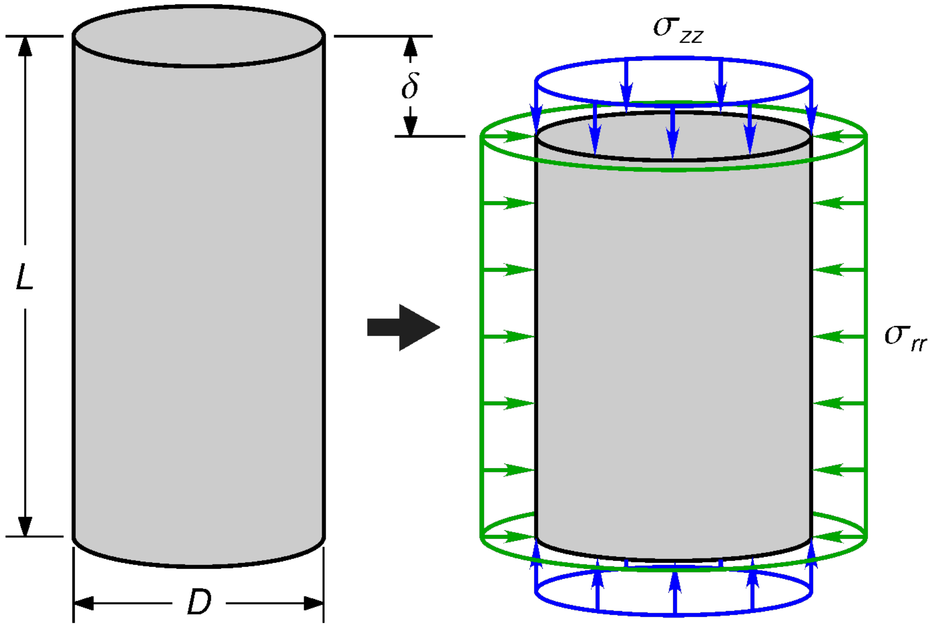

$$\frac{L}{D} = 2$$

$$\varepsilon_{zz} = \ln\left(1 + \frac{\delta}{L}\right)$$

$$\tilde{\sigma} = |\sigma_{zz} - \sigma_{rr}|$$

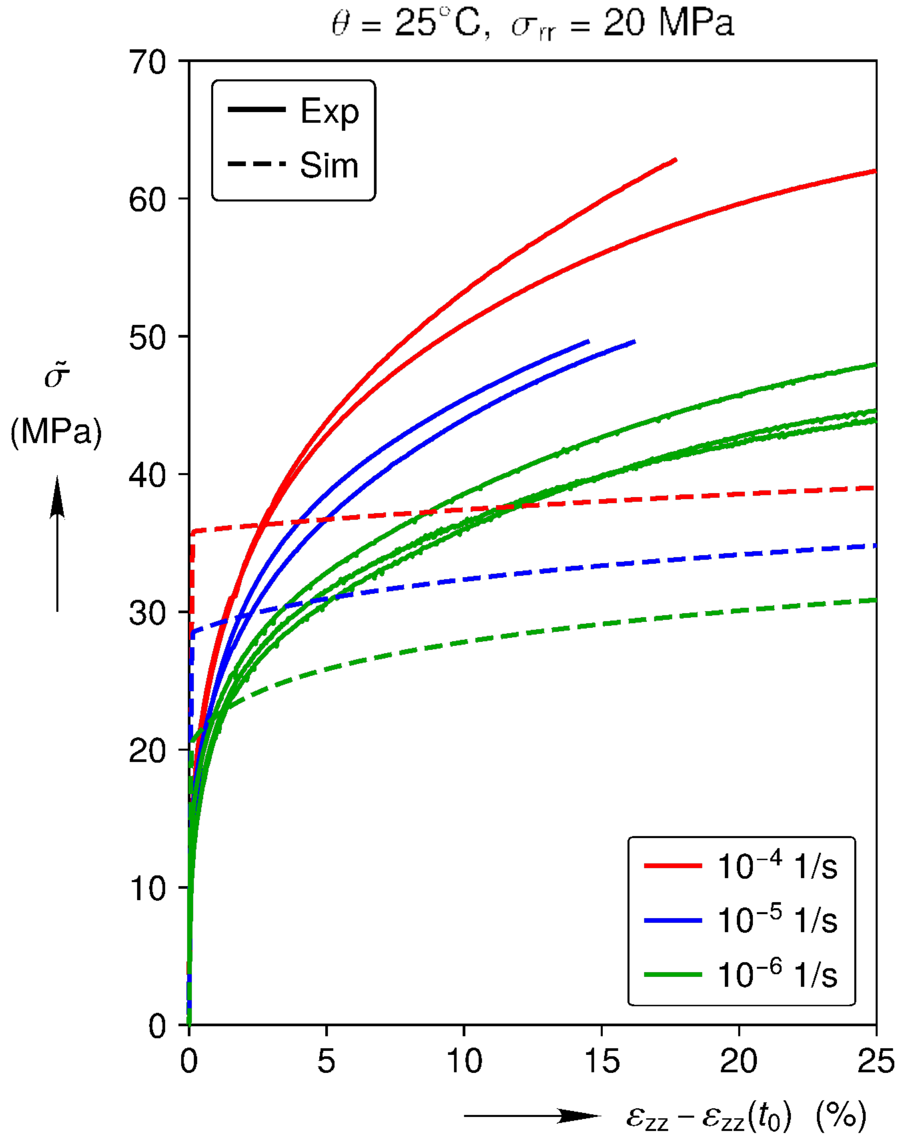

Experimental measurements from: Salzer et al. (2015) and Düsterloh et al. (2015).

Model Overview

Viscoplastic Branches

Pressure Solution and Dislocation Glide

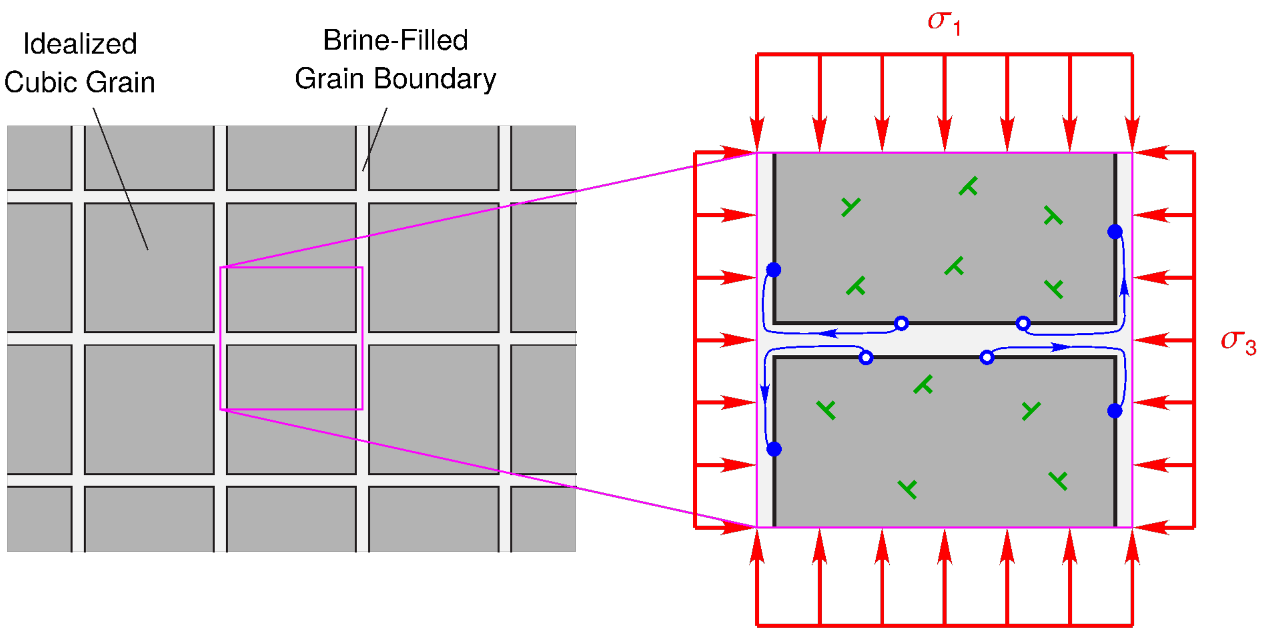

Strain Rate Decomposition
(proportional, monotonic, loading)

$$\dot{\tilde{\varepsilon}}^{vp} = \dot{\tilde{\varepsilon}}^{ps} + \dot{\tilde{\varepsilon}}^{dg}$$

A (Rough) Steady-State Deformation Mechanism Map

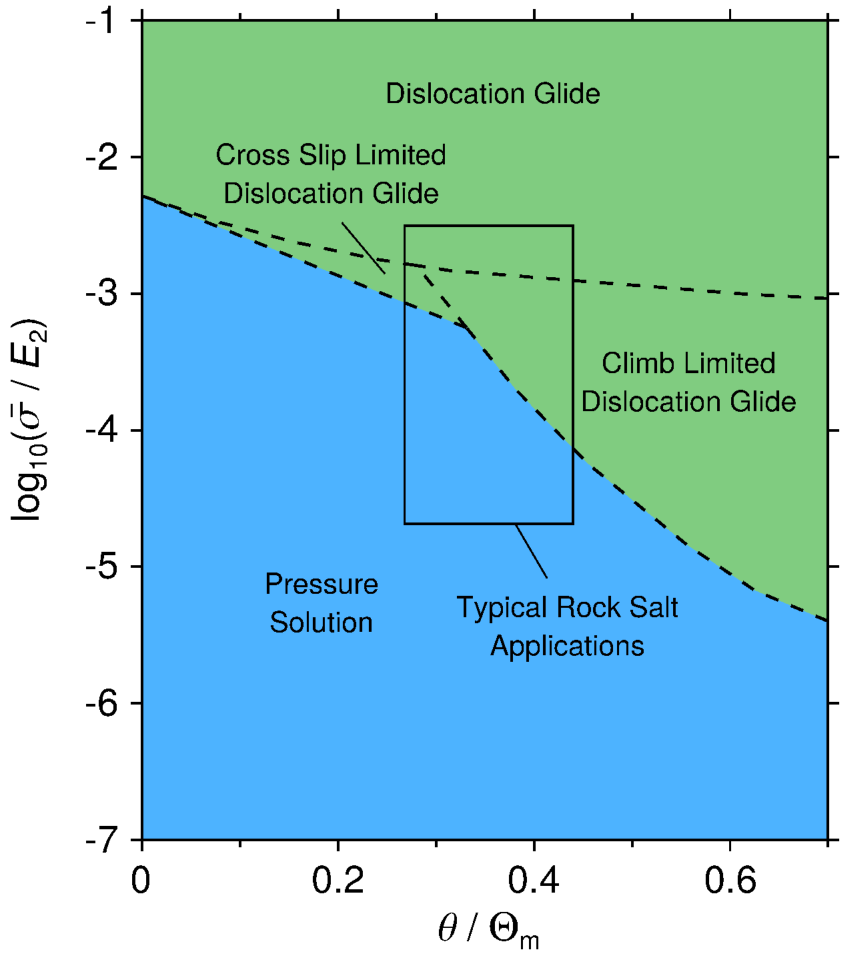

Θ_m = 1077 K
E_2 = 10 GPa
Average grain size = 10 mm

Microstructural Observations

Wavy Slip Bands

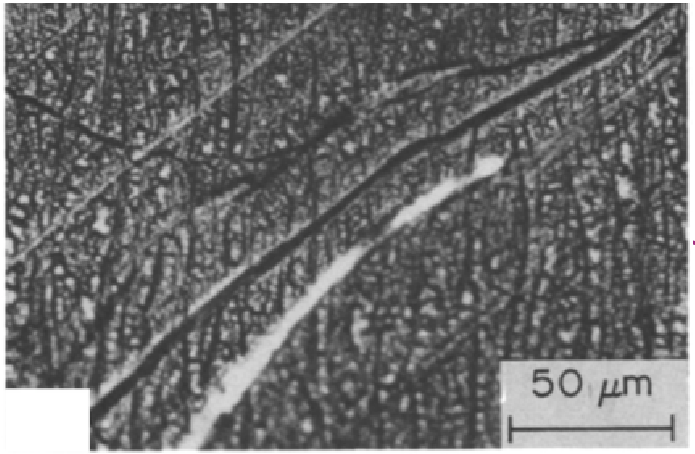

A (Rough) Steady-State Deformation Mechanism Map

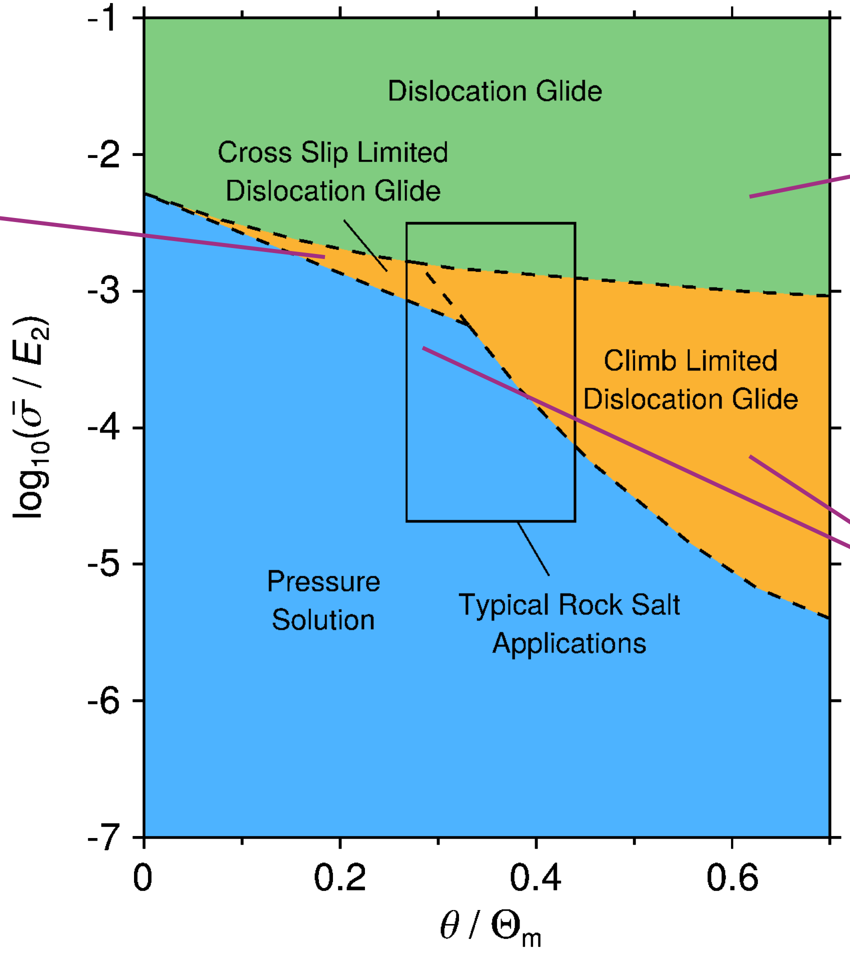

Θ_m = 1077 K
E_2 = 10 GPa
Average grain size = 10 mm

Uniform Dislocation Density

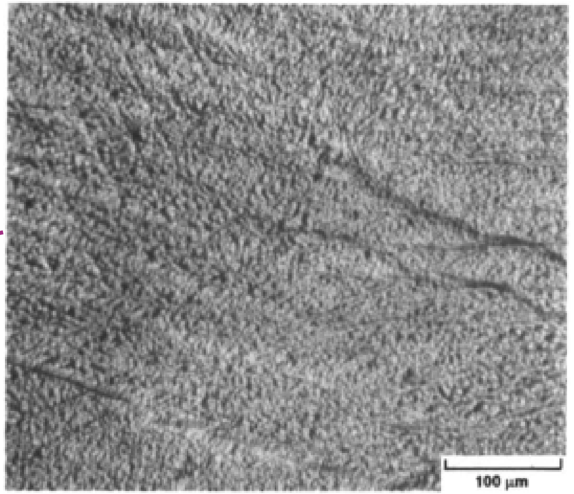

Subgrains

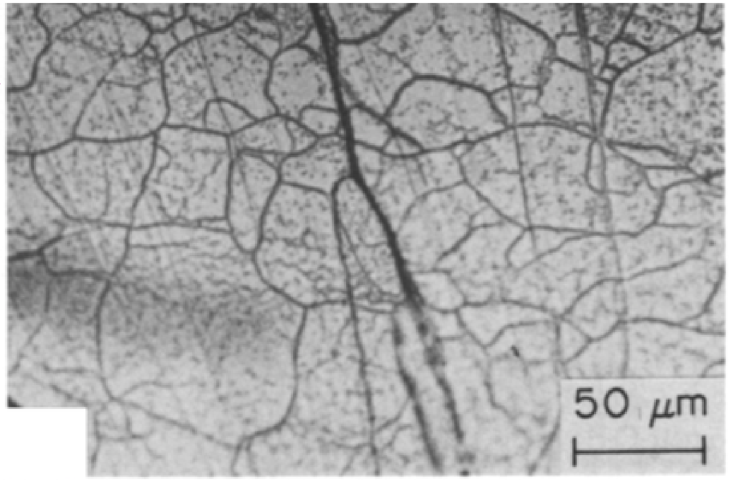

Raj, S. V. and Pharr, G. (1989). “Creep substructure formation in sodium chloride single crystals in the power law and exponential creep regimes”. In: Materials Science and Engineering: A 122.2, pp. 233–242.

Carter, NL, Horseman, ST, Russell, JE, and Handin, J (1993). Rheology of rocksalt. Journal of Structural Geology. Vol 15. No 9-10. pp 1257-1271.

Steady-State Strain Rate Calibration

Steady-State Strain Rates

$$\dot{\varepsilon}^{\text{ps}} = P_1 \exp\left(-\frac{P_2}{\theta}\right) \frac{\tilde{\sigma}}{\theta}$$

$$\dot{\varepsilon}^{\text{dg}} = Y_3 \exp\left(-\frac{G_2}{\theta}\right) \left[\sinh\left(\frac{\tilde{\sigma}}{Y_4}\right)\right]^{Y_5}$$

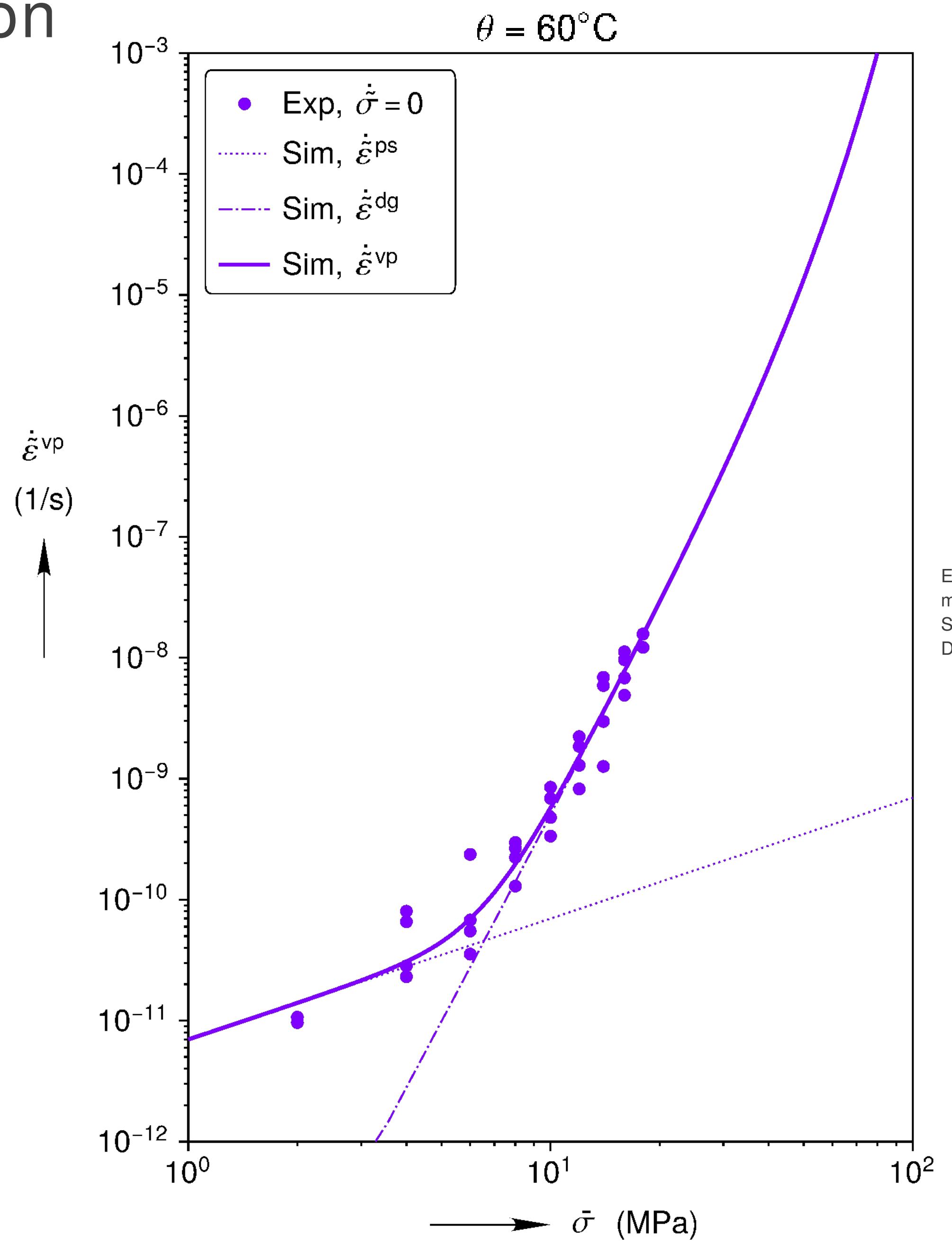

Experimental measurements from: Salzer et al. (2015) and Düsterloh et al. (2015).

Spiers, C., Schutjens, P., Brzesowsky, R., Peach, C., Liezenberg, J., and Zwart, H. (1990). Experimental determination of constitutive parameters governing creep of rocksalt by pressure solution. In: Geological Society, London, Special Publications 54.1, pp. 215–227.

Garofalo, F. (1963). An empirical relation defining the stress dependence of minimum creep rate in metals. In: Trans. AIME 227, pp. 351–356.

Steady-State Strain Rate Calibration

Steady-State Strain Rates

$$\dot{\tilde{\varepsilon}}^{ps} = P_1 \exp\left(-\frac{P_2}{\theta}\right) \frac{\tilde{\sigma}}{\theta}$$

$$\dot{\tilde{\varepsilon}}^{dg} = Y_3 \exp\left(-\frac{G_2}{\theta}\right) \left[\sinh\left(\frac{\tilde{\sigma}}{Y_4}\right)\right]^{Y_5}$$

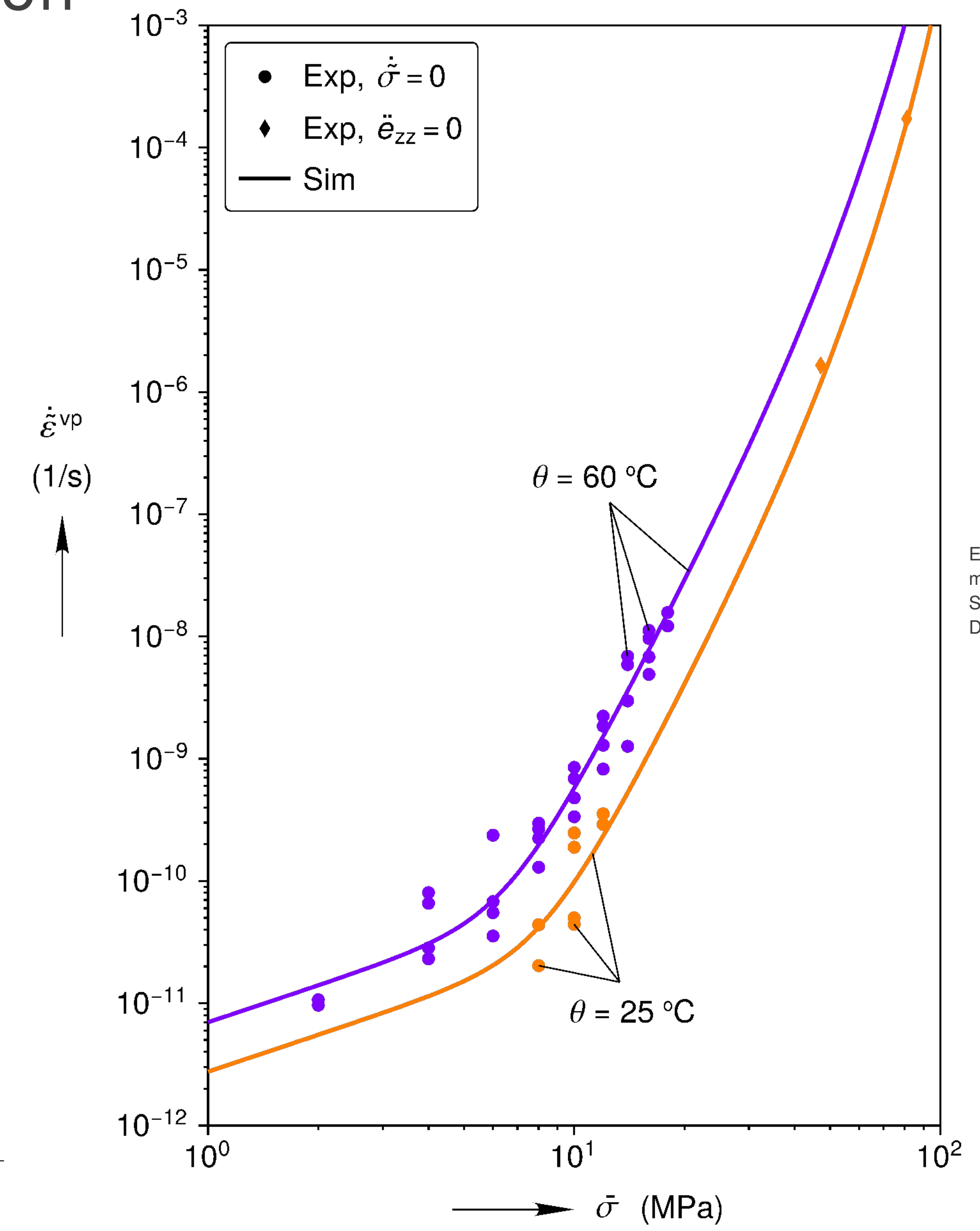

Experimental measurements from: Salzer et al. (2015) and Düsterloh et al. (2015).

Spiers, C., Schutjens, P., Brzesowsky, R., Peach, C., Liezenberg, J., and Zwart, H. (1990). Experimental determination of constitutive parameters governing creep of rocksalt by pressure solution. In: Geological Society, London, Special Publications 54.1, pp. 215–227.

Garofalo, F. (1963). An empirical relation defining the stress dependence of minimum creep rate in metals. In: Trans. AIME 227, pp. 351–356.

Strain Rates While Hardening

Strain Rates
(proportional, monotonic, loading)

$$\dot{\tilde{\varepsilon}}^{\mathrm{ps}} = P_1 \exp\left(-\frac{P_2}{\theta}\right) \frac{\tilde{\sigma}}{\theta}$$

$$\dot{\tilde{\varepsilon}}^{\mathrm{dg}} = G_1 \exp\left(-\frac{G_2}{\theta}\right) \left[\sinh\left(\frac{\tilde{\sigma} - \tilde{b}}{y}\right)\right]^{G_3}$$

Strain Rates While Hardening

Strain Rates
(proportional, monotonic, loading)

$$\dot{\tilde{\varepsilon}}^{ps} = P_1 \exp\left(-\frac{P_2}{\theta}\right) \frac{\tilde{\sigma}}{\theta}$$

$$\dot{\tilde{\varepsilon}}^{dg} = G_1 \exp\left(-\frac{G_2}{\theta}\right) \left[\sinh\left(\frac{\tilde{\sigma} - \tilde{b}}{y}\right)\right]^{G_3}$$

Low Constant Stress

$\tilde{\sigma}$ = 4 MPa, θ = 60°C

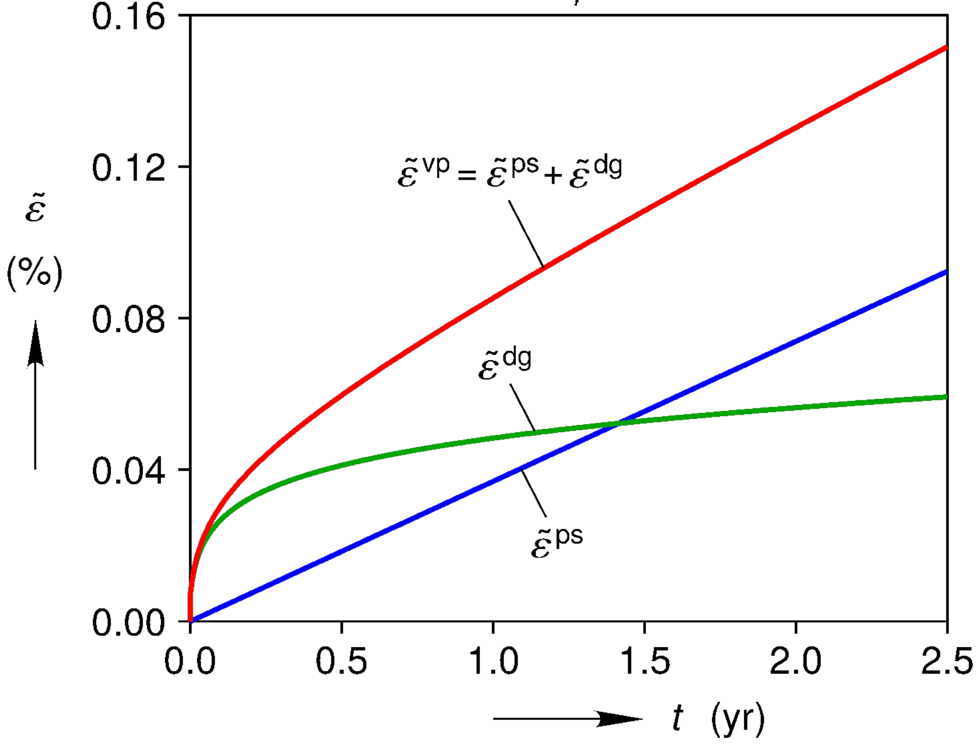

Strain Rates While Hardening

Strain Rates
(proportional, monotonic, loading)

$$\dot{\tilde{\varepsilon}}^{ps} = P_1 \exp\left(-\frac{P_2}{\theta}\right) \frac{\tilde{\sigma}}{\theta}$$

$$\dot{\tilde{\varepsilon}}^{dg} = G_1 \exp\left(-\frac{G_2}{\theta}\right) \left[\sinh\left(\frac{\tilde{\sigma} - \tilde{b}}{y}\right)\right]^{G_3}$$

Dislocation Glide Hardening

Equivalent Stress Decomposition
(proportional, monotonic, loading)

$$\tilde{\sigma} = \tilde{b} + \tilde{\sigma}^{dg}$$

Drag Stress Contribution

$$\tilde{\sigma}^{dg} = y \sinh^{-1}\left\{\left[\frac{\dot{\tilde{\varepsilon}}^{dg}}{G_1 \exp\left(-G_2/\theta\right)}\right]^{1/G_3}\right\}$$

Uniform Dislocation Density

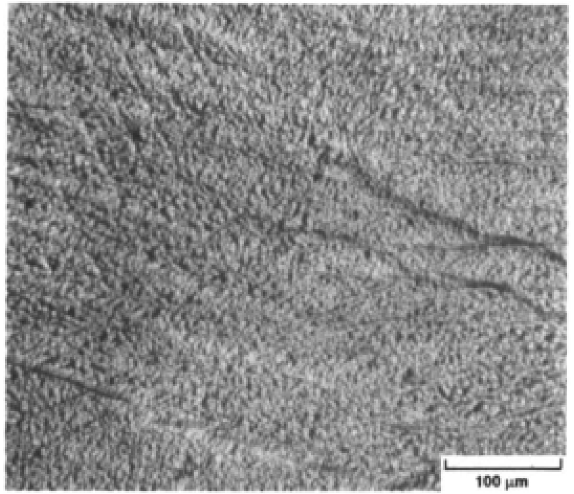

Non-Uniform Dislocation Density

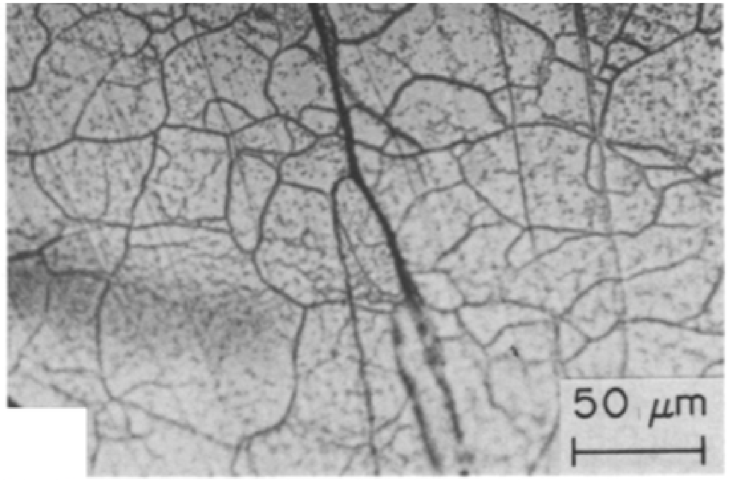

Raj, S. V. and Pharr, G. (1989). "Creep substructure formation in sodium chloride single crystals in the power law and exponential creep regimes". In: Materials Science and Engineering: A 122.2, pp. 233–242.

Carter, NL, Horseman, ST, Russell, JE, and Handin, J (1993). Rheology of rocksalt. Journal of Structural Geology. Vol 15. No 9-10. pp 1257-1271.

Constant Strain Rate Behavior

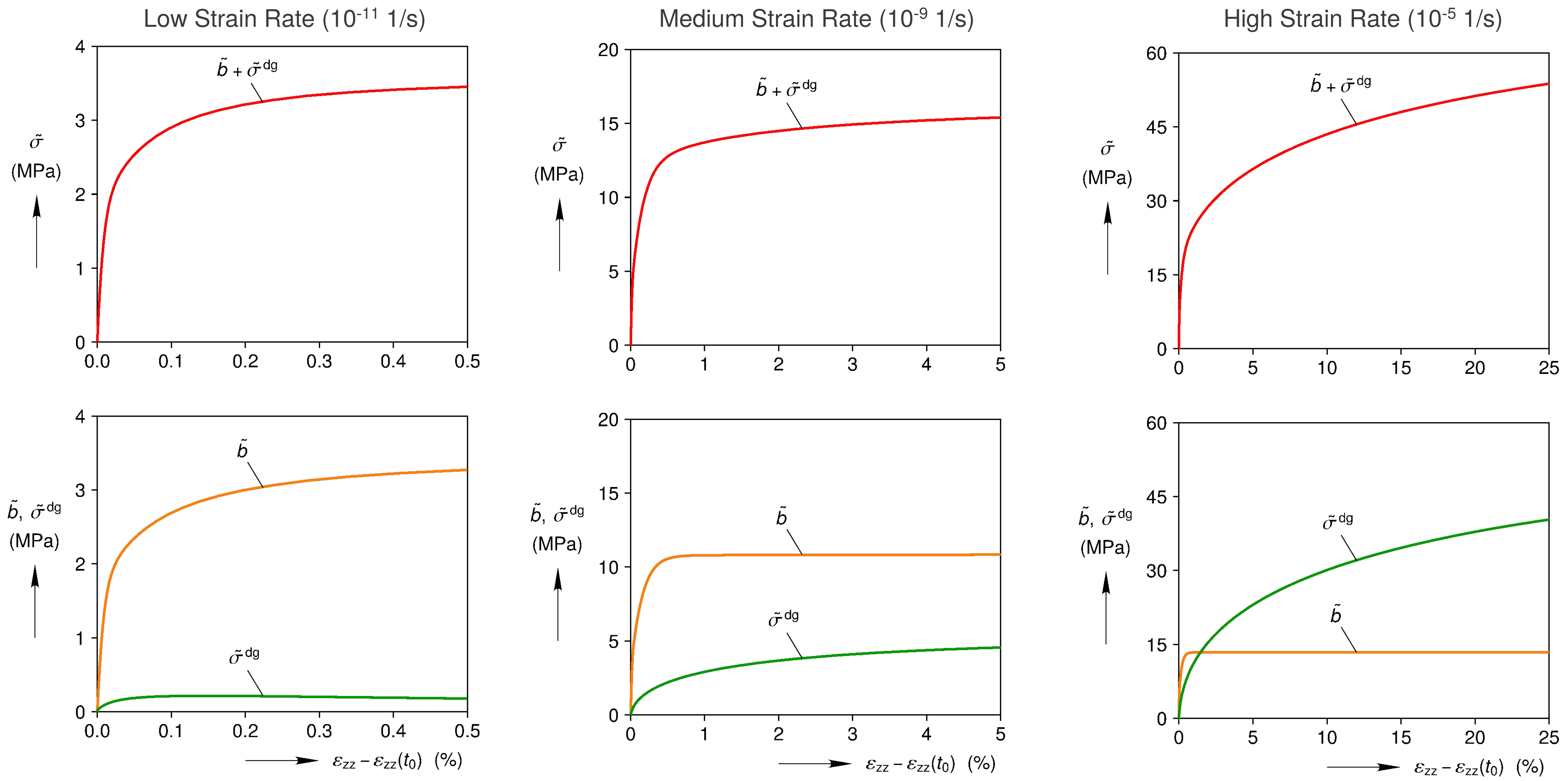

Calibrations

Hardening Transition from Low to Medium Stresses (Strain Rates)

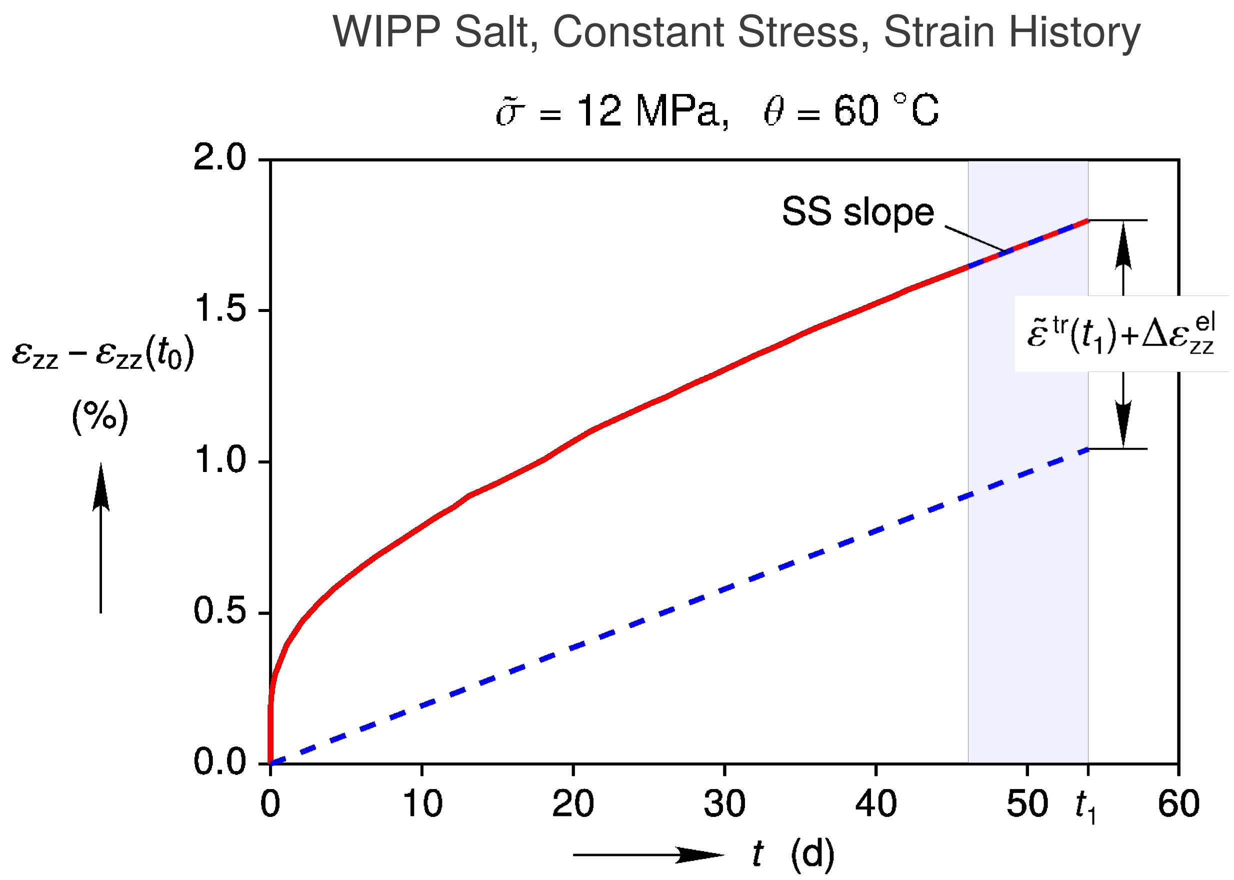

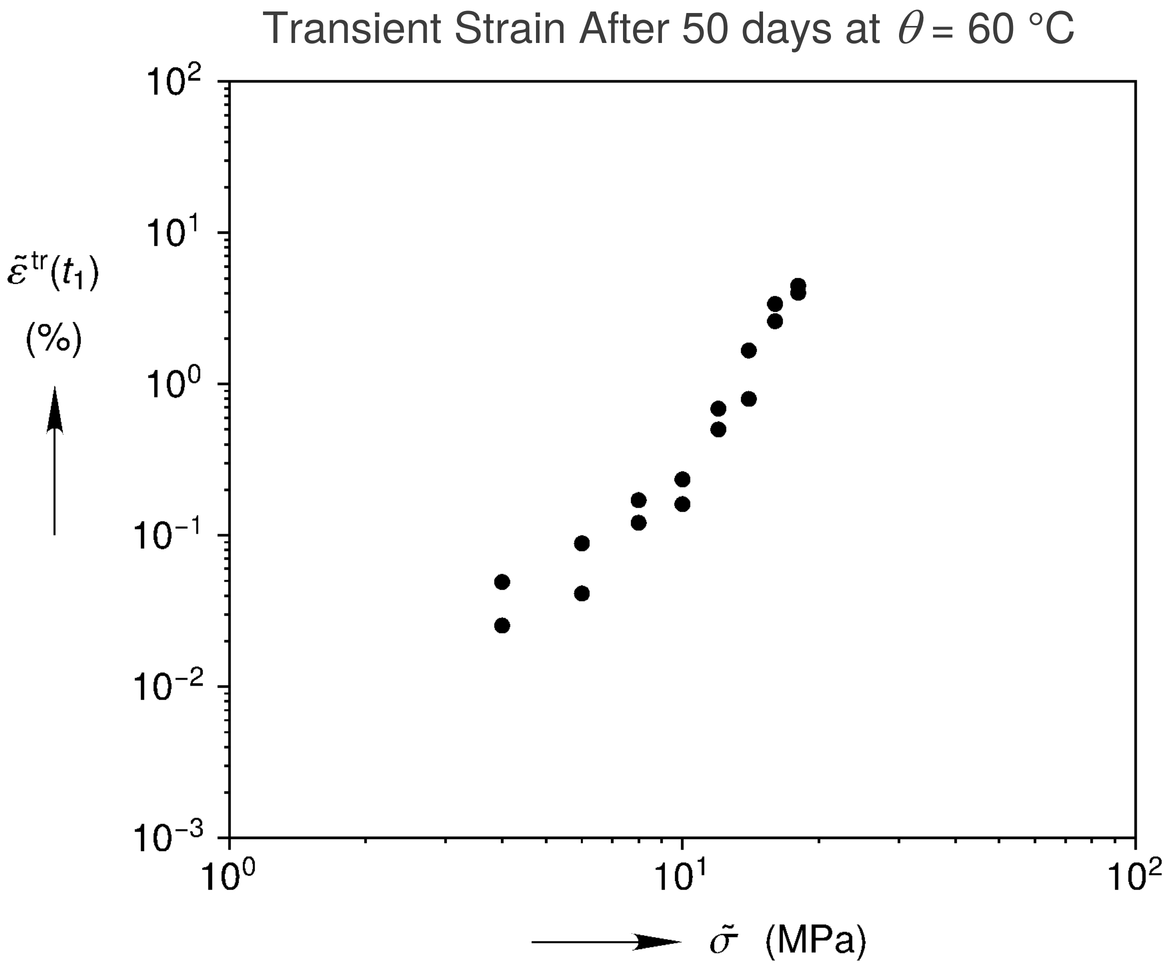

Experimental measurements from: Salzer et al. (2015) and Düsterloh et al. (2015).

Hardening Transition from Low to Medium Stresses (Strain Rates)

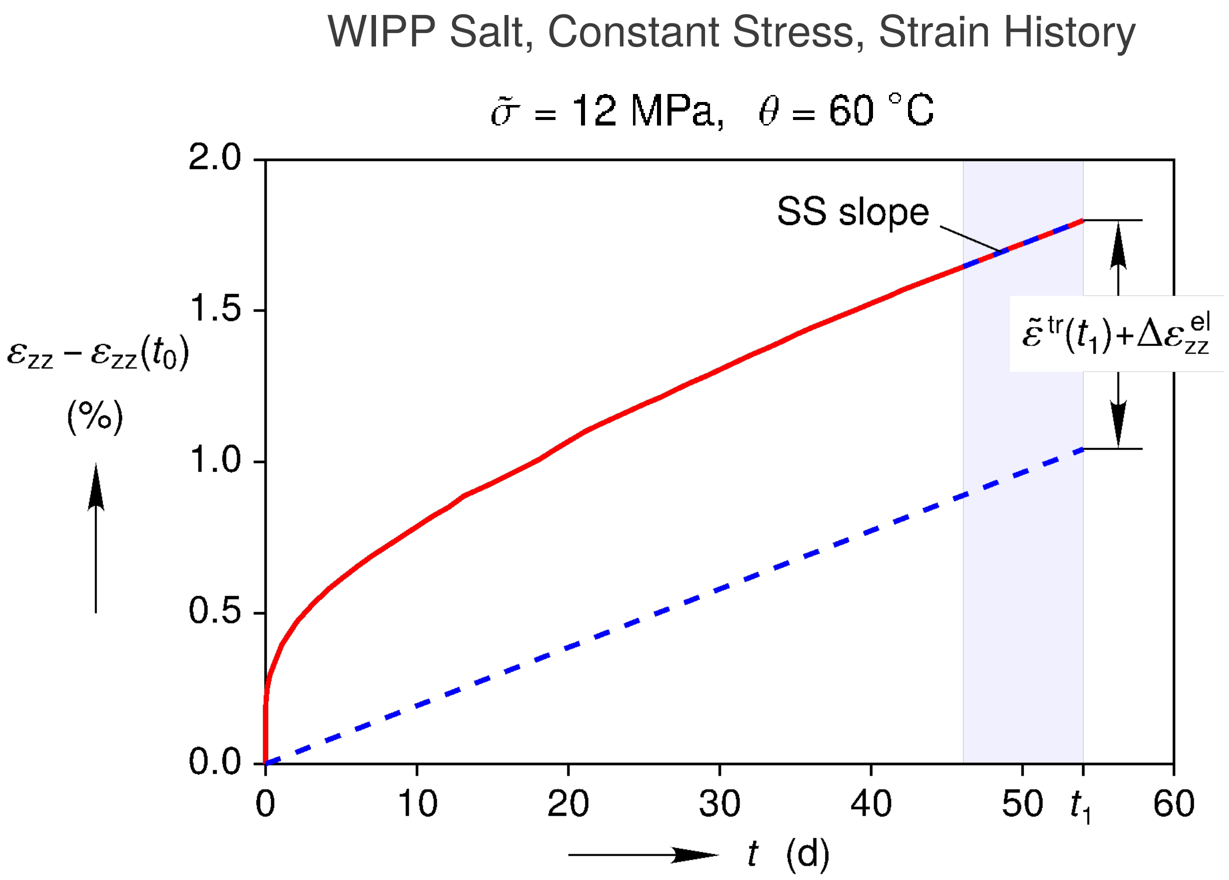

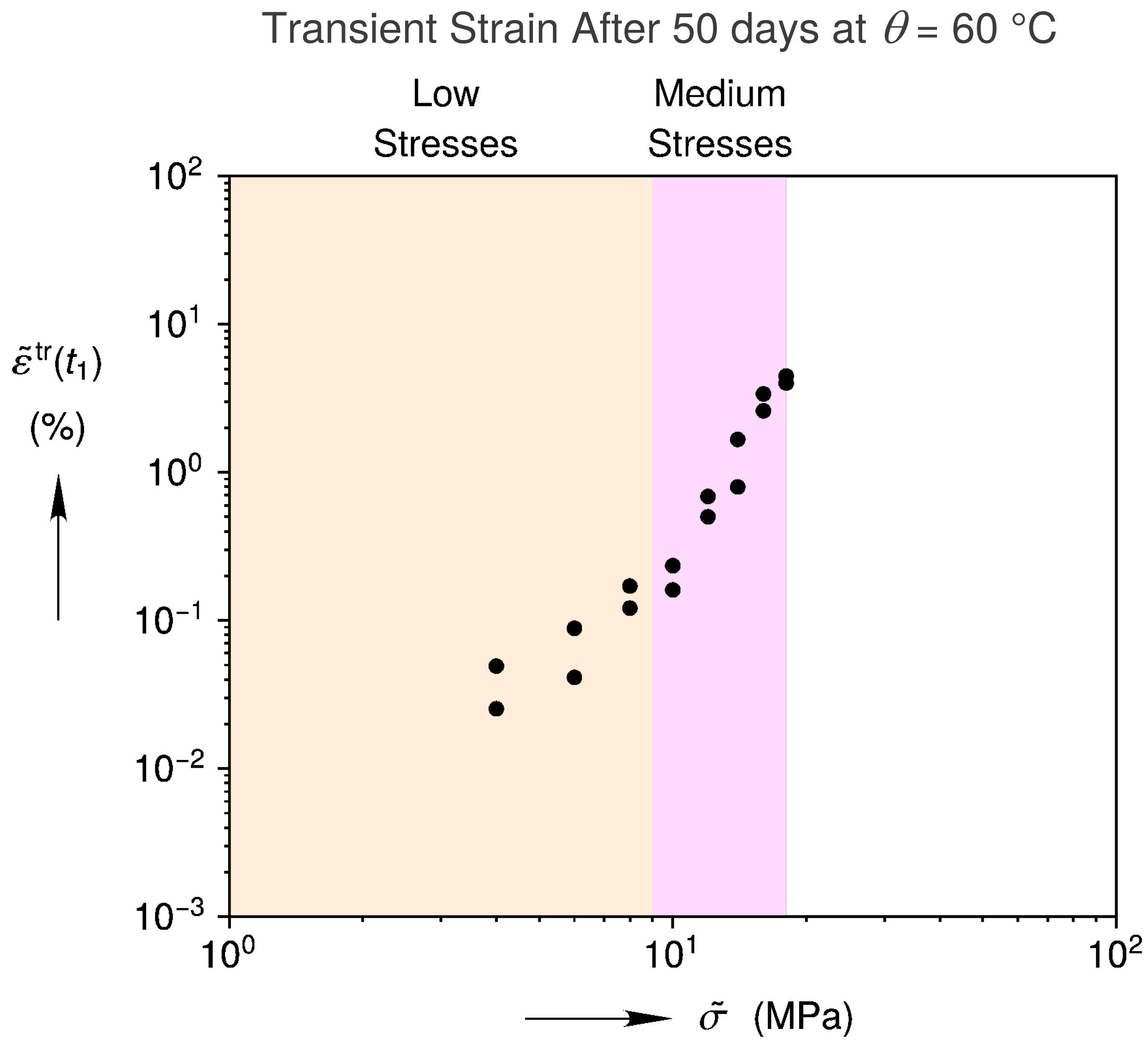

Experimental measurements from: Salzer et al. (2015) and Düsterloh et al. (2015).

Selected Hardening Measurements on WIPP Salt

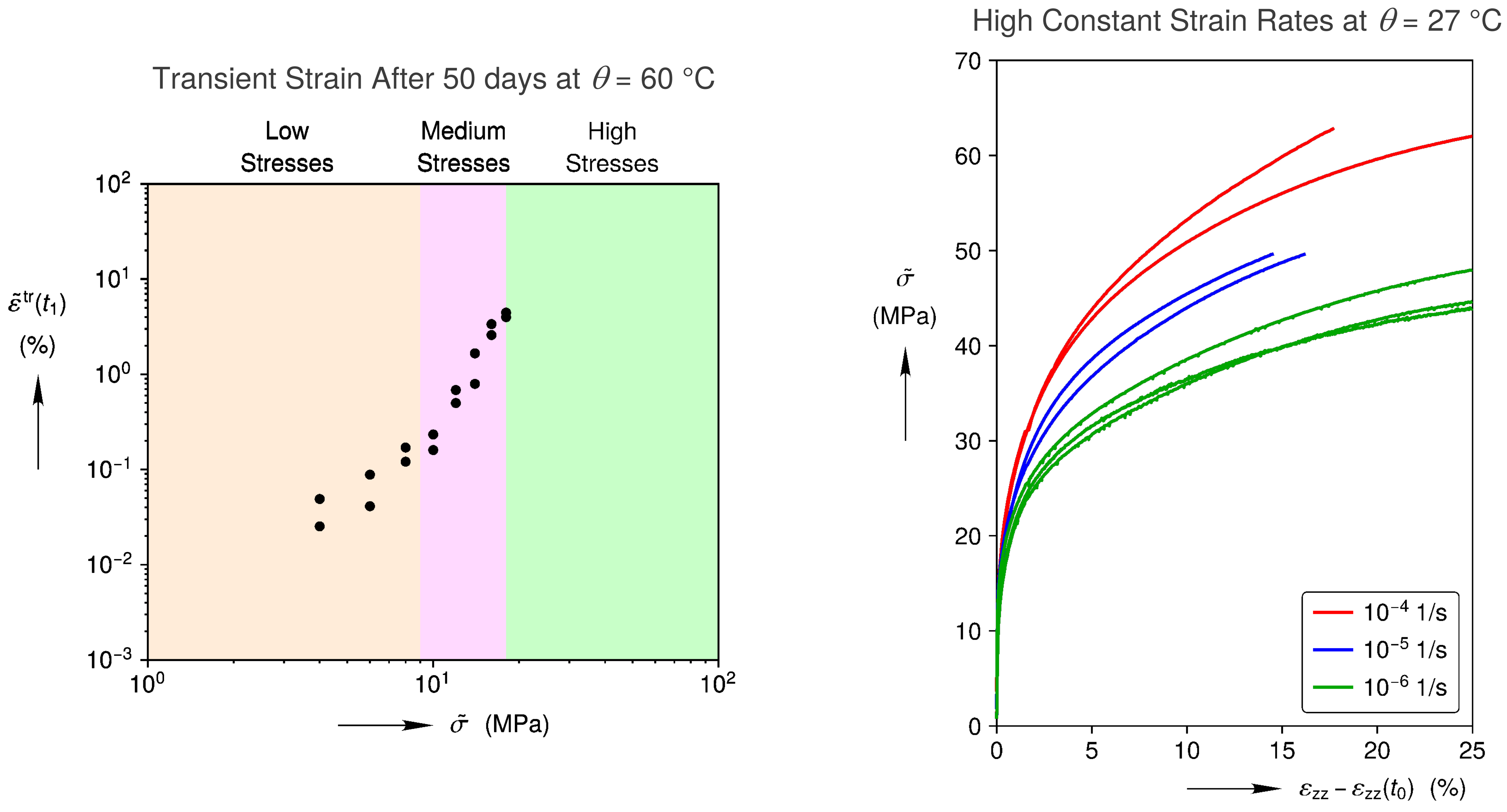

Experimental measurements from: Salzer et al. (2015) and Düsterloh et al. (2015).

Calibration 1A1: Drag Stress Only

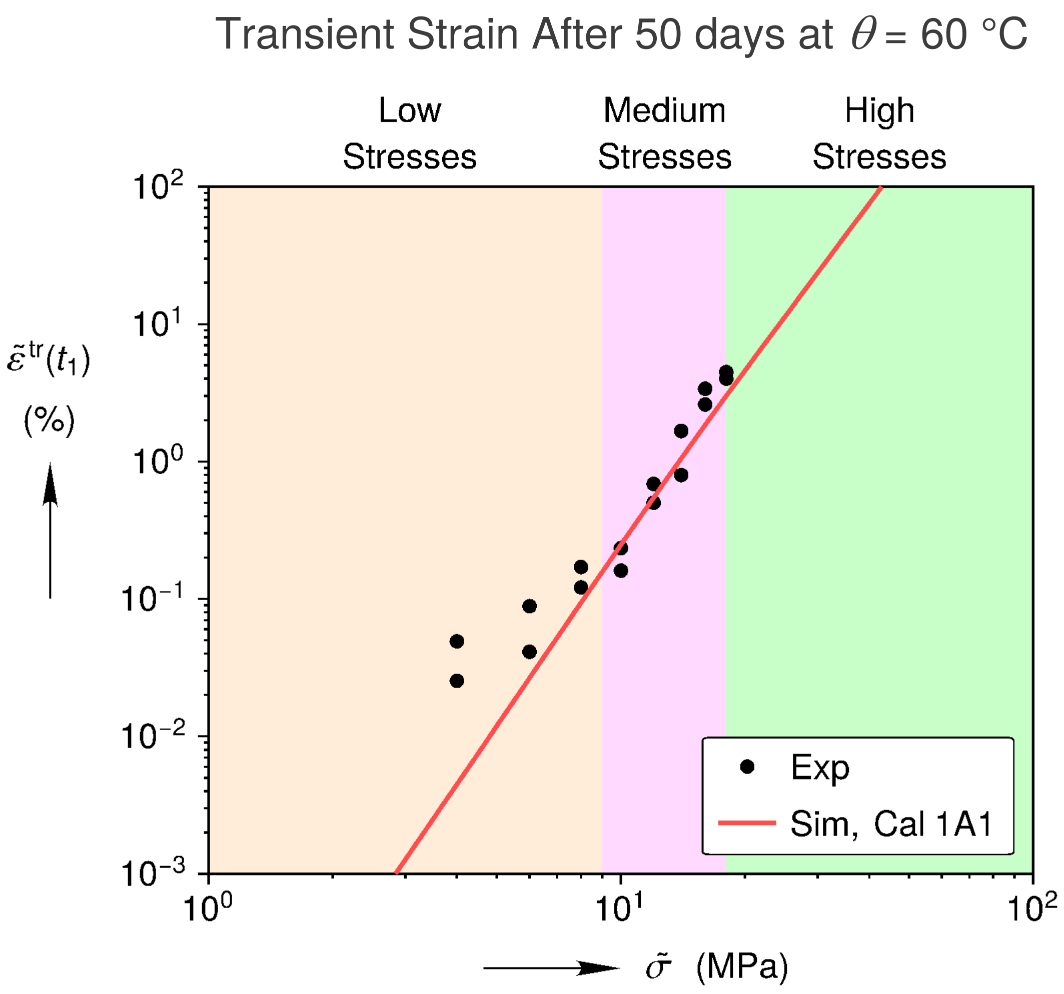

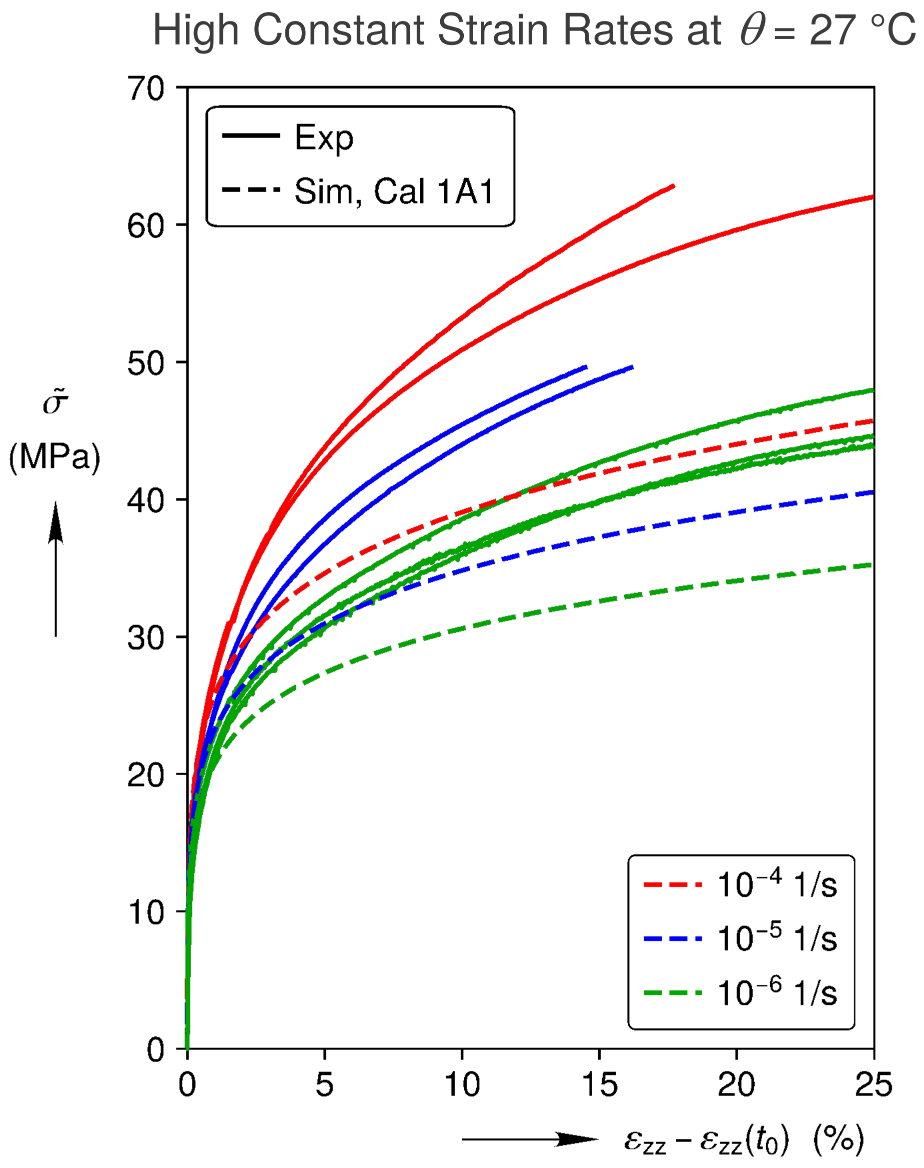

Experimental measurements from: Salzer et al. (2015) and Düsterloh et al. (2015).

Calibration 1A2: Drag Stress Only

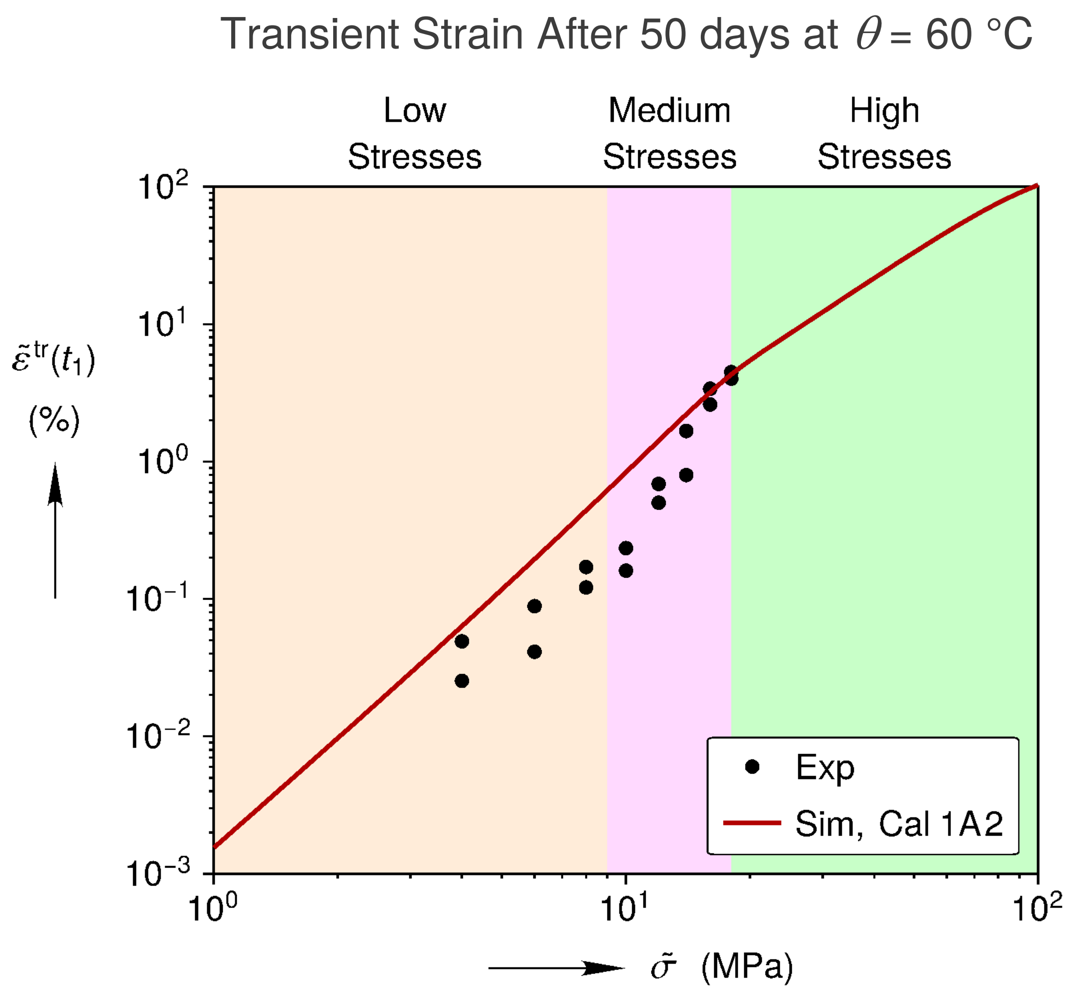

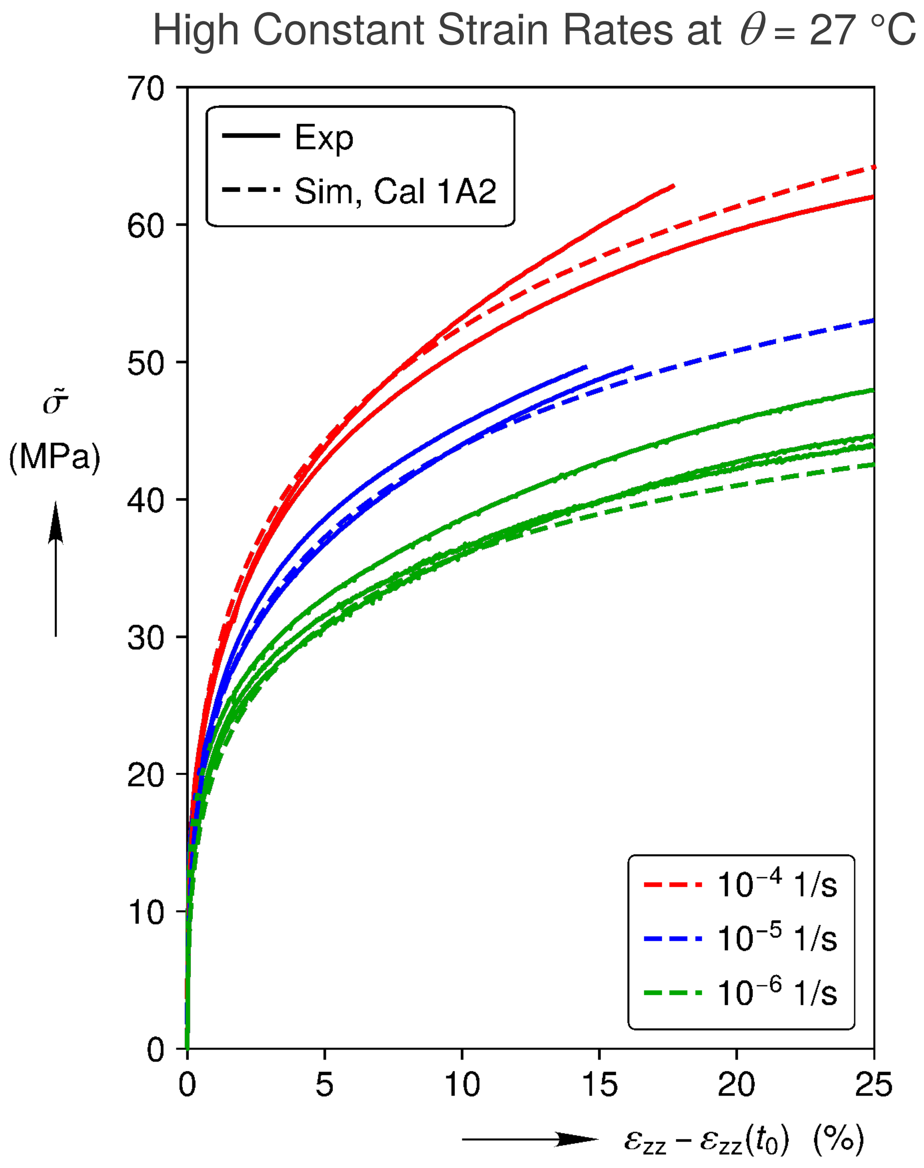

Experimental measurements from: Salzer et al. (2015) and Düsterloh et al. (2015).

Calibration 1C: Drag Stress and Back Stress

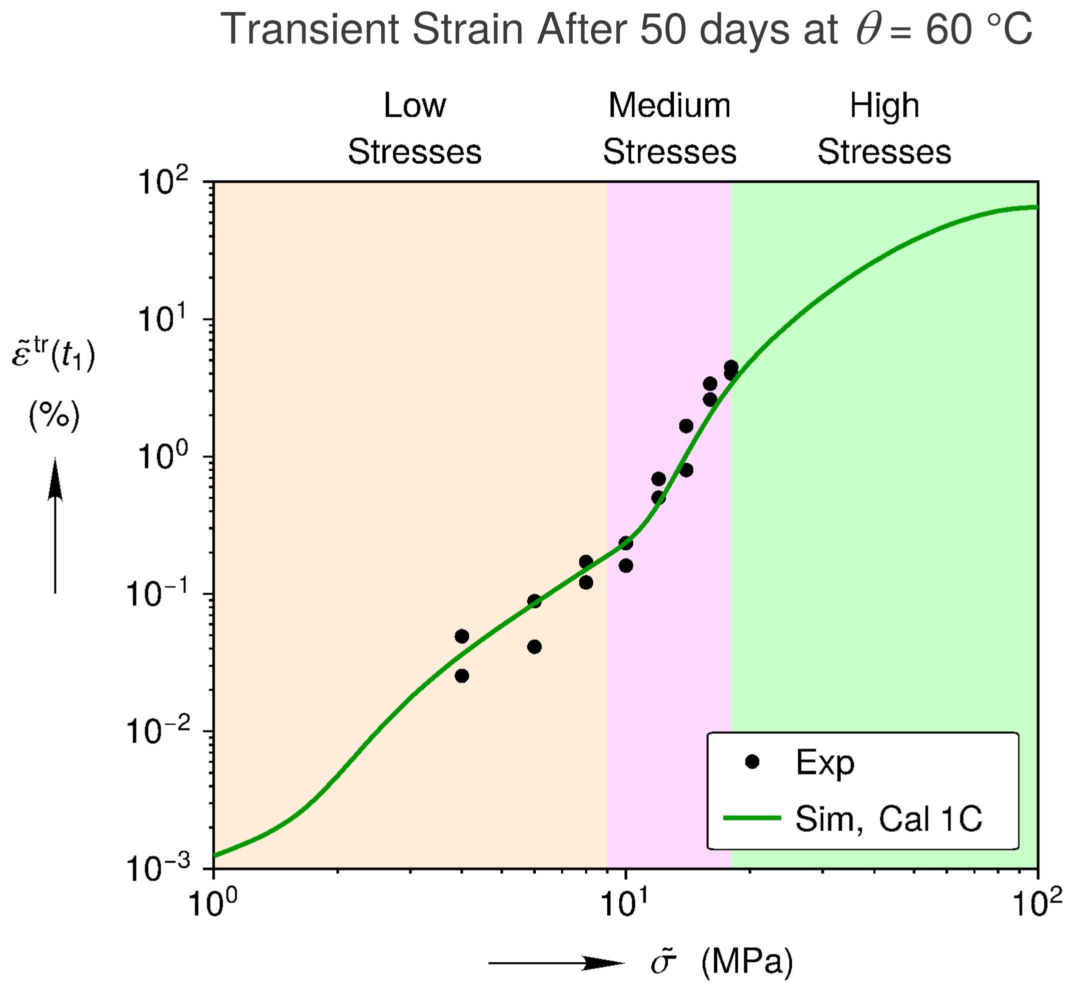

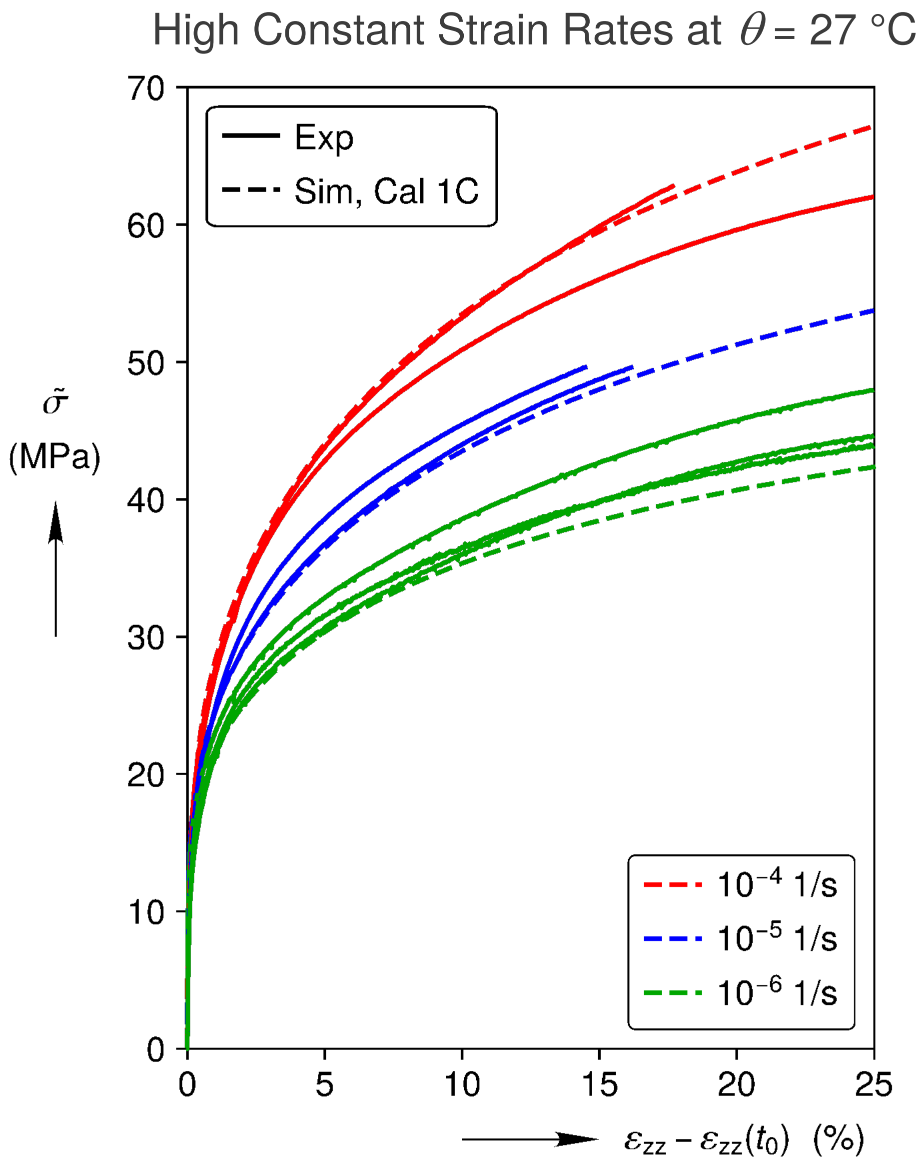

Experimental measurements from: Salzer et al. (2015) and Düsterloh et al. (2015).

Non-Monotonic Loading

A "Gedankenexperiment"

Subgrains

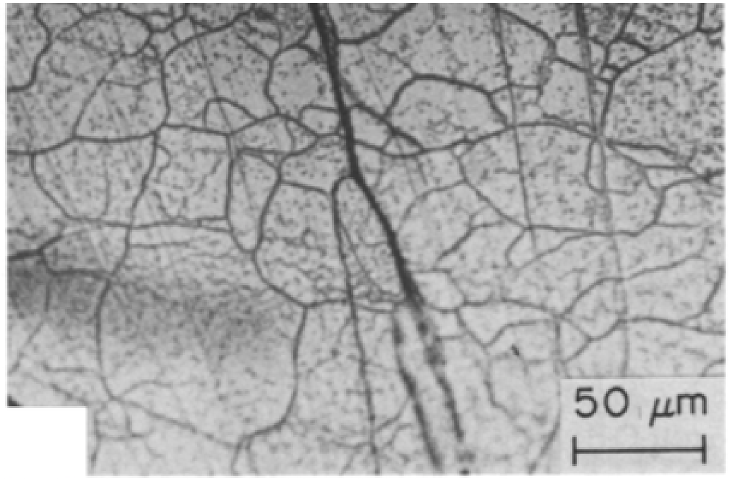

Schematic

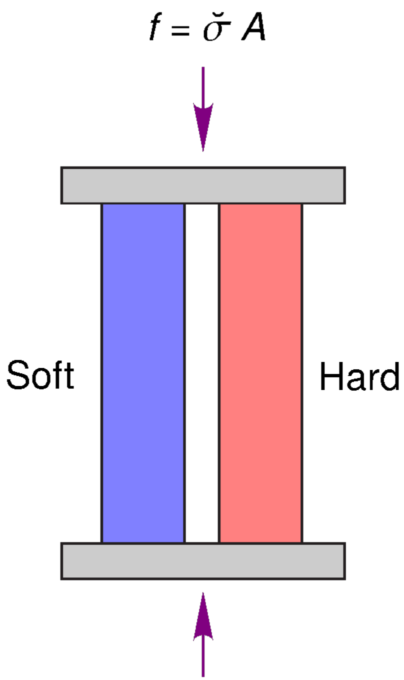

Mechanical Responses

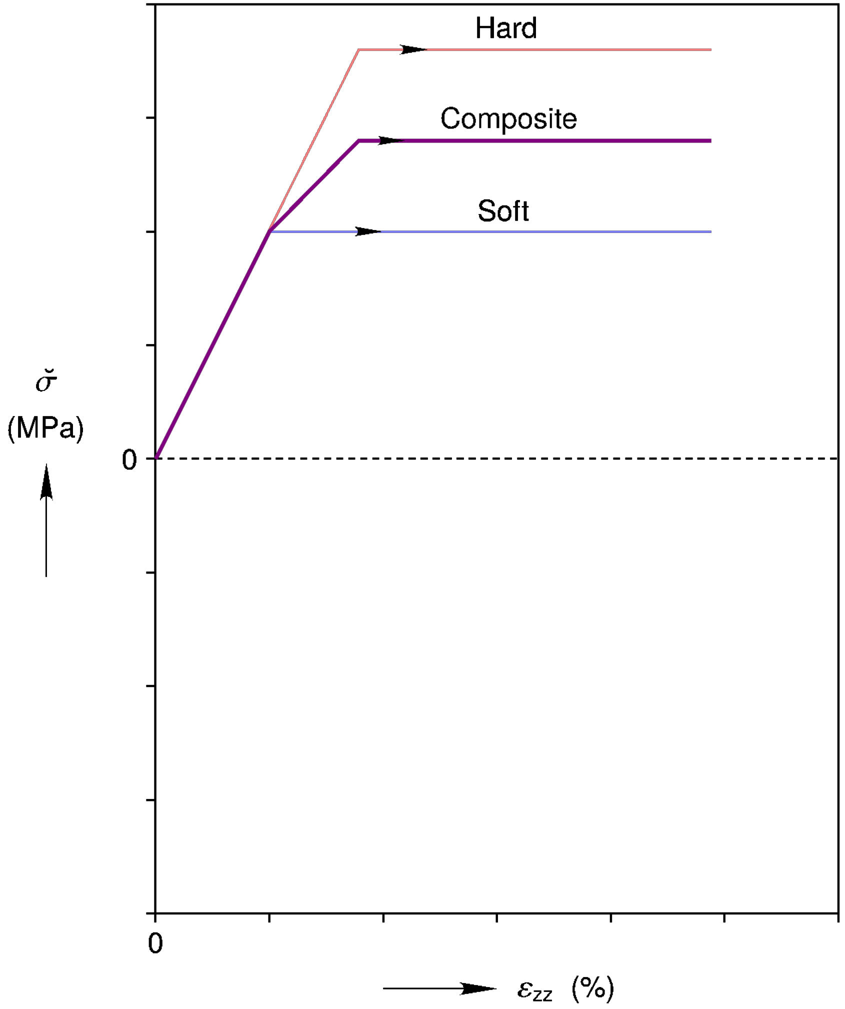

Original "Gedankenexperiment" from: Mughrabi, H. (1983) Dislocation wall and cell structures and long-range internal stresses in deformed metal crystals. Acta Metallurgica. Vol. 31. No. 9. pg. 1367-1379

A “Gedankenexperiment”

Subgrains

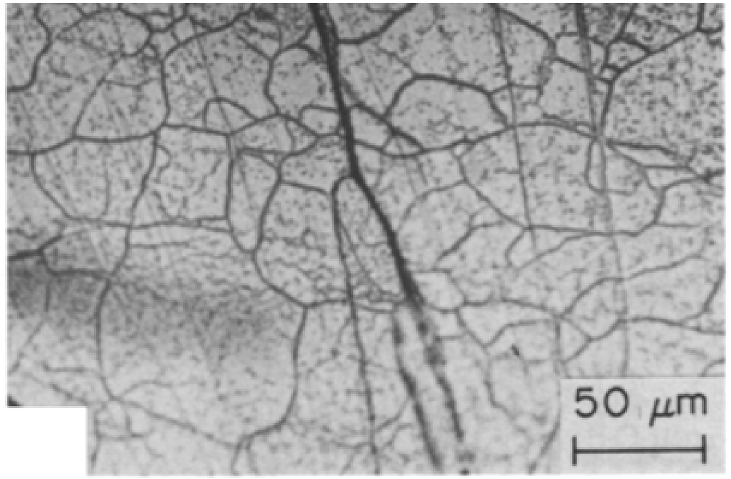

Schematic

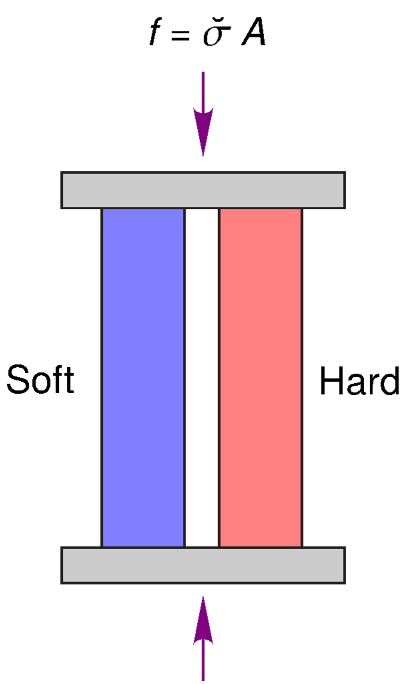

Mechanical Responses

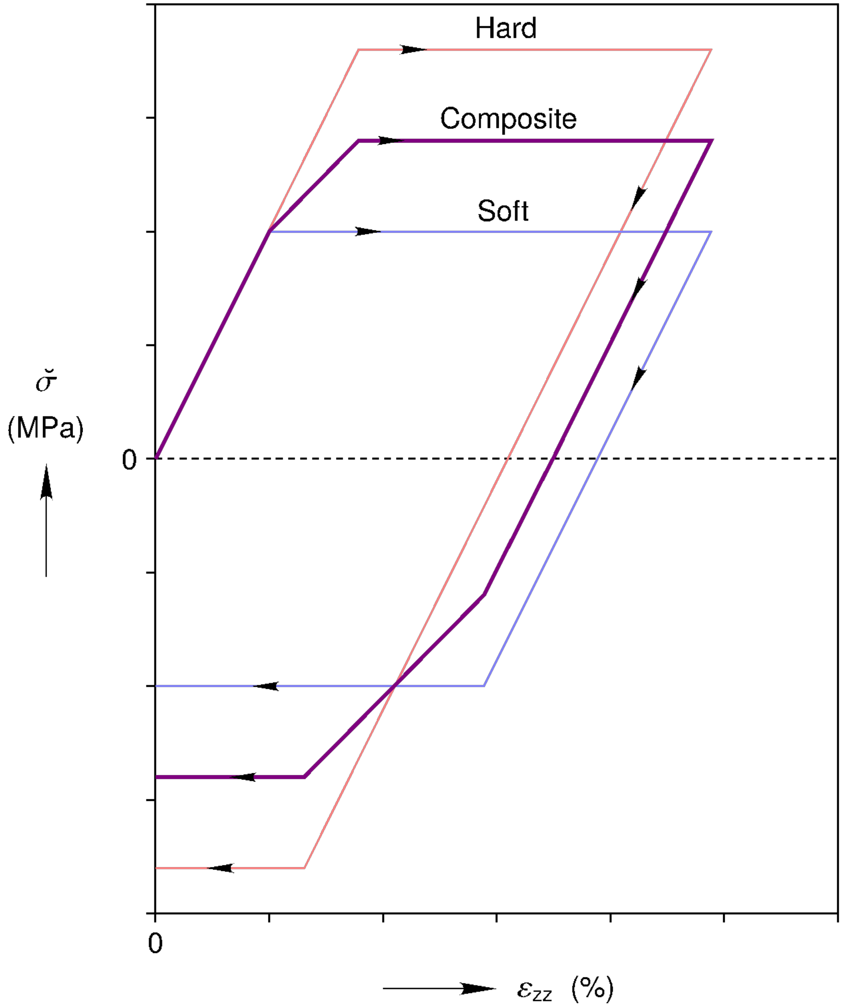

Original "Gedankenexperiment" from: Mughrabi, H. (1983) Dislocation wall and cell structures and long-range internal stresses in deformed metal crystals. Acta Metallurgica. Vol. 31. No. 9. pg. 1367-1379

Bauschinger Effect

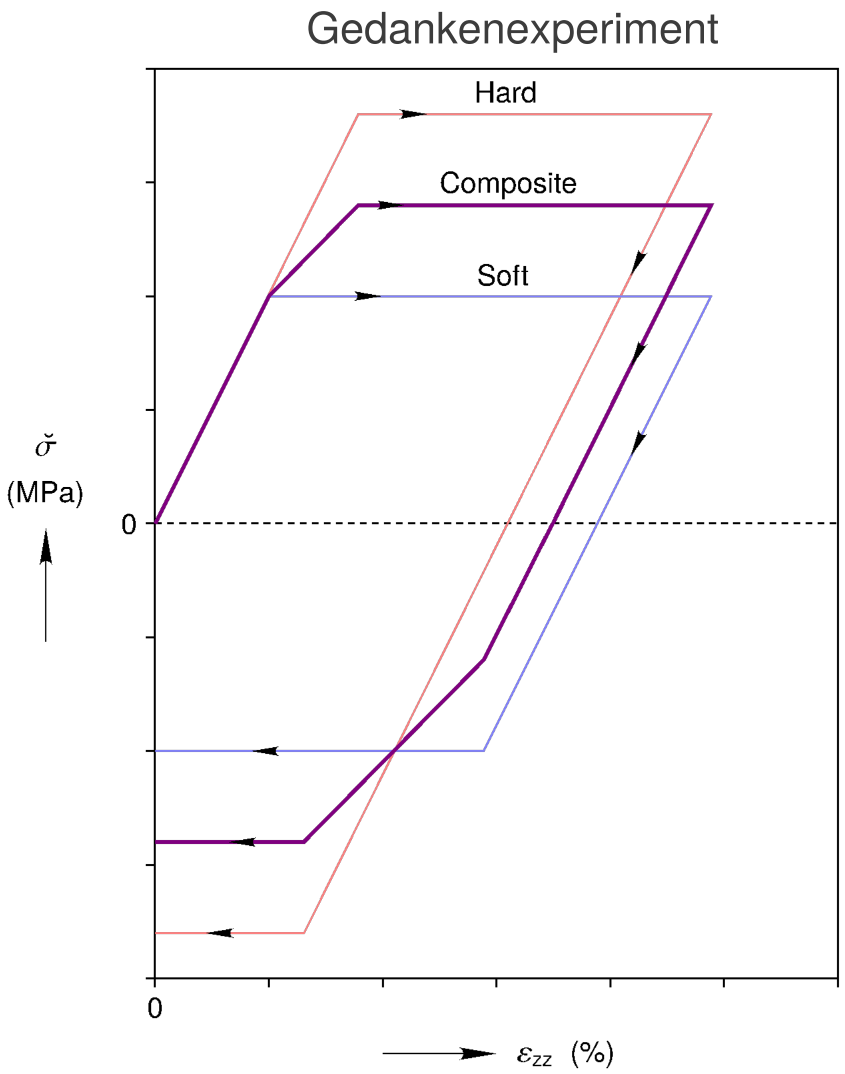

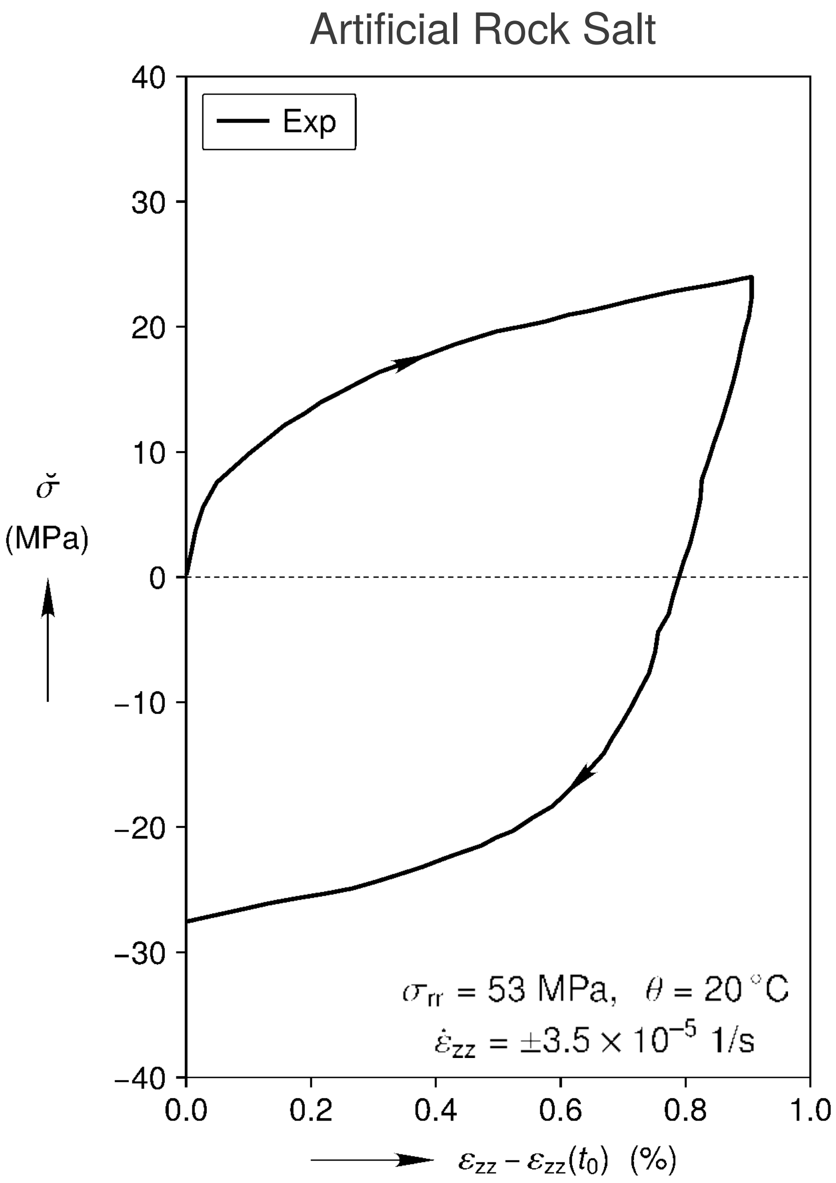

Experimental measurements from Aubertin et al. (1999)

Re-hardening during Non-Monotonic Loading

Constant Strain Rate Test on Artificial Salt

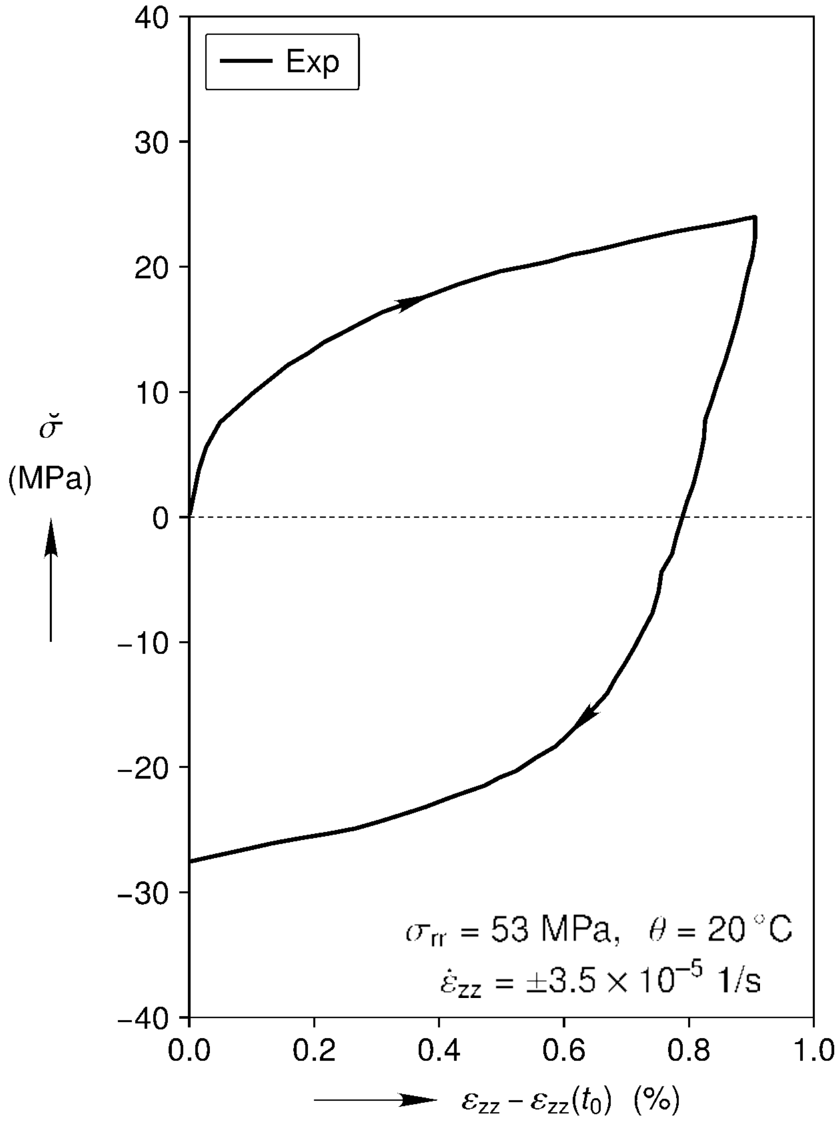

Experimental measurements from: Aubertin et al. (1999)

Multi-Stage Constant Stress Test on Cayuta Salt

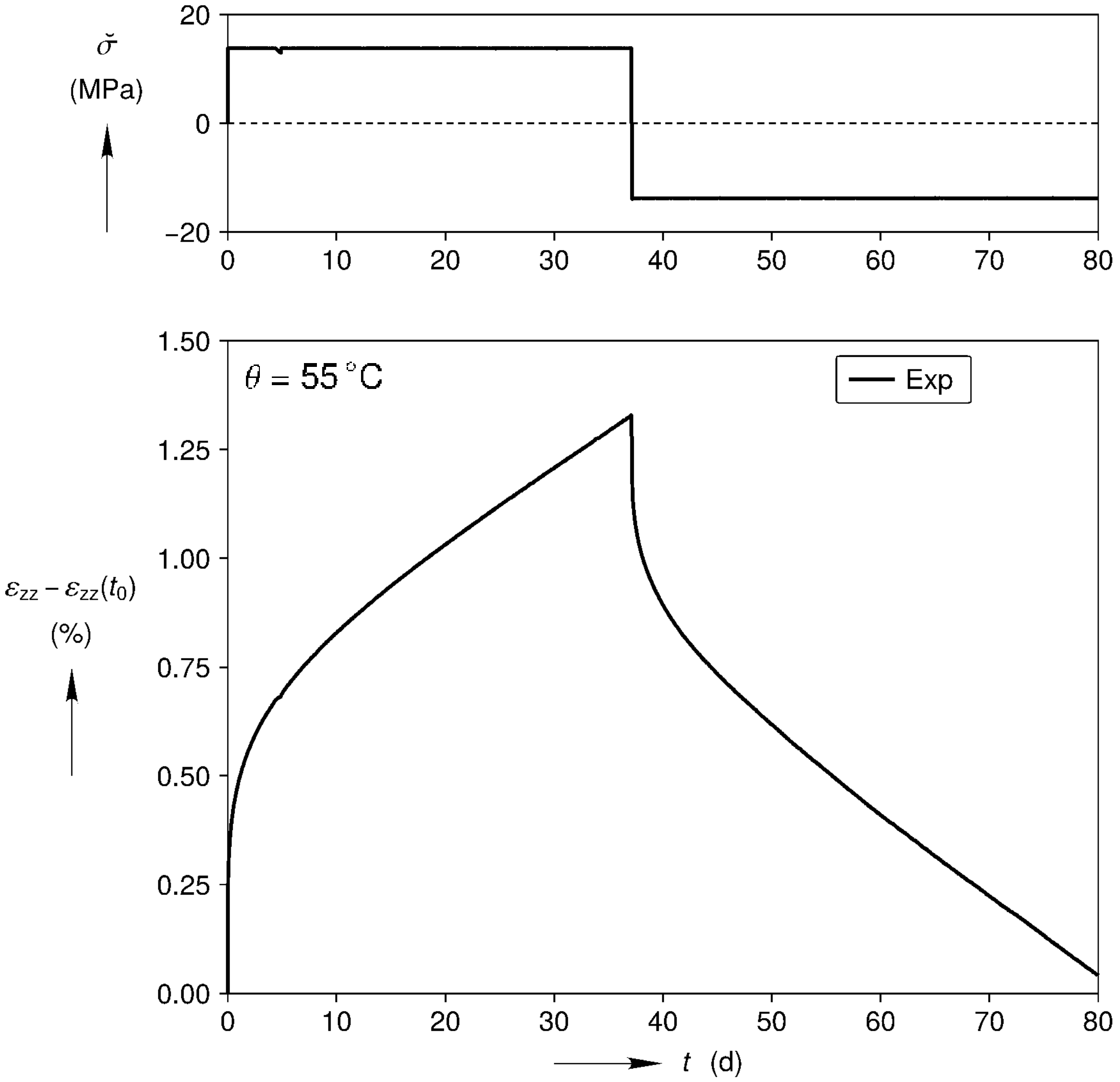

Experimental measurements from: Mellegard et al. (2007)

Re-hardening during Non-Monotonic Loading

Constant Strain Rate Test on Artificial Salt

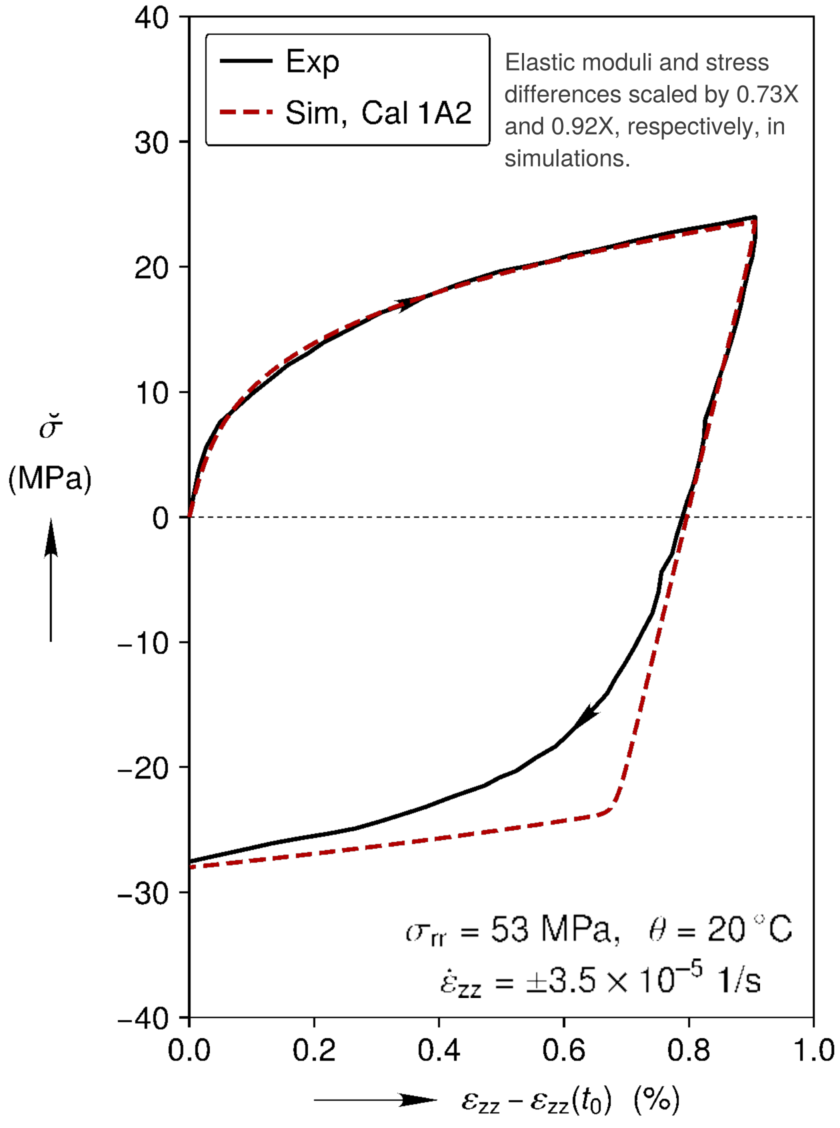

Experimental measurements from: Aubertin et al. (1999)

Multi-Stage Constant Stress Test on Cayuta Salt

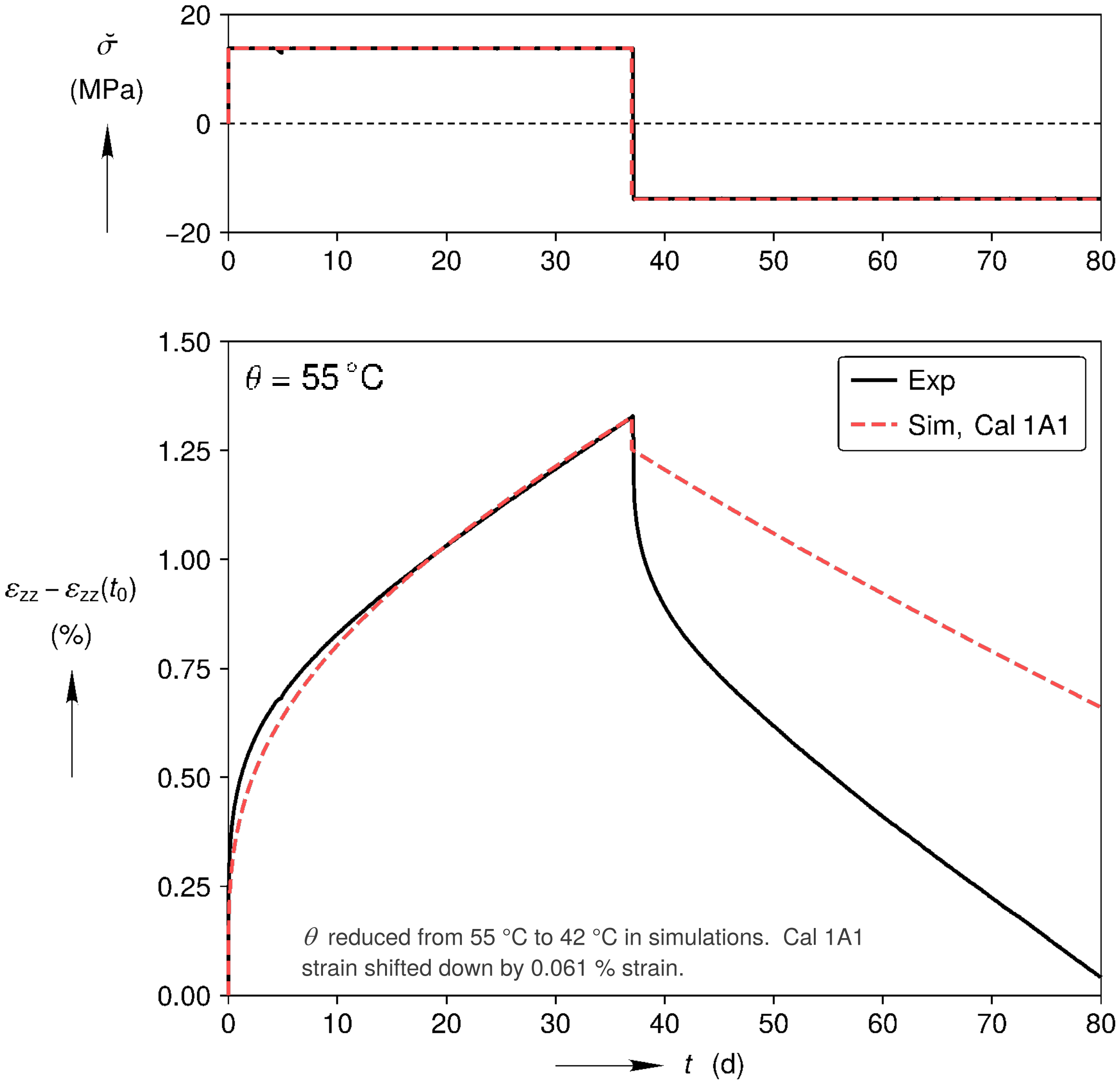

Experimental measurements from: Mellegard et al. (2007)

Re-hardening during Non-Monotonic Loading

Constant Strain Rate Test on Artificial Salt

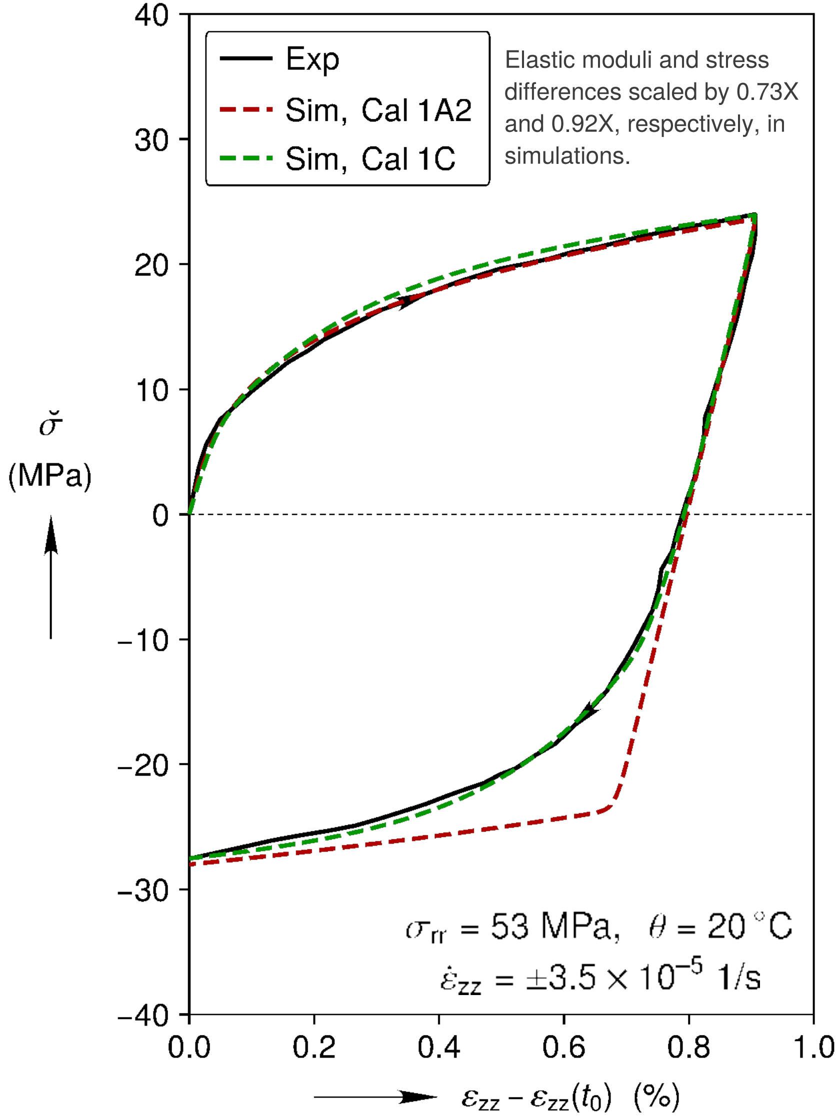

Experimental measurements from: Aubertin et al. (1999)

Multi-Stage Constant Stress Test on Cayuta Salt

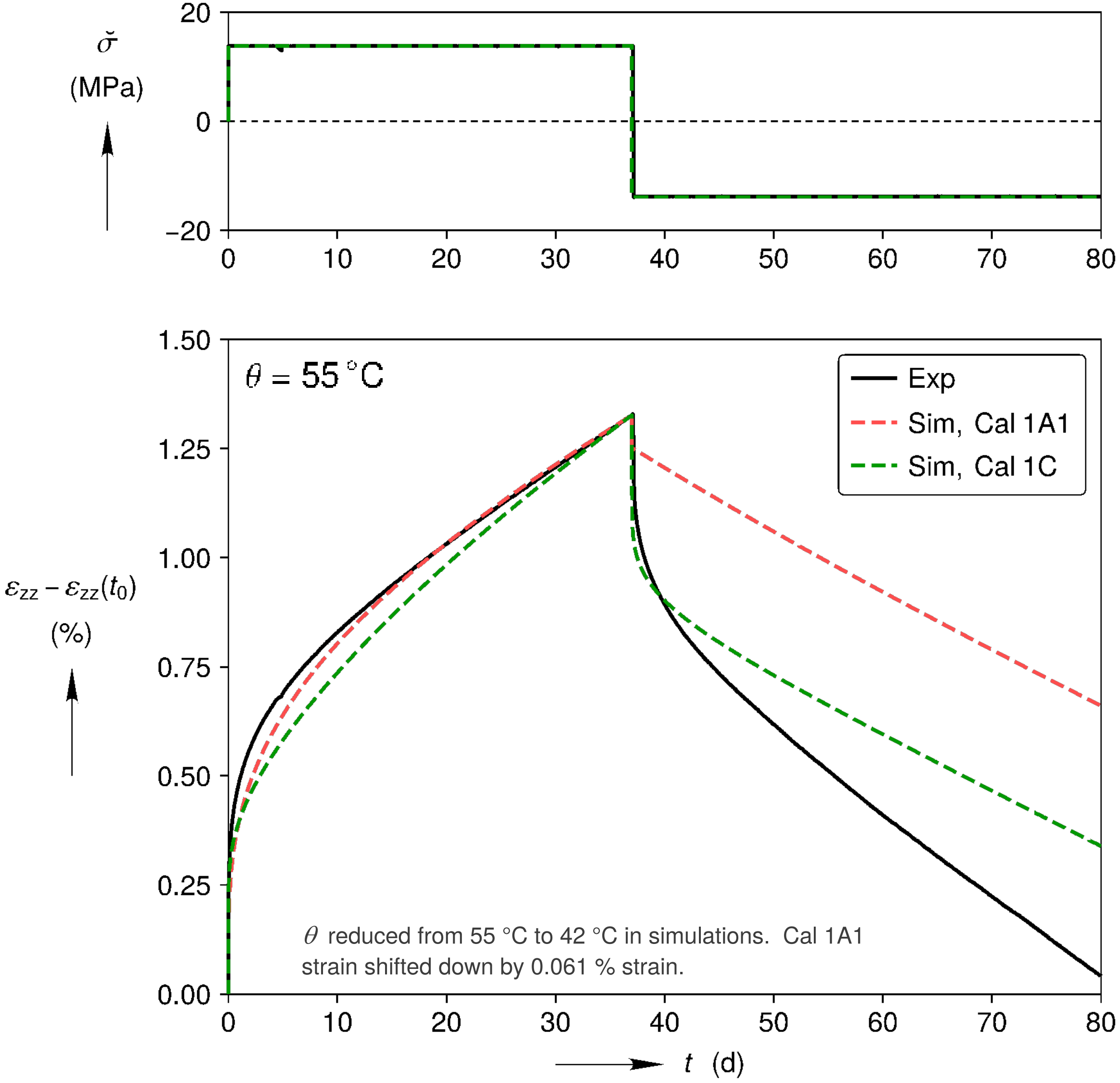

Experimental measurements from: Mellegard et al. (2007)

Summary & Future Work

Summary & Future Work

1. Summary
    1. Largely phenomenological model, but key decisions were motivated by micro-physical observations.
    2. Pressure solution and dislocation glide branches
    3. Combined drag and back stress hardening enables one to capture hardening at low, medium, and high strain rates, as well as re-hardening behavior after non-monotonic loading.
2. Future work
    1. Polish numerical implementation
    2. Simulate more underground structures
    3. Add damage and healing

Extra Slides

Hardening Transition from Medium to High Strain Rates (Stresses)

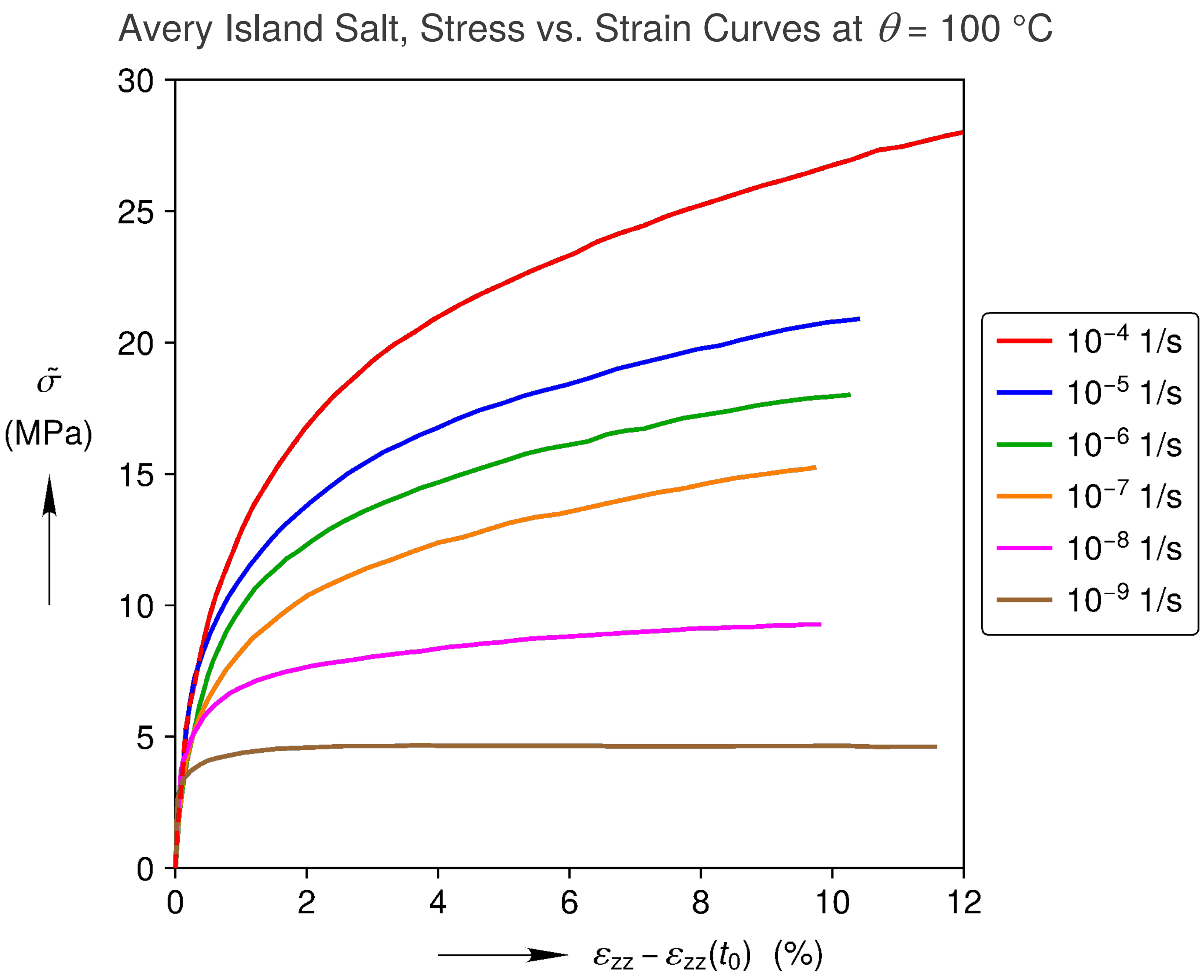

Experimental measurements from: Horseman, ST and Handin, J. (1990) and Carter, NL, Horseman, ST, Russell, JE, and Handin, J (1993)

Hardening Transition from Medium to High Strain Rates (Stresses)

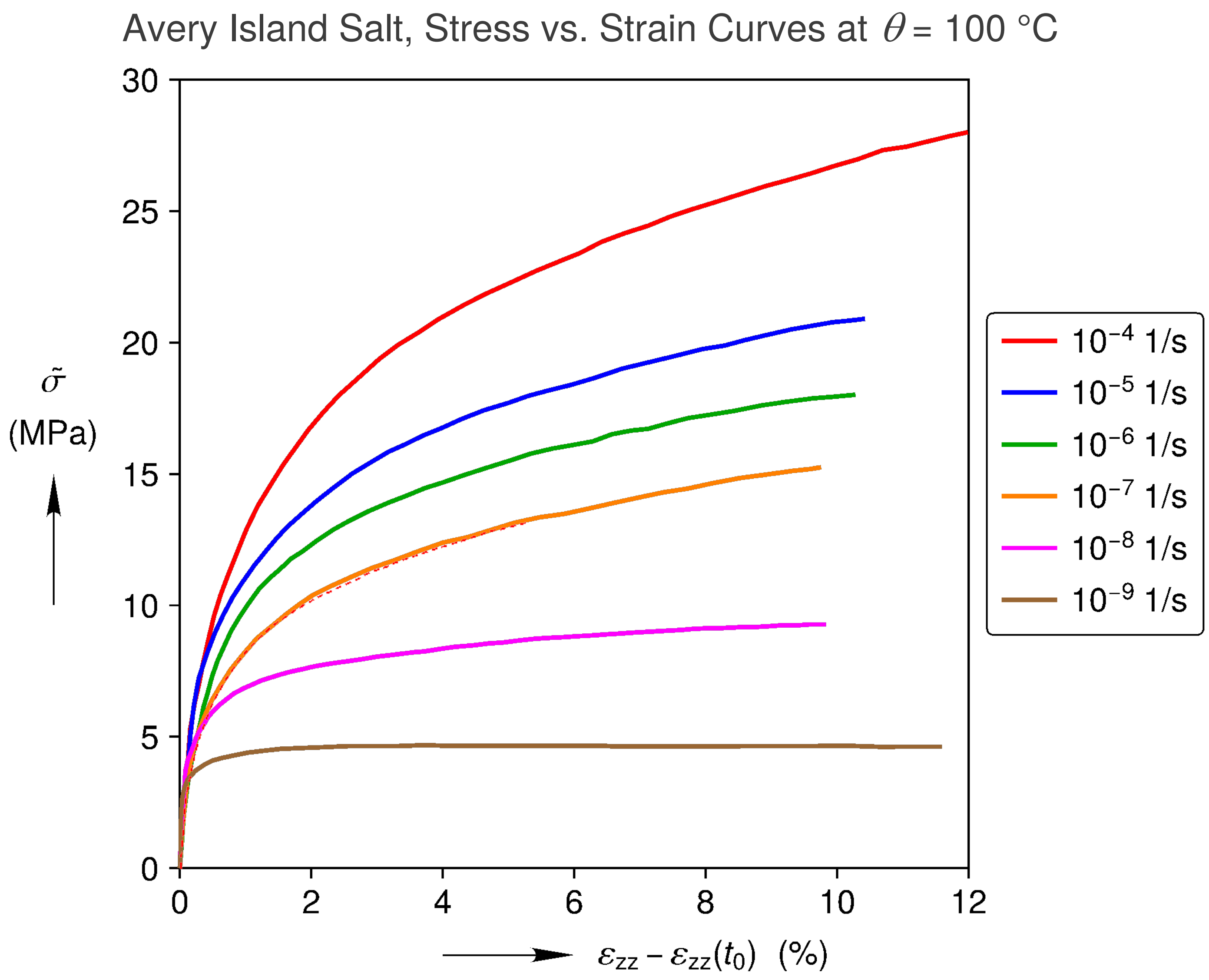

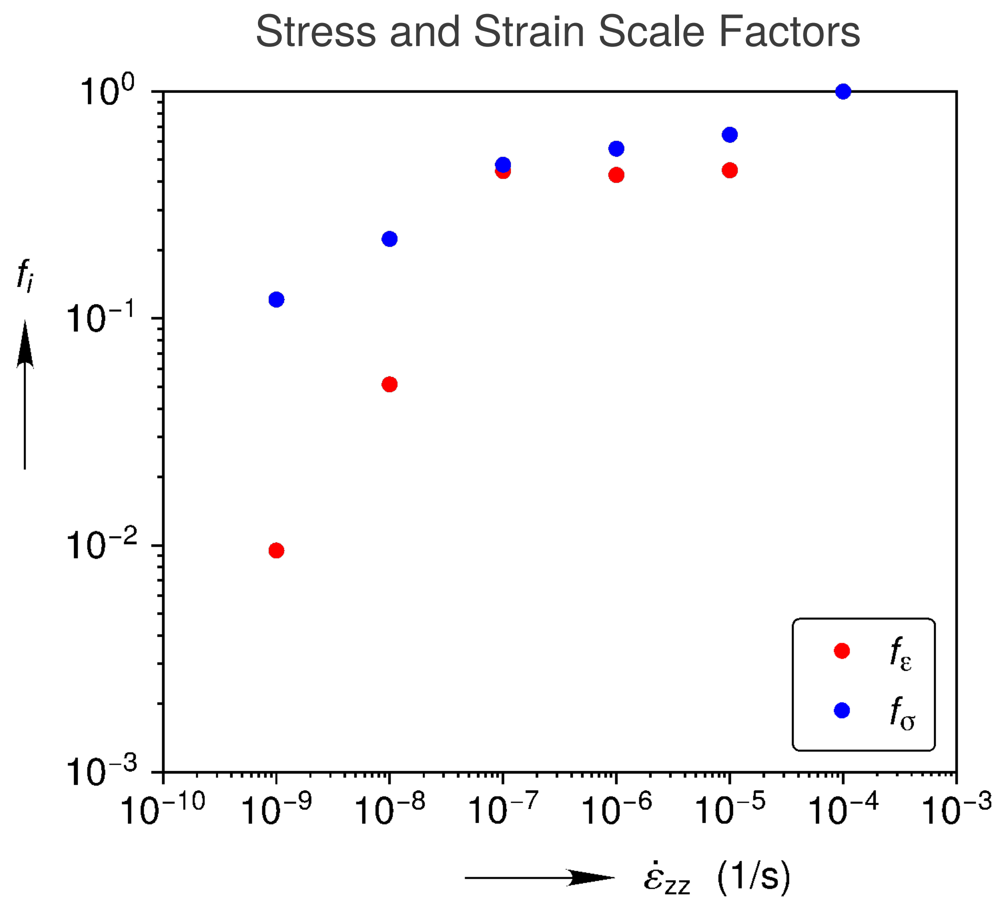

Experimental measurements from: Horseman, ST and Handin, J. (1990) and Carter, NL, Horseman, ST, Russell, JE, and Handin, J (1993)

Hardening Transition from Medium to High Strain Rates (Stresses)

Avery Island Salt, Stress vs. Strain Curves at θ = 100 °C

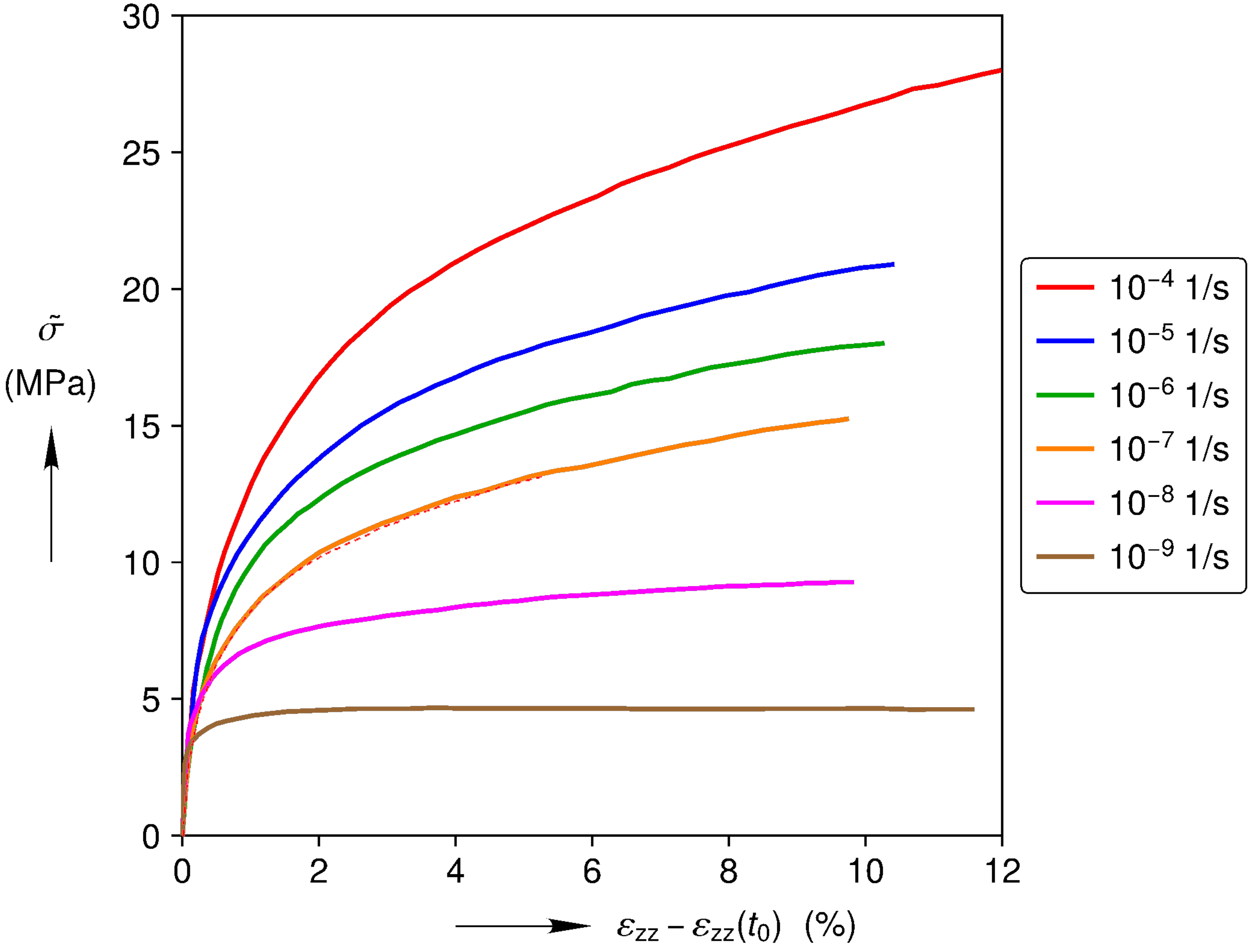

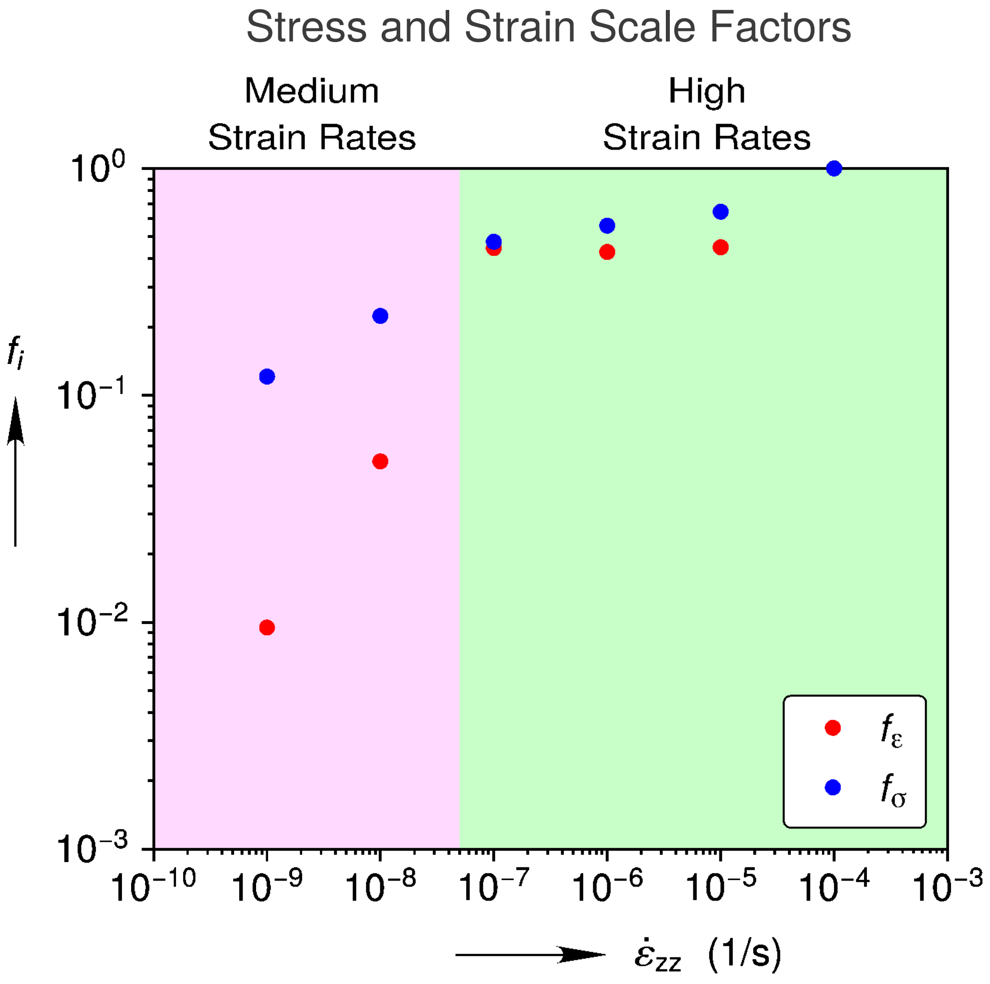

Experimental measurements from: Horseman, ST and Handin, J. (1990) and Carter, NL, Horseman, ST, Russell, JE, and Handin, J (1993)

Re-hardening During Non-Monotonic Loading

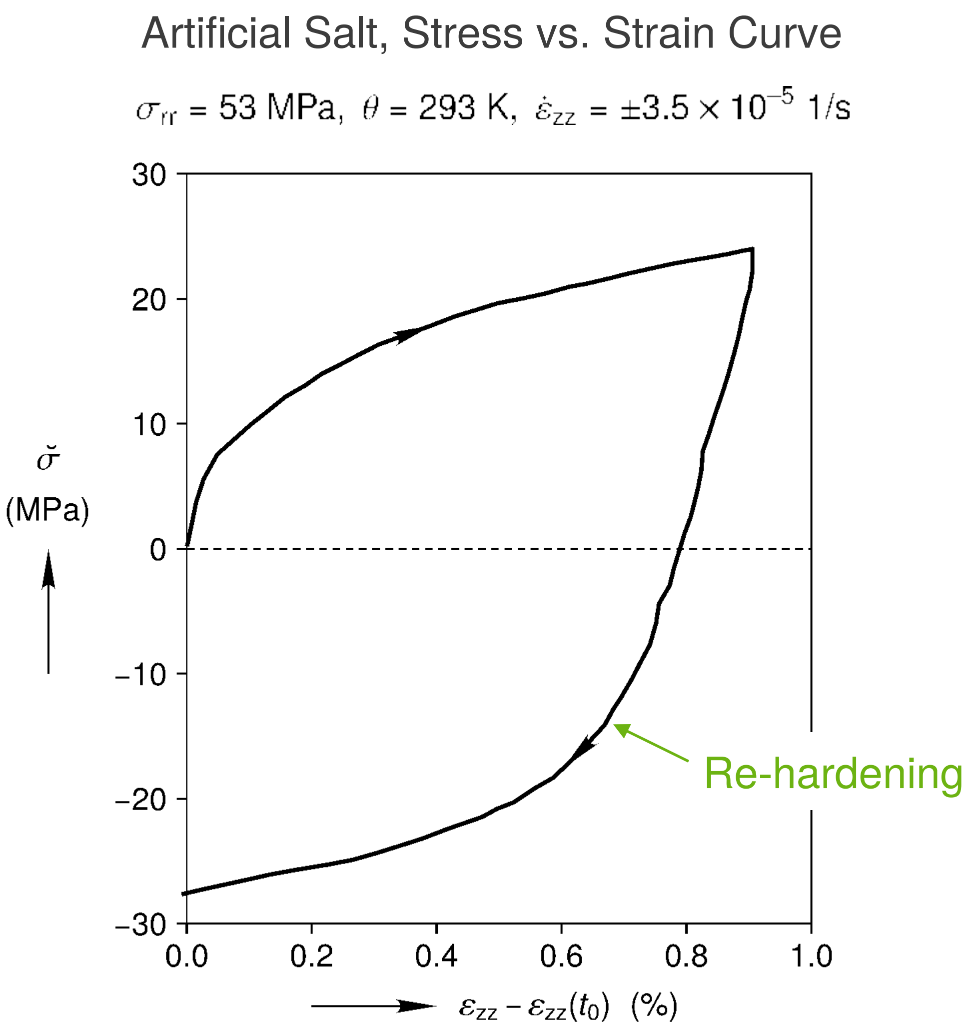

Experimental measurements from Aubertin et al. (1999)

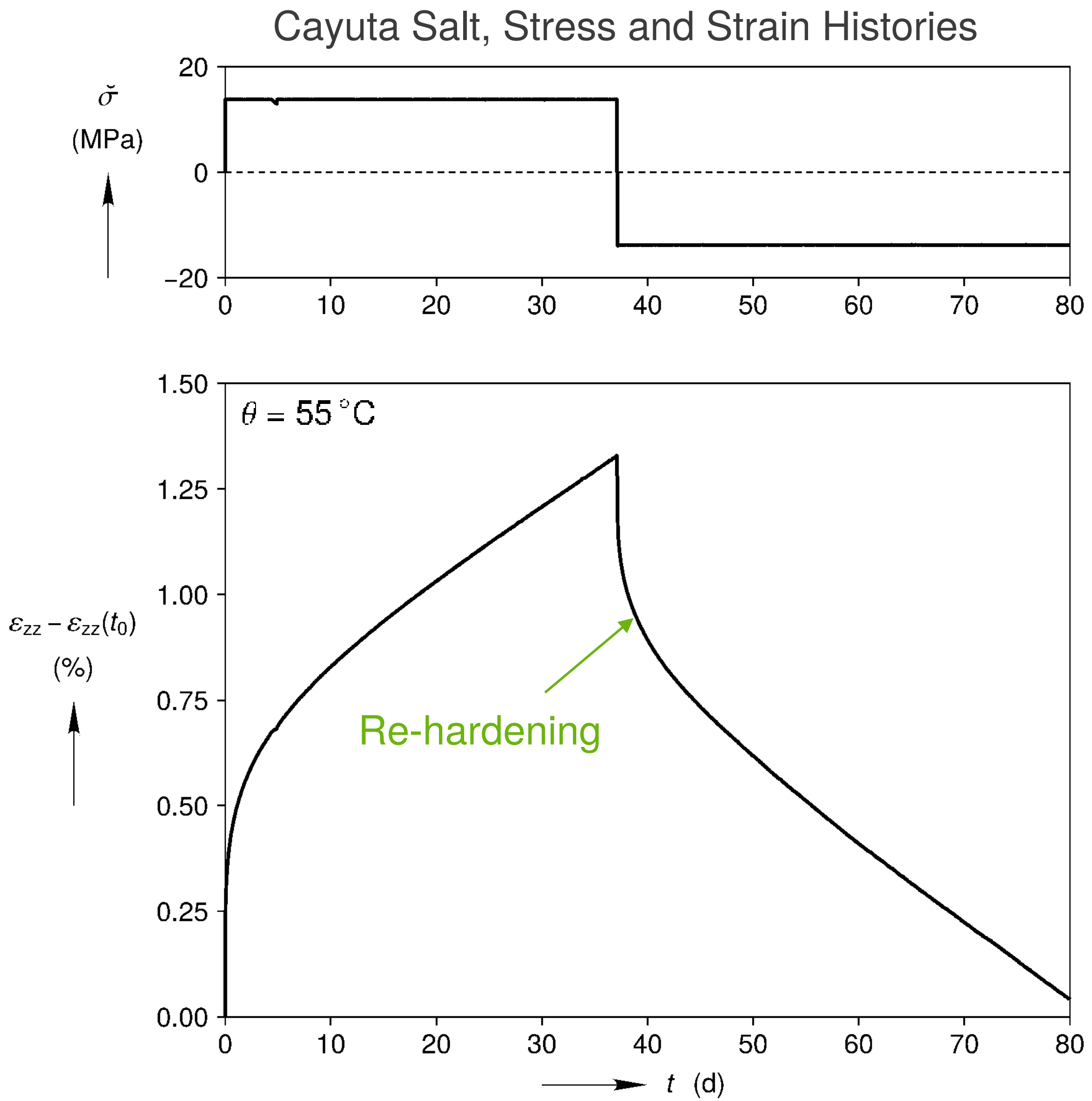

Experimental measurements from: Mellegard et al. (2007)

Dislocation Glide Hardening

Drag Stress Evolution Equation

$$\dot{y} = Y_1 \left(\frac{Y_1}{y}\right)^{Y_2} \left(1 - \frac{y}{\bar{y}}\right) \dot{\tilde{\varepsilon}}^{dg}$$

Back Stress Evolution Equation
(proportional, monotonic, loading)

$$\dot{\tilde{b}} = B_1 \left(1 - \frac{\tilde{b}}{\bar{b}}\right) \dot{\tilde{\varepsilon}}^{dg}$$

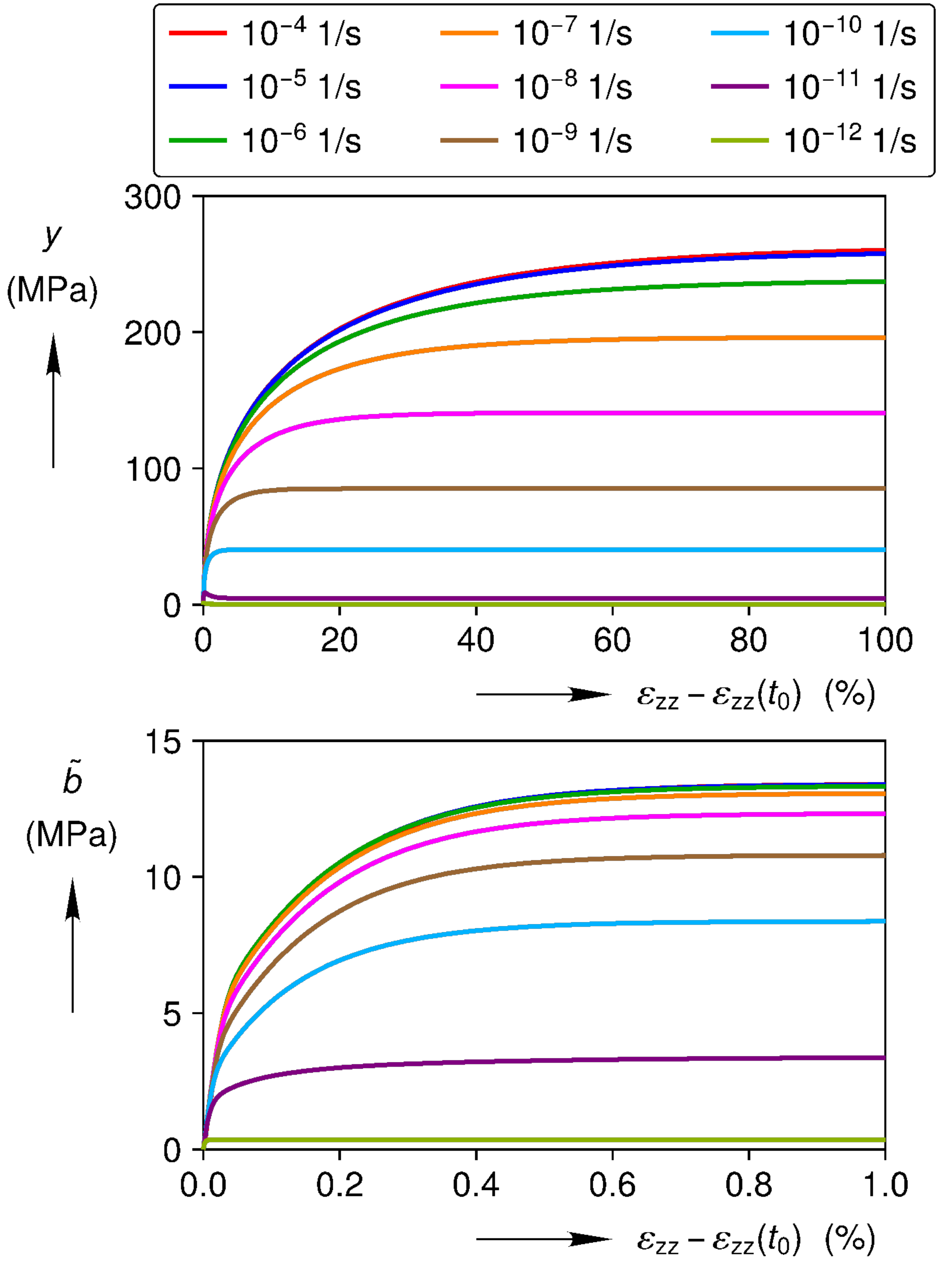

Dislocation Glide Hardening

Drag Stress Evolution Equation

$$\dot{y} = Y_1 \left(\frac{Y_1}{y}\right)^{Y_2} \left(1 - \frac{y}{\bar{y}}\right) \dot{\tilde{\varepsilon}}^{\text{dg}}$$

Back Stress Evolution Equation
(proportional, monotonic, loading)

$$\dot{\tilde{b}} = B_1 \left(1 - \frac{\tilde{b}}{\bar{b}}\right) \dot{\tilde{\varepsilon}}^{\text{dg}}$$

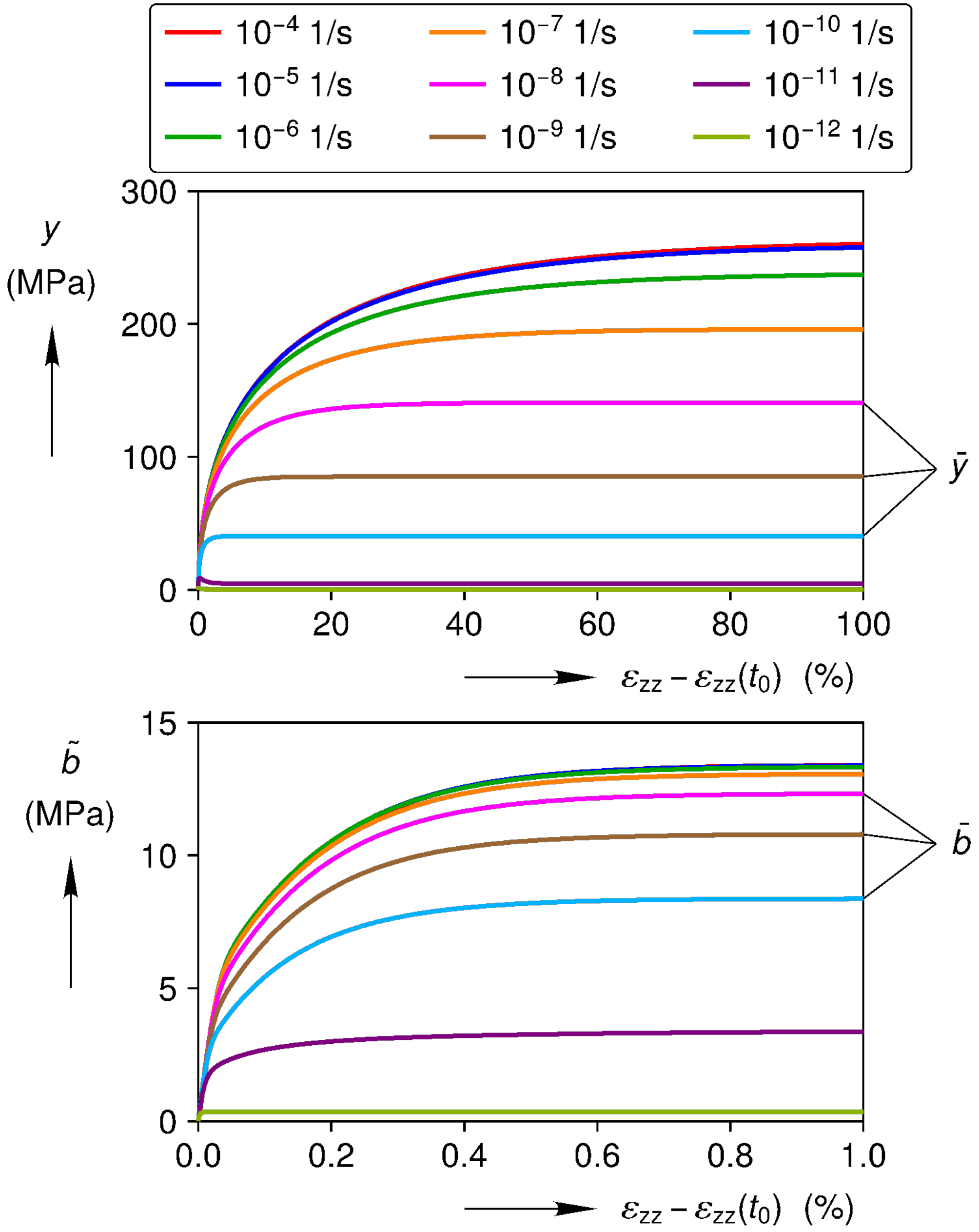

Dislocation Glide Hardening

Strain Rates
(proportional, monotonic, loading)

$$\dot{\tilde{\varepsilon}}^{ps} = P_1 \exp\left(-\frac{P_2}{\theta}\right)\frac{\tilde{\sigma}}{\theta}$$

$$\dot{\tilde{\varepsilon}}^{dg} = G_1 \exp\left(-\frac{G_2}{\theta}\right)\left[\sinh\left(\frac{\tilde{\sigma}-\tilde{b}}{y}\right)\right]^{G_3}$$

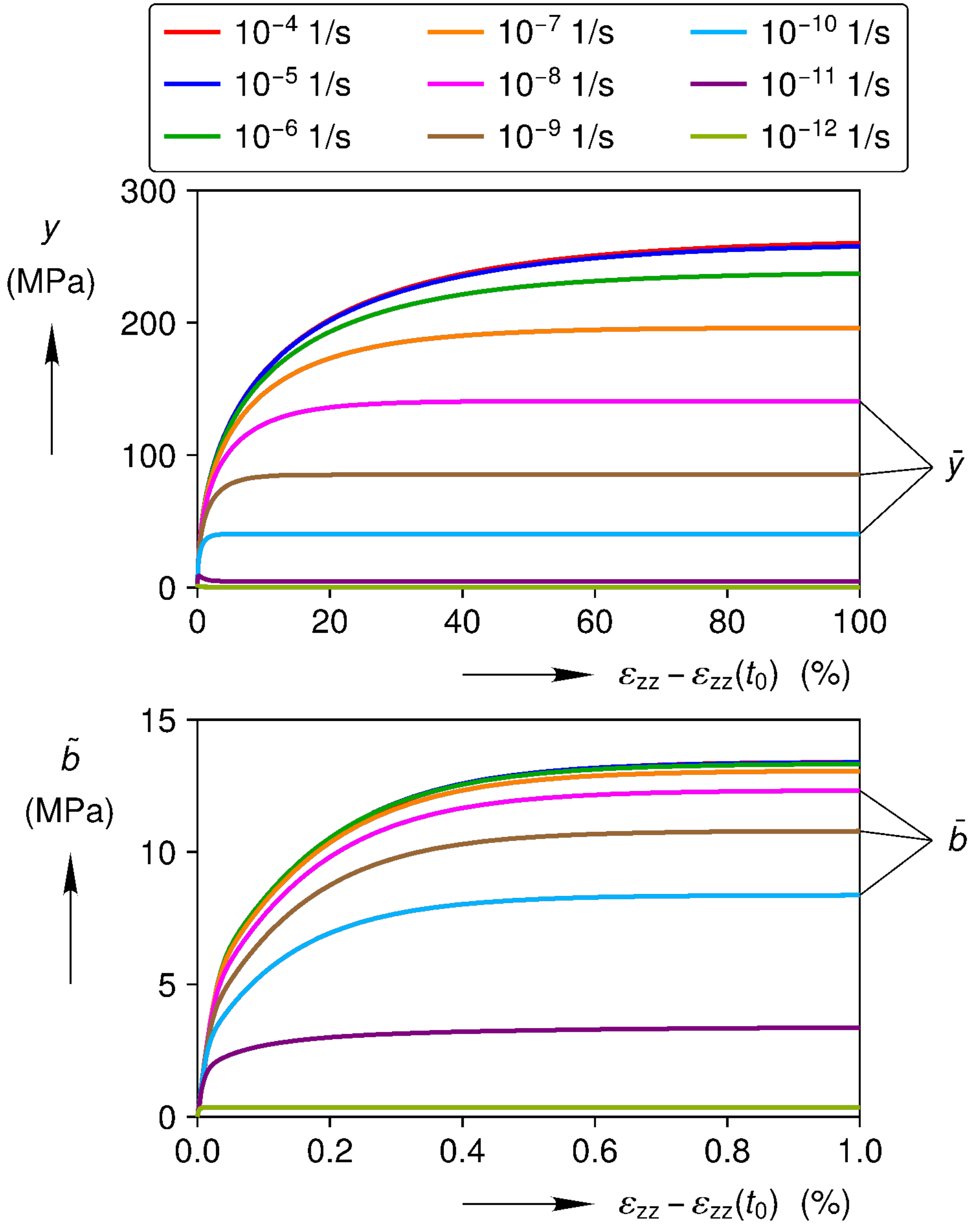

Dislocation Glide Steady-State

Steady-State Strain Rates

$$\dot{\tilde{\varepsilon}}^{ps} = P_1 \exp\left(-\frac{P_2}{\theta}\right)\frac{\tilde{\sigma}}{\theta}$$

$$\dot{\tilde{\varepsilon}}^{dg} = G_1 \exp\left(-\frac{G_2}{\theta}\right)\left[\sinh\left(\frac{\tilde{\sigma}-\bar{b}}{\bar{y}}\right)\right]^{G_3}$$

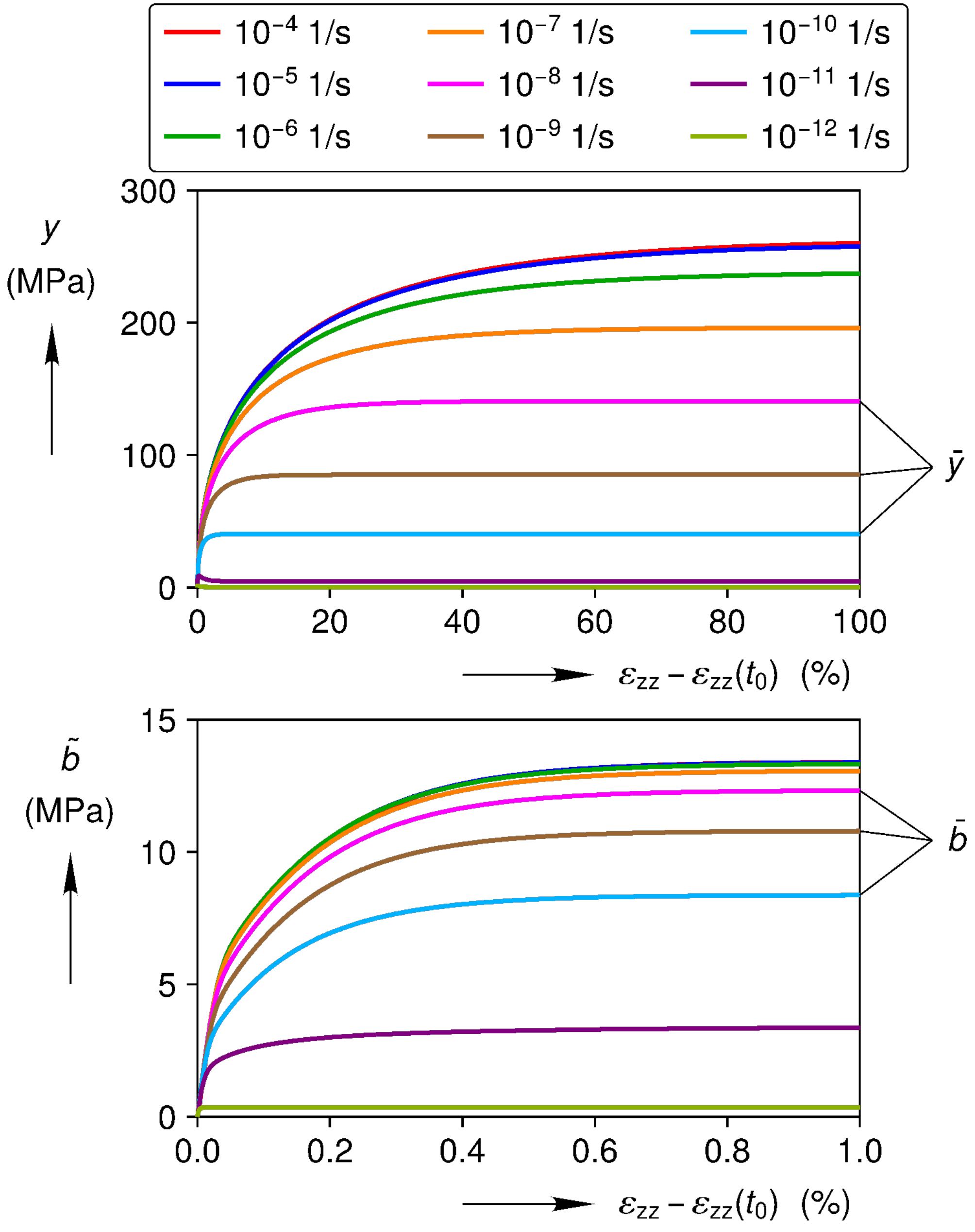

Dislocation Glide Steady-State

Steady-State Strain Rates

$$\dot{\tilde{\varepsilon}}^{\mathrm{ps}} = P_1 \exp\left(-\frac{P_2}{\theta}\right)\frac{\tilde{\sigma}}{\theta}$$

$$\dot{\tilde{\varepsilon}}^{\mathrm{dg}} = Y_3 \exp\left(-\frac{G_2}{\theta}\right)\left[\sinh\left(\frac{\tilde{\sigma}}{Y_4}\right)\right]^{Y_5}$$

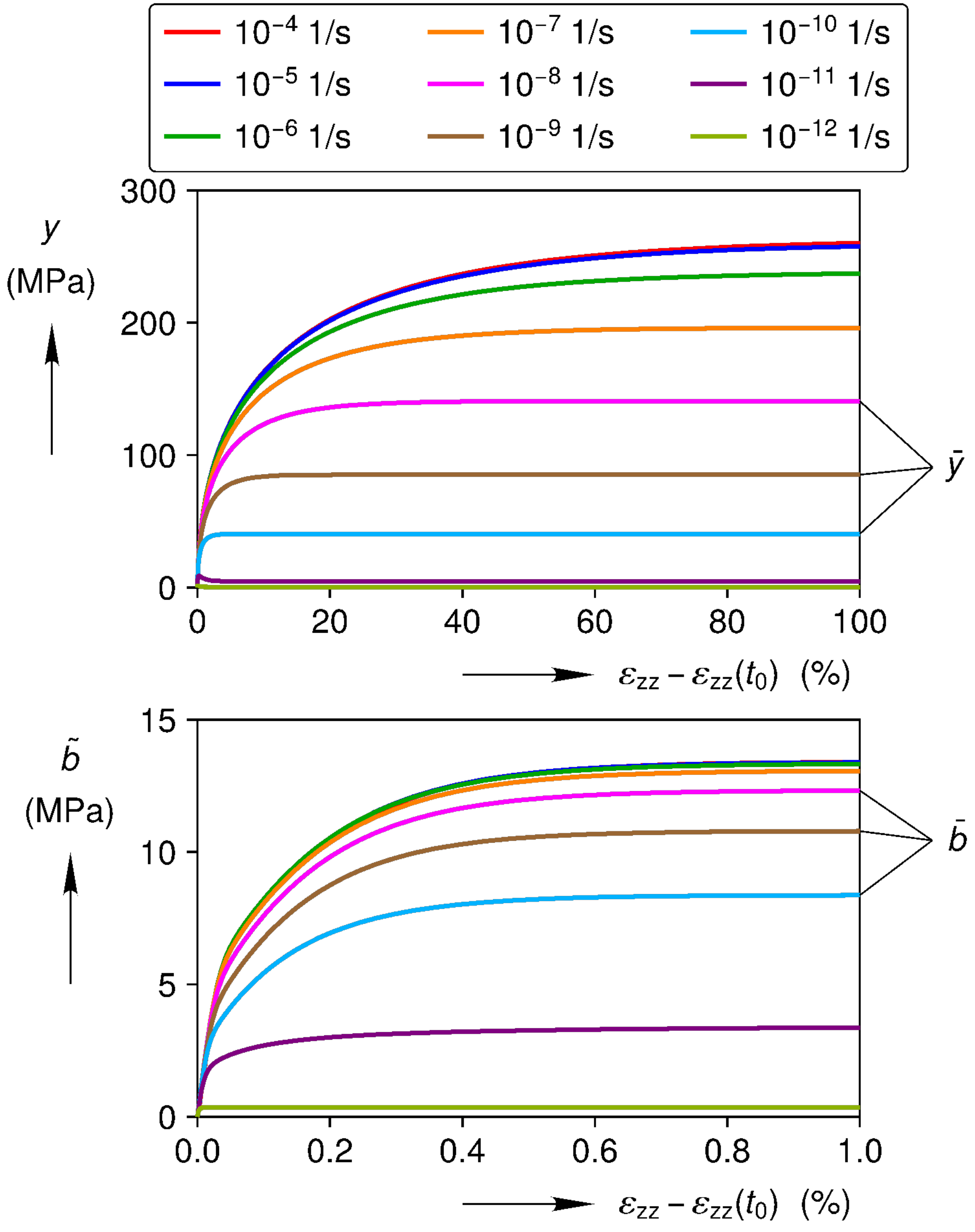

Dislocation Glide Hardening

Equivalent Dislocation Glide Strain Rate

$$\dot{\bar{\varepsilon}}^{\mathrm{dg}} = G_1 \exp\left(-\frac{G_2}{\theta}\right)\left[\sinh\left(\frac{\tilde{\sigma}^{\mathrm{dg}}}{y}\right)\right]^{G_3}$$

Isotropic Dislocation Glide Hardening

Equivalent Dislocation Glide Strain Rate

$$\dot{\tilde{\varepsilon}}^{dg} = G_1 \exp\left(-\frac{G_2}{\theta}\right)\left[\sinh\left(\frac{\tilde{\sigma}}{y}\right)\right]^{G_3}$$

Equivalent Dislocation Glide Stress

$$\tilde{\sigma} = \sqrt{\frac{3}{2}\,\boldsymbol{\sigma}^{dev} : \boldsymbol{\sigma}^{dev}}$$

Flow Rule

$$\boldsymbol{\varepsilon}^{dg} = \dot{\tilde{\varepsilon}}^{dg}\frac{\partial f_i}{\partial \boldsymbol{\sigma}}$$

Isotropic Dislocation Glide Hardening

Dynamic Yield Surface

$$f_i = \tilde{\sigma} - y \sinh^{-1}\left\{\left[\frac{\dot{\bar{\varepsilon}}^{dg}}{G_1 \exp(-G_2/\theta)}\right]^{1/G_3}\right\} = 0$$

Equivalent Dislocation Glide Stress

$$\tilde{\sigma} = \sqrt{\frac{3}{2}\boldsymbol{\sigma}^{dev} : \boldsymbol{\sigma}^{dev}}$$

Flow Rule

$$\dot{\boldsymbol{\varepsilon}}^{dg} = \dot{\bar{\varepsilon}}^{dg}\frac{\partial f_i}{\partial \boldsymbol{\sigma}}$$

Deviatoric Plane

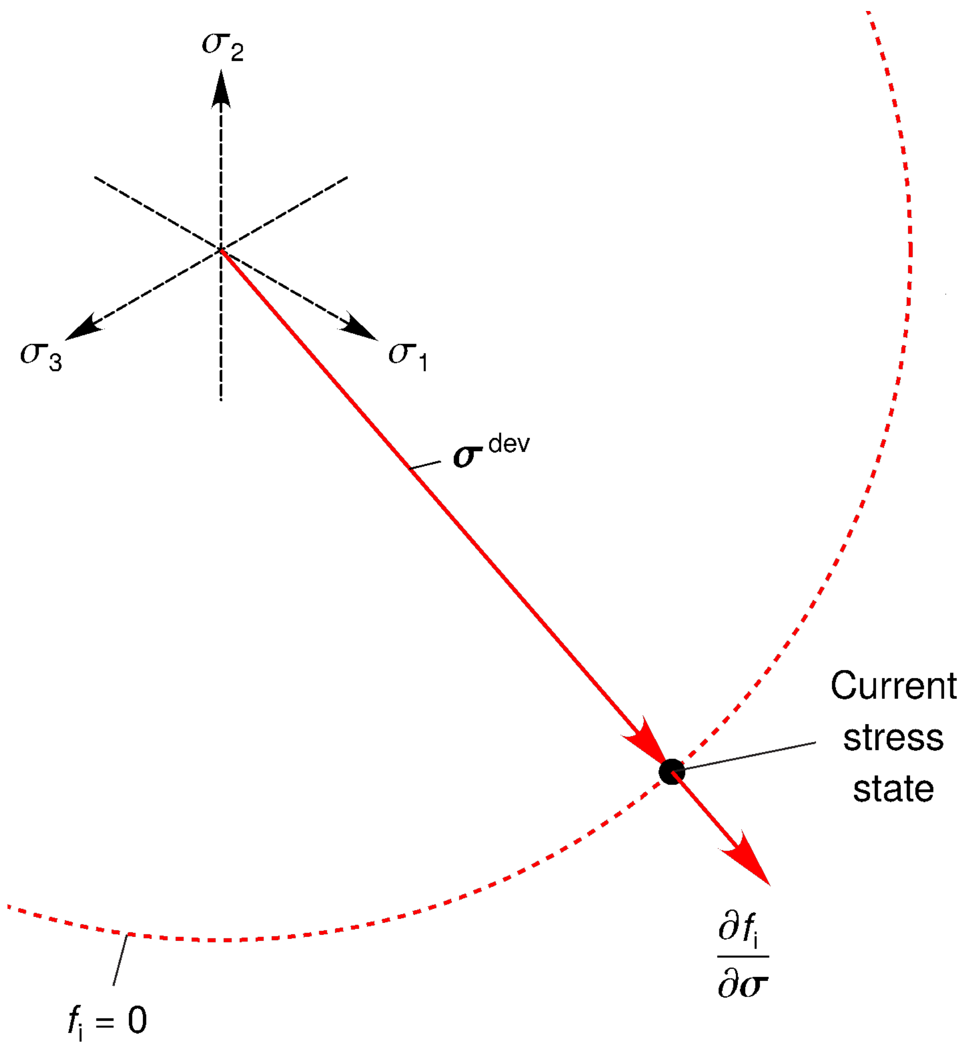

Isotropic Dislocation Glide Hardening

Dynamic Yield Surface

$$f_i = \tilde{\sigma} - y \sinh^{-1}\left\{\left[\frac{\dot{\tilde{\varepsilon}}^{dg}}{G_1 \exp(-G_2/\theta)}\right]^{1/G_3}\right\} = 0$$

Equivalent Dislocation Glide Stress

$$\tilde{\sigma} = \sqrt{\frac{3}{2}\,\boldsymbol{\sigma}^{dev} : \boldsymbol{\sigma}^{dev}}$$

Flow Rule

$$\dot{\boldsymbol{\varepsilon}}^{dg} = \dot{\tilde{\varepsilon}}^{dg}\,\frac{\partial f_i}{\partial \boldsymbol{\sigma}}$$

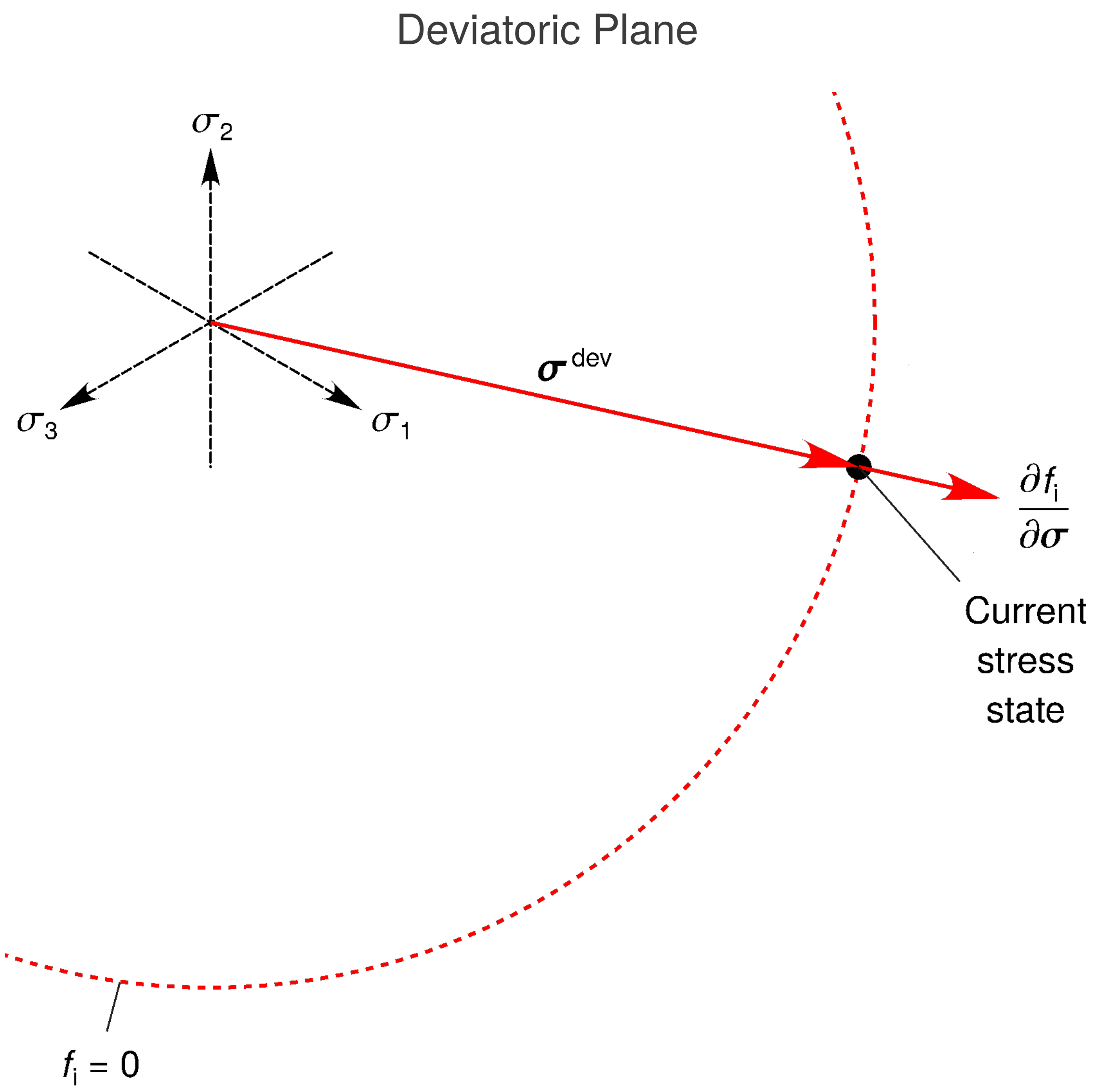

Isotropic and Kinematic Dislocation Glide Hardening

Dynamic Yield Surface

$$f_{ik} = \tilde{\sigma}^{dg} - y \sinh^{-1}\left\{\left[\frac{\dot{\tilde{\varepsilon}}^{dg}}{G_1 \exp(-G_2/\theta)}\right]^{1/G_3}\right\} = 0$$

Dislocation Glide Stress

$$\boldsymbol{\sigma}^{dg} = \boldsymbol{\sigma}^{dev} - \boldsymbol{b}$$

$$\tilde{\sigma}^{dg} = \sqrt{\tfrac{3}{2}\boldsymbol{\sigma}^{dg} : \boldsymbol{\sigma}^{dg}}$$

Flow Rule

$$\dot{\boldsymbol{\varepsilon}}^{dg} = \dot{\tilde{\varepsilon}}^{dg} \frac{\partial f_{ik}}{\partial \boldsymbol{\sigma}}$$

Deviatoric Plane

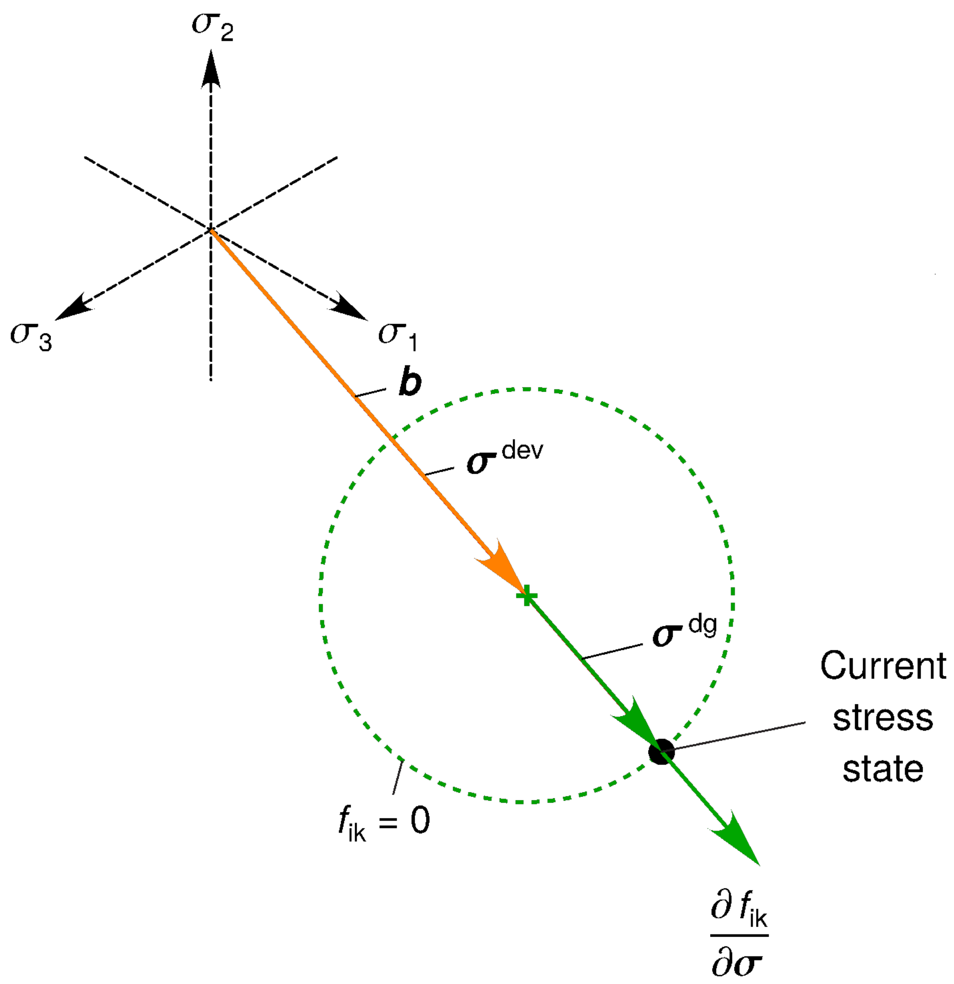

Isotropic and Kinematic Dislocation Glide Hardening

Dynamic Yield Surface

$$f_{ik} = \tilde{\sigma}^{dg} - y \sinh^{-1}\left\{\left[\frac{\dot{\tilde{\varepsilon}}^{dg}}{G_1 \exp(-G_2/\theta)}\right]^{1/G_3}\right\} = 0$$

Dislocation Glide Stress

$$\boldsymbol{\sigma}^{dg} = \boldsymbol{\sigma}^{dev} - \boldsymbol{b}$$

$$\tilde{\sigma}^{dg} = \sqrt{\tfrac{3}{2}\boldsymbol{\sigma}^{dg} : \boldsymbol{\sigma}^{dg}}$$

Flow Rule

$$\dot{\boldsymbol{\varepsilon}}^{dg} = \dot{\tilde{\varepsilon}}^{dg} \frac{\partial f_{ik}}{\partial \boldsymbol{\sigma}}$$

Deviatoric Plane

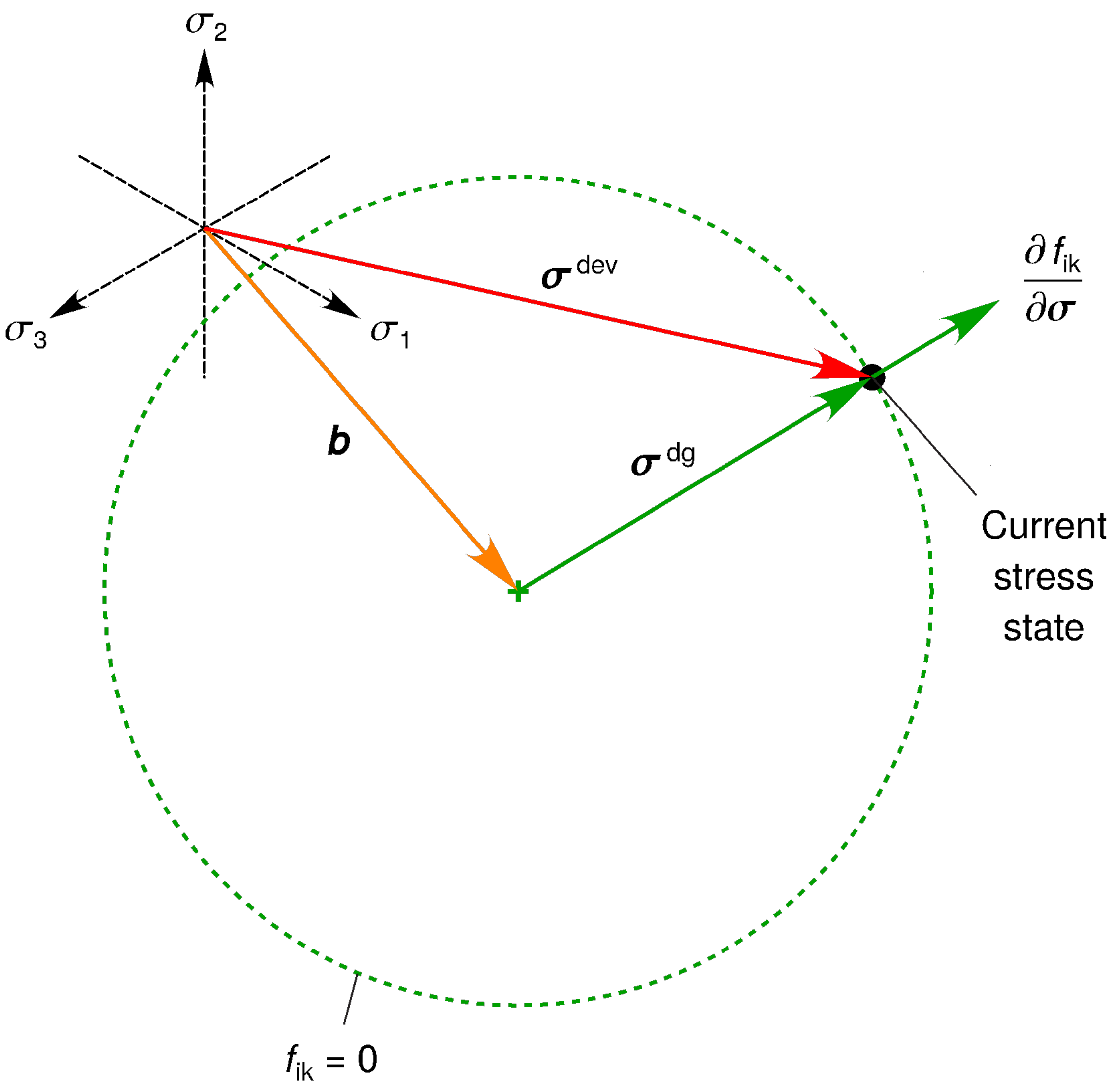

Isotropic and Kinematic Dislocation Glide Hardening

Dynamic Yield Surface

$$f_{ik} = \tilde{\sigma}^{dg} - y \sinh^{-1}\left\{\left[\frac{\dot{\tilde{\varepsilon}}^{dg}}{G_1 \exp(-G_2/\theta)}\right]^{1/G_3}\right\} = 0$$

Dislocation Glide Stress

$$\boldsymbol{\sigma}^{dg} = \boldsymbol{\sigma}^{dev} - \boldsymbol{b}$$

$$\tilde{\sigma}^{dg} = \sqrt{\tfrac{3}{2}\boldsymbol{\sigma}^{dg} : \boldsymbol{\sigma}^{dg}}$$

Flow Rule

$$\dot{\boldsymbol{\varepsilon}}^{dg} = \dot{\tilde{\varepsilon}}^{dg}\frac{\partial f_{ik}}{\partial \boldsymbol{\sigma}}$$

Deviatoric Plane

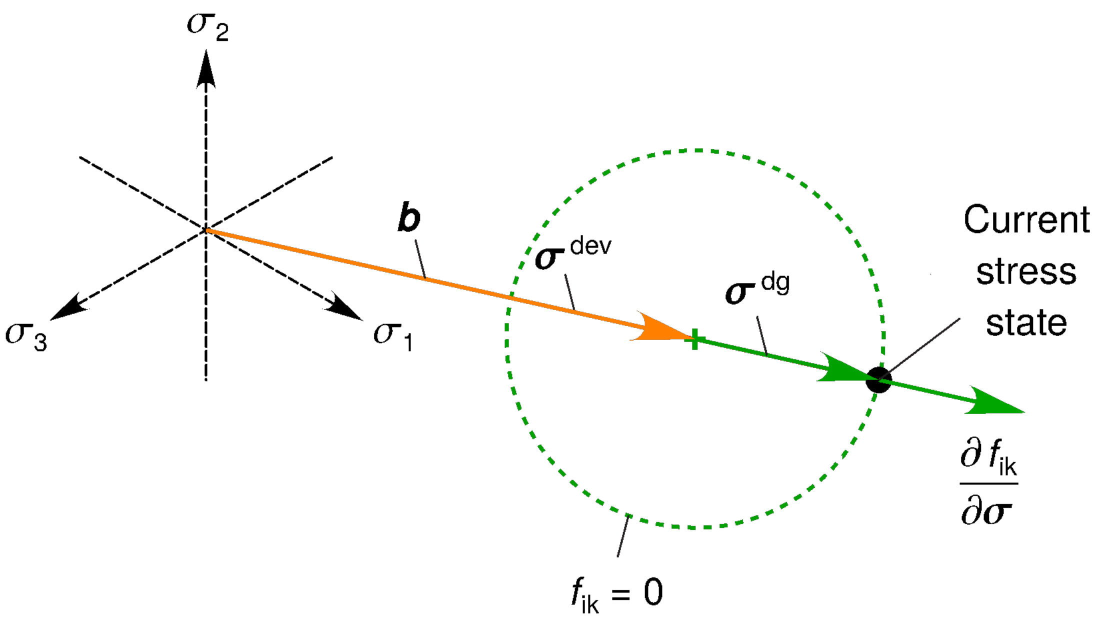

Isotropic and Kinematic Dislocation Glide Hardening

Dynamic Yield Surface

$$f_{ik} = \tilde{\sigma}^{dg} - y \sinh^{-1} \left\{ \left[\frac{\dot{\tilde{\varepsilon}}^{dg}}{G_1 \exp(-G_2/\theta)} \right]^{1/G_3} \right\} = 0$$

Equivalent Dislocation Glide Stress
(proportional, monotonic, loading, or steady-state)

$$\tilde{\sigma}^{dg} = \tilde{\sigma} - \tilde{b}$$

Flow Rule

$$\dot{\boldsymbol{\varepsilon}}^{dg} = \dot{\tilde{\varepsilon}}^{dg} \frac{\partial f_{ik}}{\partial \boldsymbol{\sigma}}$$

Deviatoric Plane

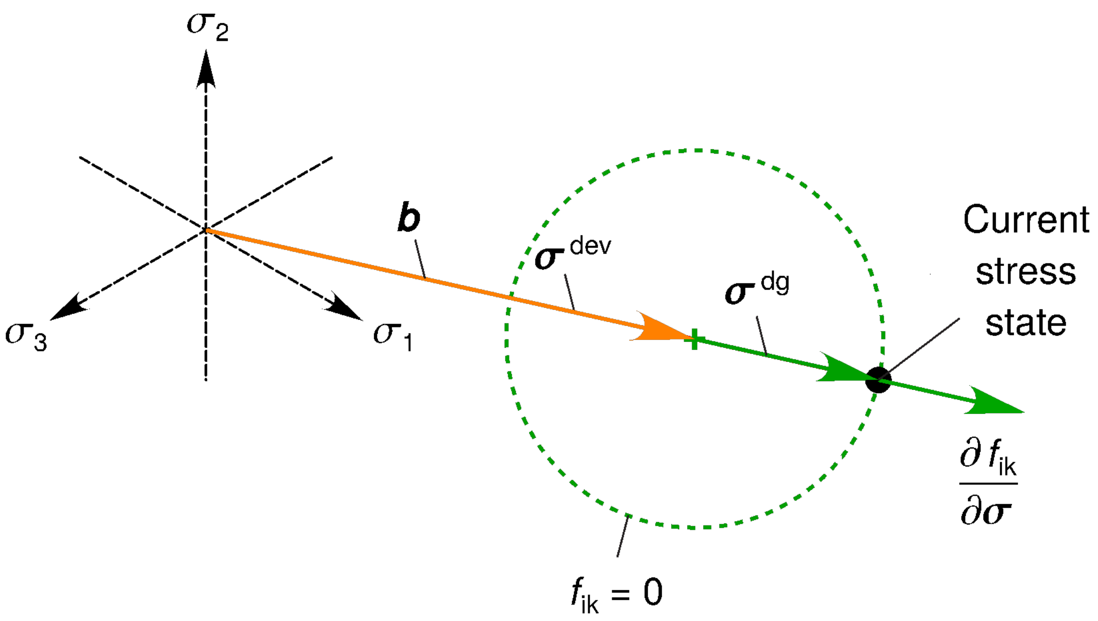

Munson-Dawson Model Constant Strain Rate Predictions

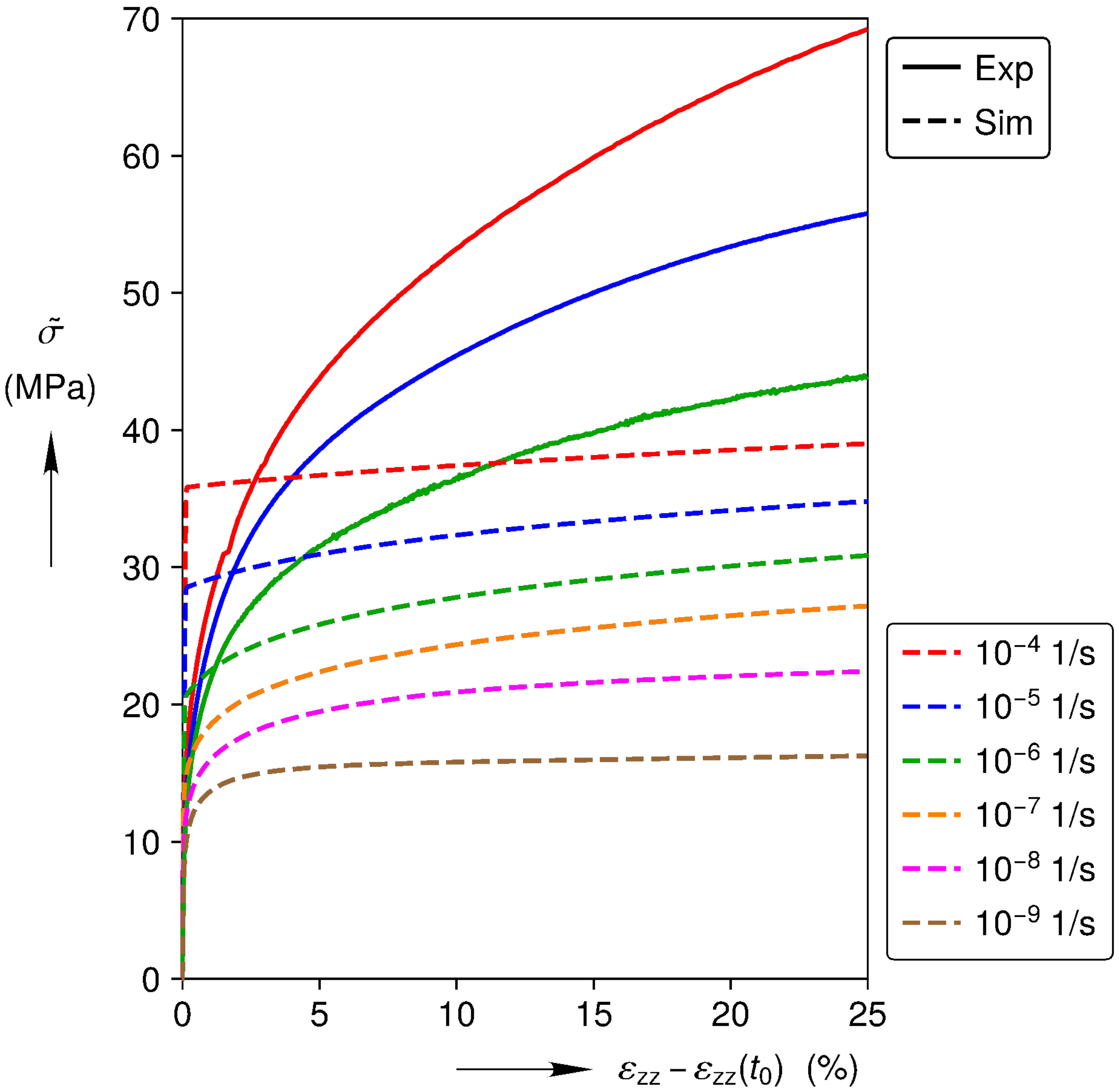

Constant Strain Rate Tests on Artificial Salt

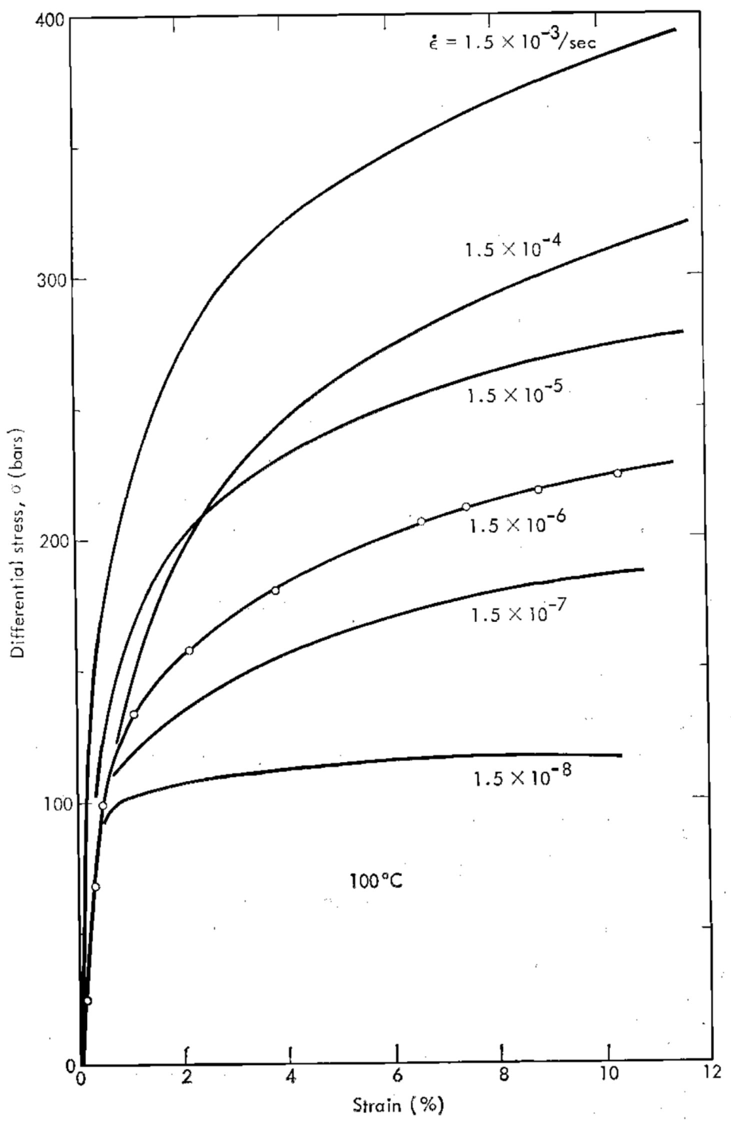

Fig. 1. Differential stress-strain curves for polycrystalline halite extended at 2 kb, $\dot{\epsilon} = 1.5 \times 10^{-3}$ to 1.5×10^{-8} sec^{-1}, and 100°C.

Heard, H. (1972). Steady-state flow in polycrystalline halite at pressure of 2 kilobars. *Flow and fracture of rocks.* Vol 16. pp 191-209.

Back Stress Measurements

Creep Responses due to Small Stress Changes Asse Rock Salt

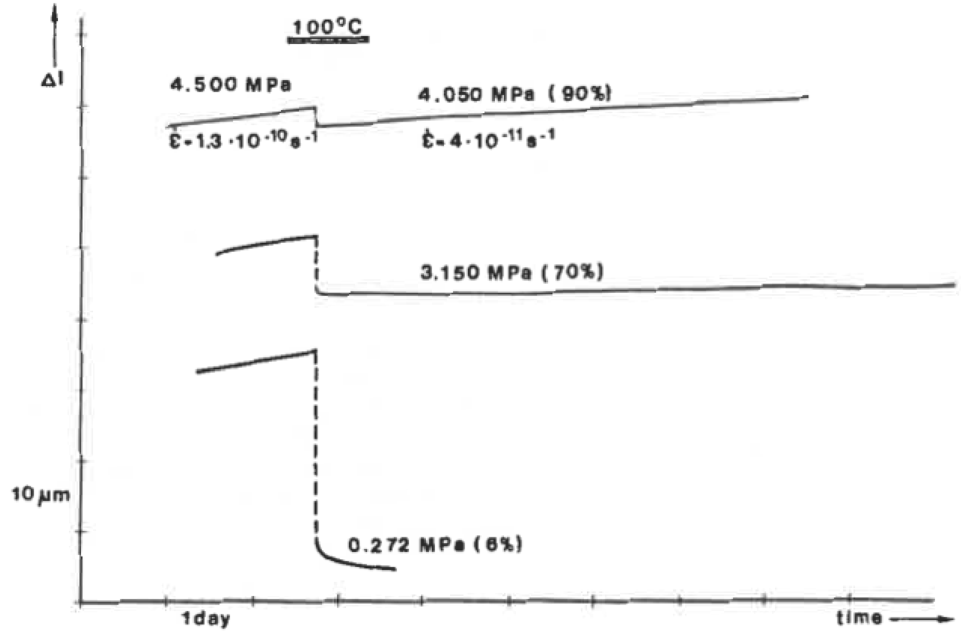

Hunsche, U. 1988. Measurement of creep in rock salt at small strain rates. Proceedings of the 2nd Conference on the Mechanical Behavior of Salt. Pg. 187-196

Dislocation Glide Strain Rate (proportional loading)

$$\dot{\varepsilon}^{dg} = G_1 \, \exp\left(-\frac{G_2}{\theta}\right) \left[\sinh\left(\frac{\left|\breve{\sigma} - \breve{b}\right|}{y}\right)\right]^{G_3} \, \mathrm{sign}\left(\breve{\sigma} - \breve{b}\right)$$

Back Stress Measurements on Single Phase Metals

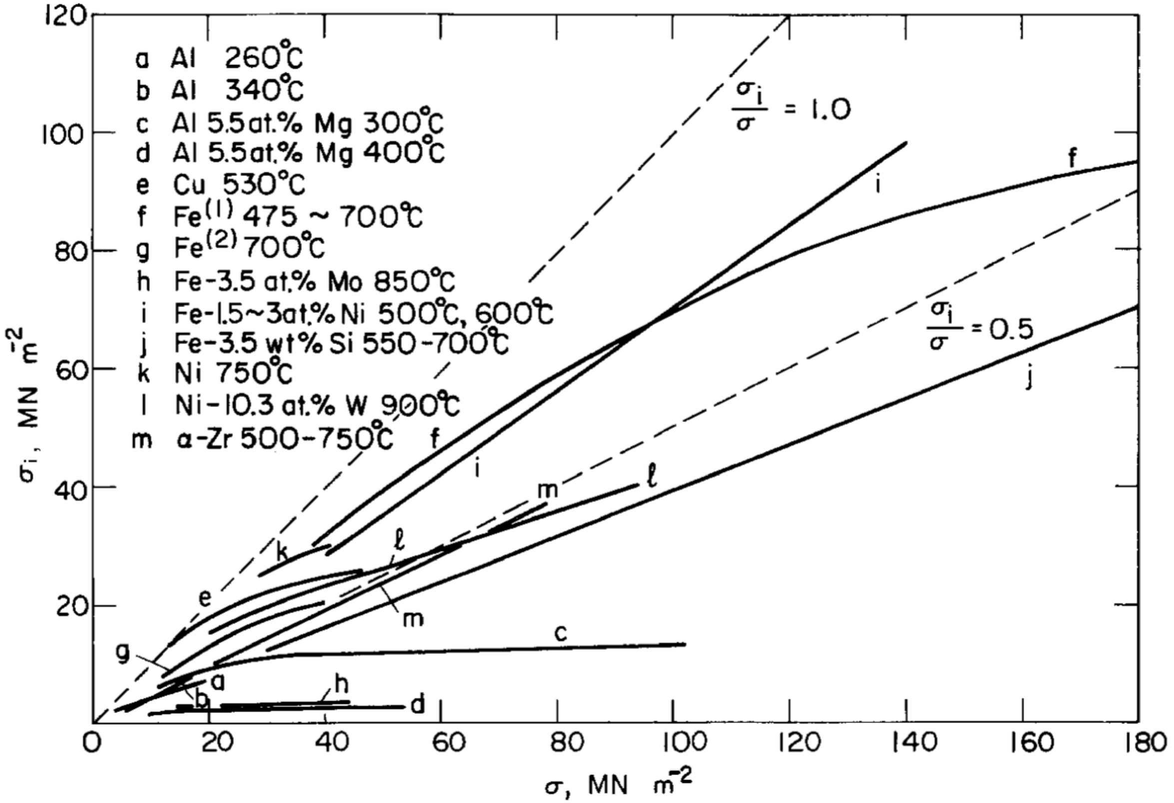

Takeuchi, S. and Argon, A. (1976). "Steady-state creep of single-phase crystalline matter at high temperature". In: Journal of Materials Science 11.8, pp. 1542–1566.

Reverse Creep at Low Stress and Room Temperature

Multi-stage Constant Stress Test on Landes Salt

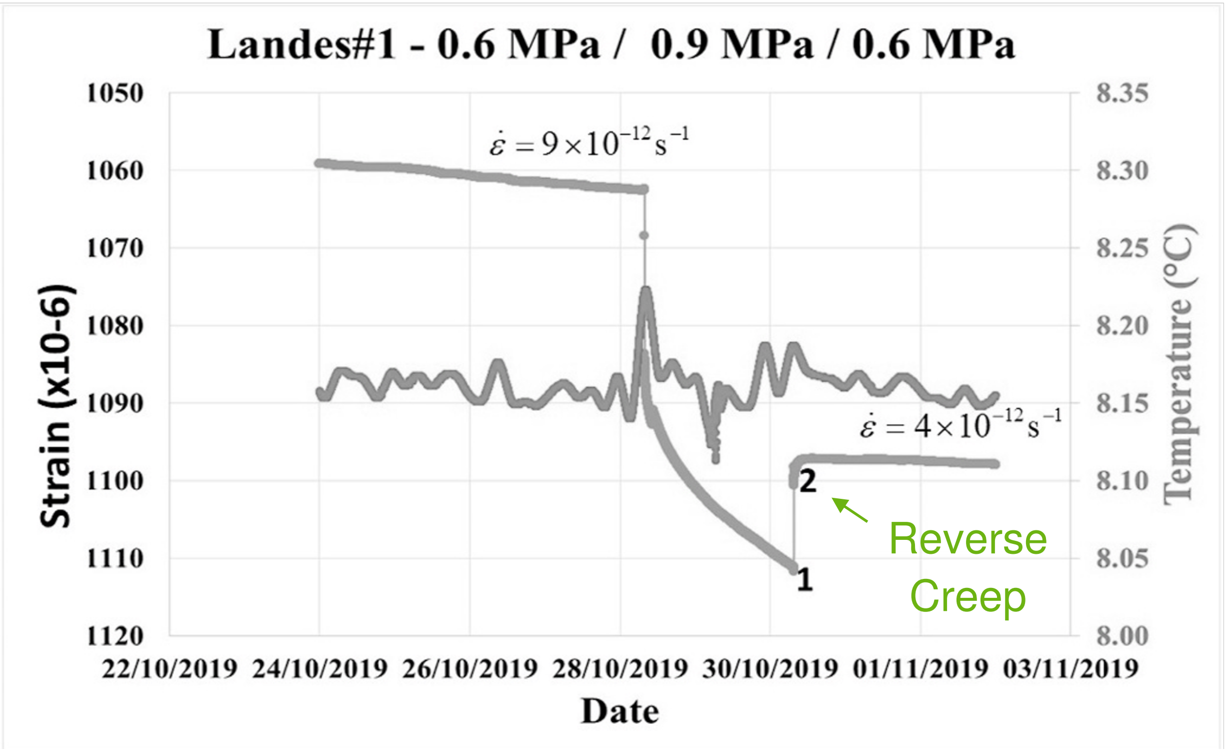

Gharbi, H., Bérest, P., Blanco-Martín, L., and Brouard, B. (Oct. 2020). “Determining upper and lower bounds for steady state strain rate during a creep test on a salt sample”. In: International Journal of Rock Mechanics and Mining Sciences 134, p. 104452

Multi-stage Constant Stress Predictions (Cal 1C)
(different stresses than on Landes salt)

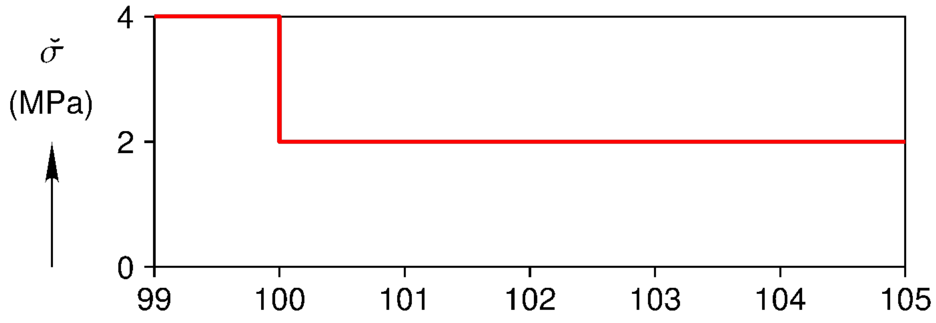

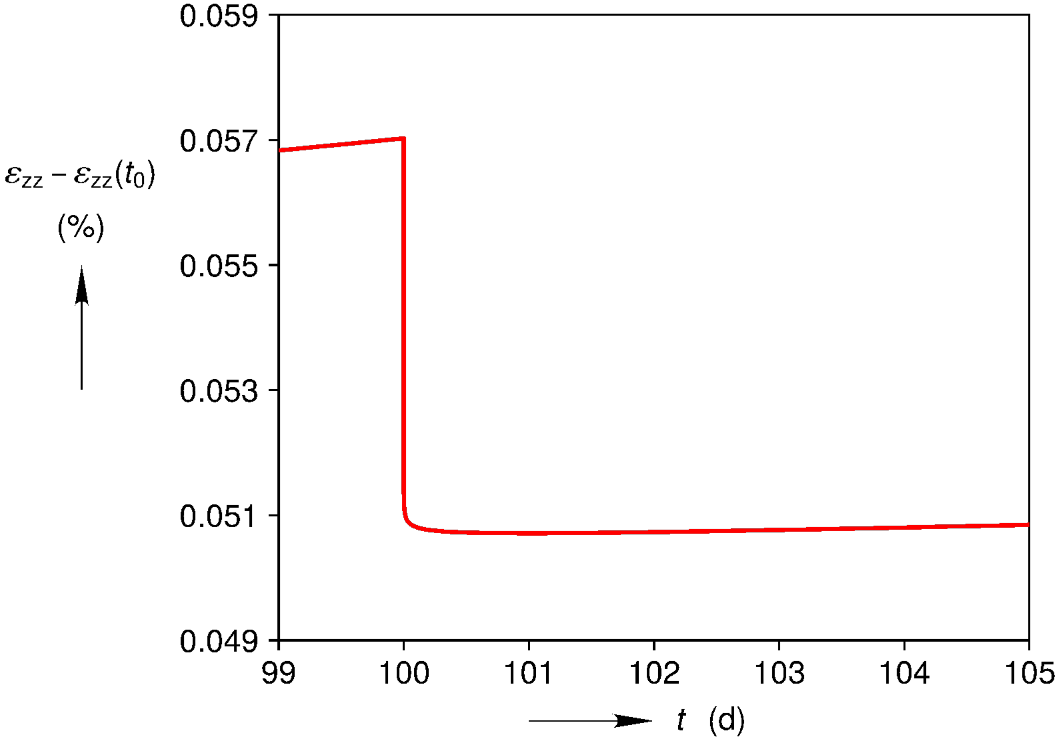

Dislocation Glide Hardening Saturation (Steady-State)

Equivalent Stress Decomposition
(proportional, monotonic, loading)

$$\bar{\sigma} = \bar{b} + \bar{\sigma}^{dg}$$

Drag Stress Contribution

$$\bar{\sigma}^{dg} = \bar{y} \sinh^{-1} \left\{ \left[\frac{\dot{\bar{\varepsilon}}^{dg}}{G_1 \exp\left(-G_2/\theta\right)} \right]^{1/G_3} \right\}$$

Contributions at Saturation

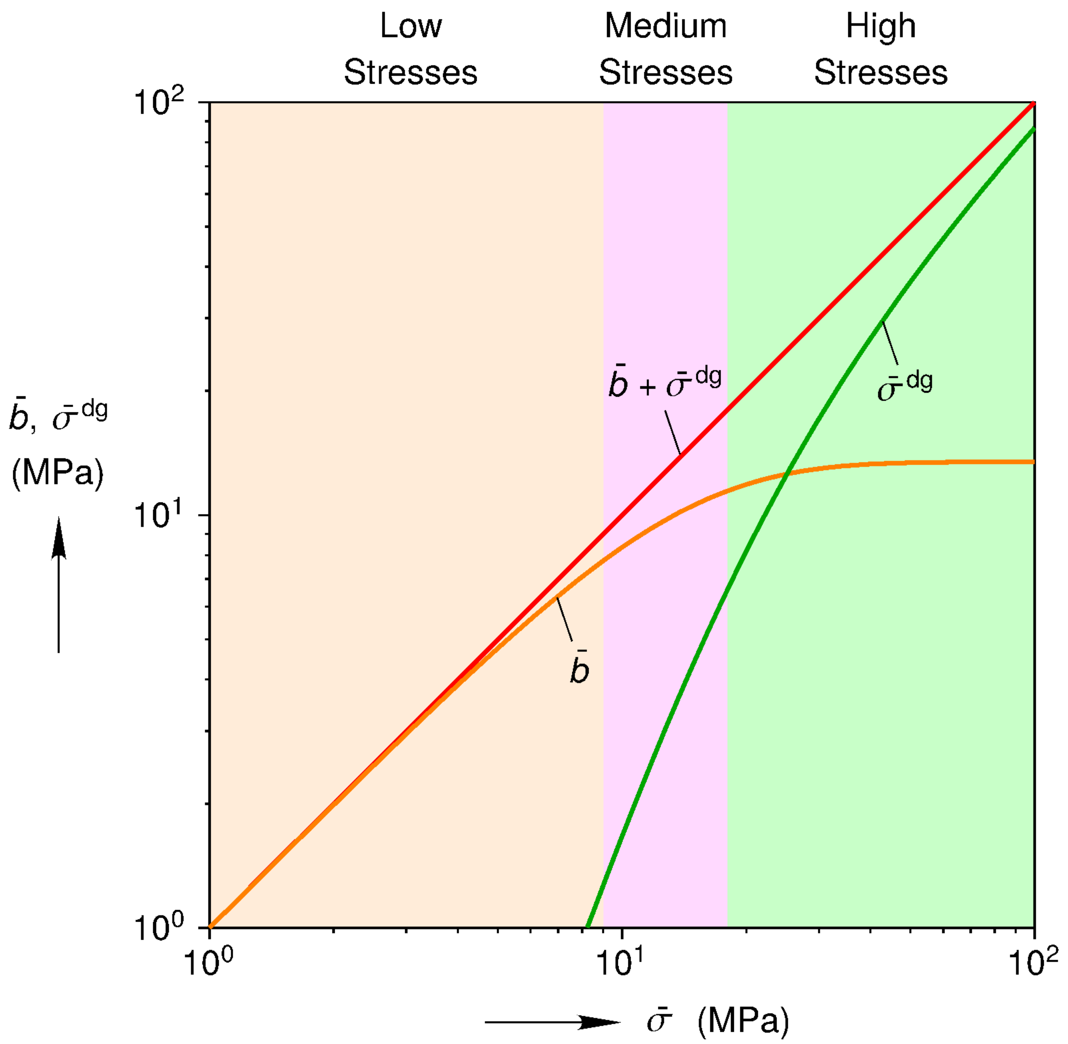

Bauschinger Effect: Isotropic Hardening Only

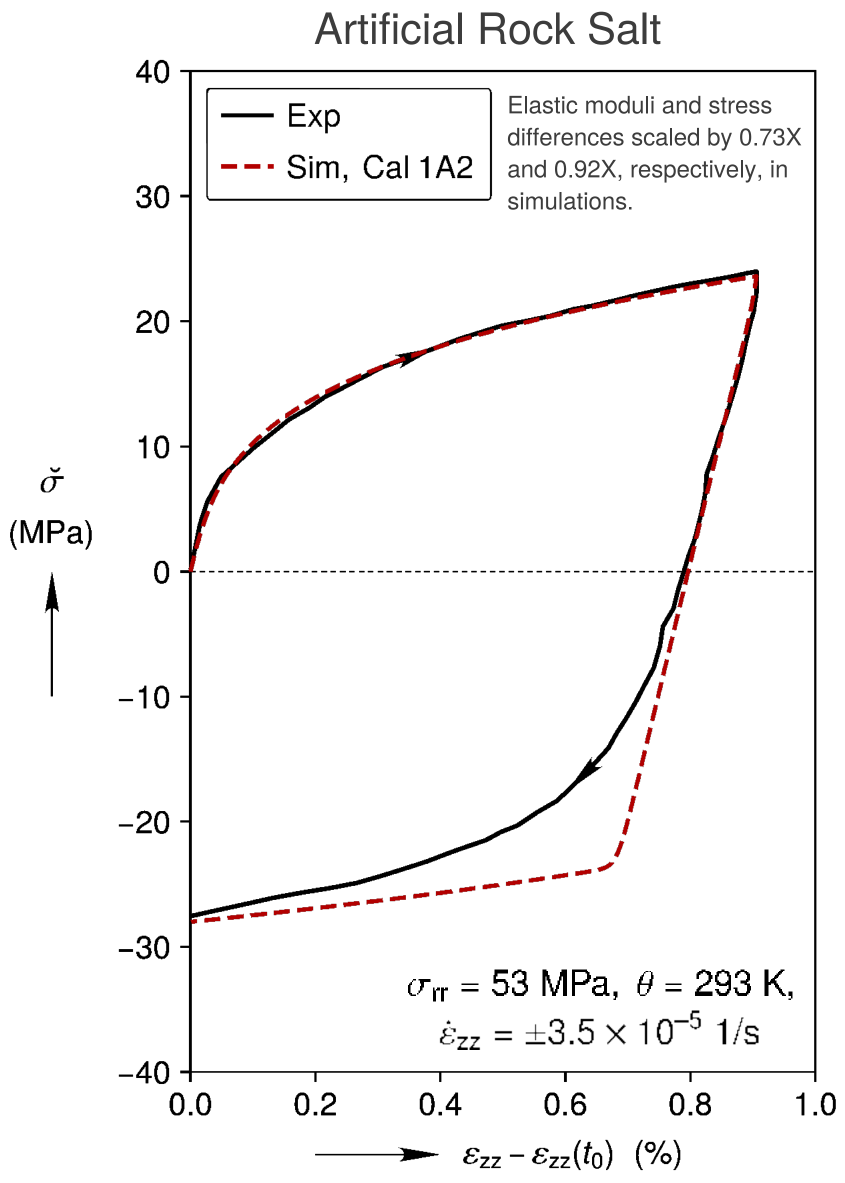

Experimental measurements from Aubertin et al. (1999)

Strain Rate

$$\dot{\varepsilon}^{dg} = G_1 \exp\left(-\frac{G_2}{\theta}\right)\left[\sinh\left(\frac{\tilde{\sigma}}{y}\right)\right]^{G_3}$$

Equivalent Stress

$$\tilde{\sigma} = \sqrt{\frac{3}{2}\,\boldsymbol{\sigma}^{dev} : \boldsymbol{\sigma}^{dev}}$$

Bauschinger Effect: Isotropic Hardening Only

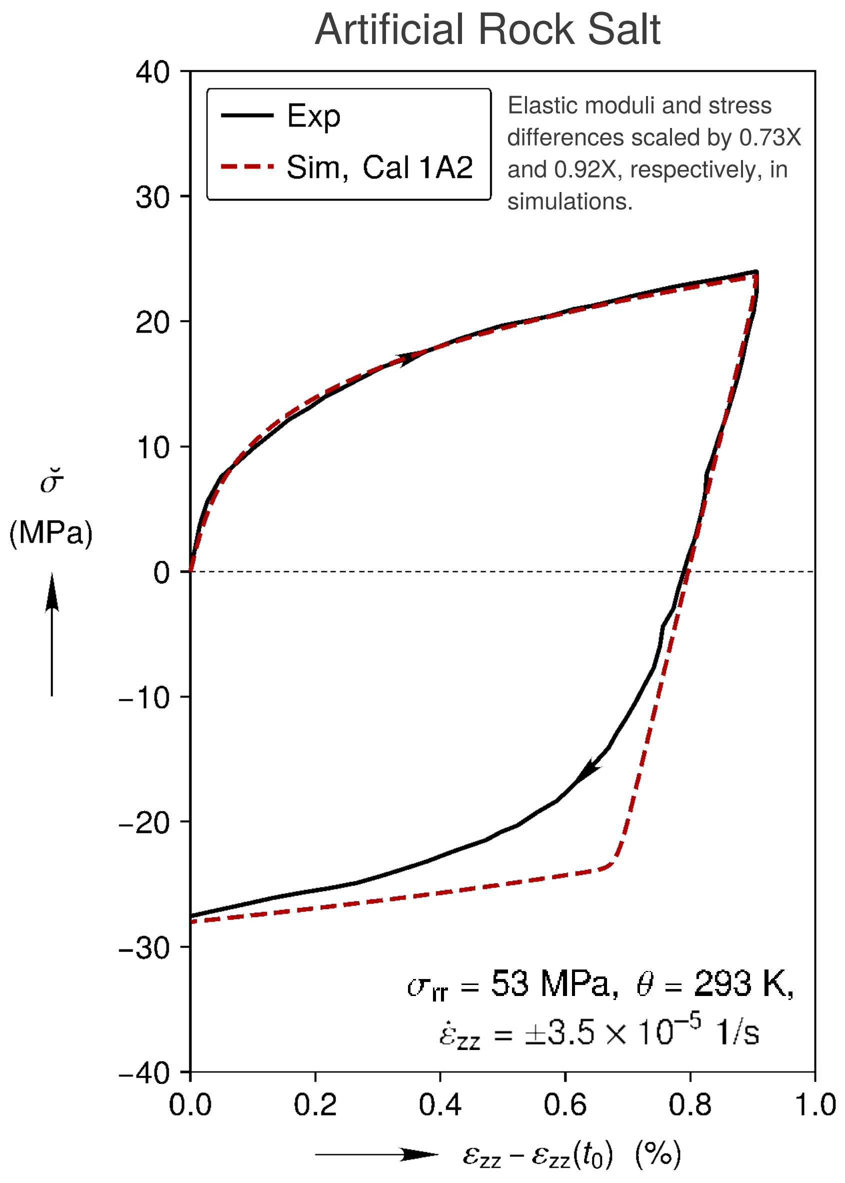

Experimental measurements from Aubertin et al. (1999)

Dynamic Yield Surface

$$f = \tilde{\sigma} - y \sinh^{-1}\left\{\left[\frac{\dot{\varepsilon}^{dg}}{G_1 \exp(-G_2/\theta)}\right]^{1/G_3}\right\} = 0$$

Equivalent Stress

$$\tilde{\sigma} = \sqrt{\frac{3}{2}\boldsymbol{\sigma}^{dev} : \boldsymbol{\sigma}^{dev}}$$

Bauschinger Effect: Isotropic Hardening Only

Artificial Rock Salt

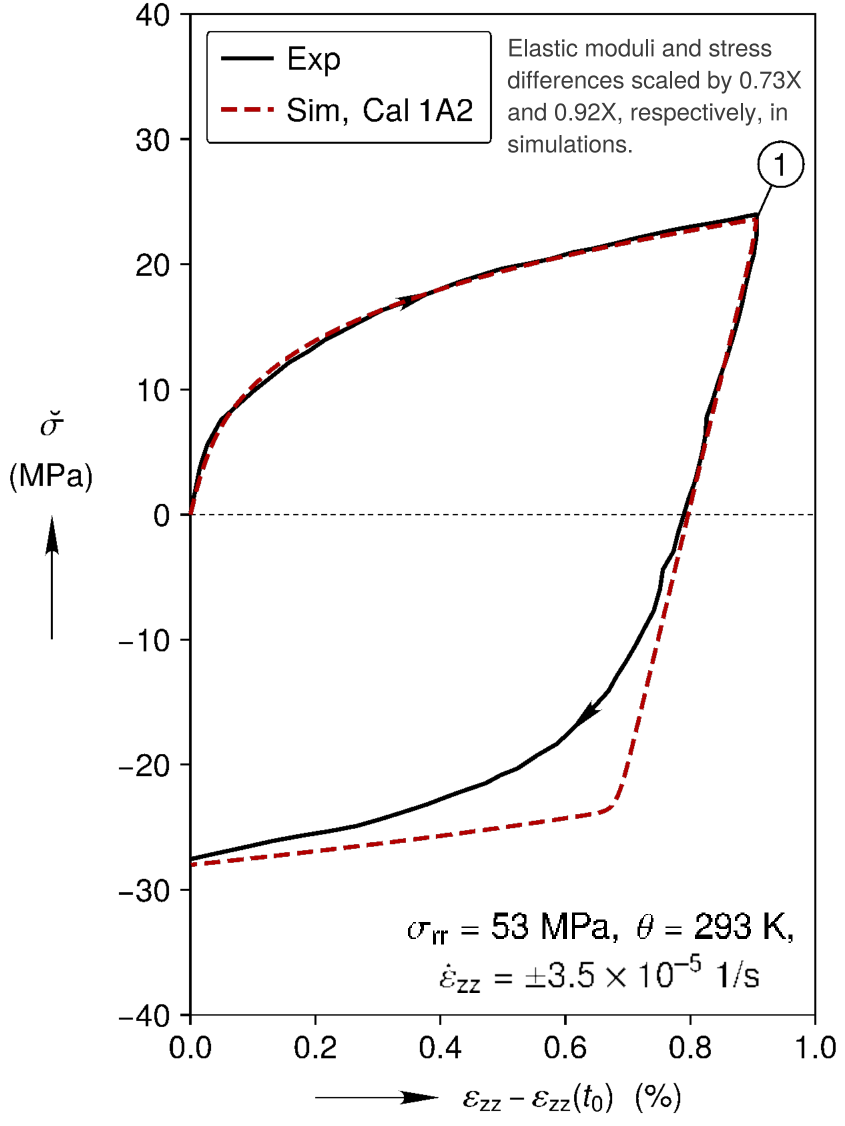

Experimental measurements from Aubertin et al. (1999)

Dynamic Yield Surface

$$f = \tilde{\sigma} - y \sinh^{-1}\left\{\left[\frac{\dot{\varepsilon}^{dg}}{G_1 \exp\left(-G_2/\theta\right)}\right]^{1/G_3}\right\} = 0$$

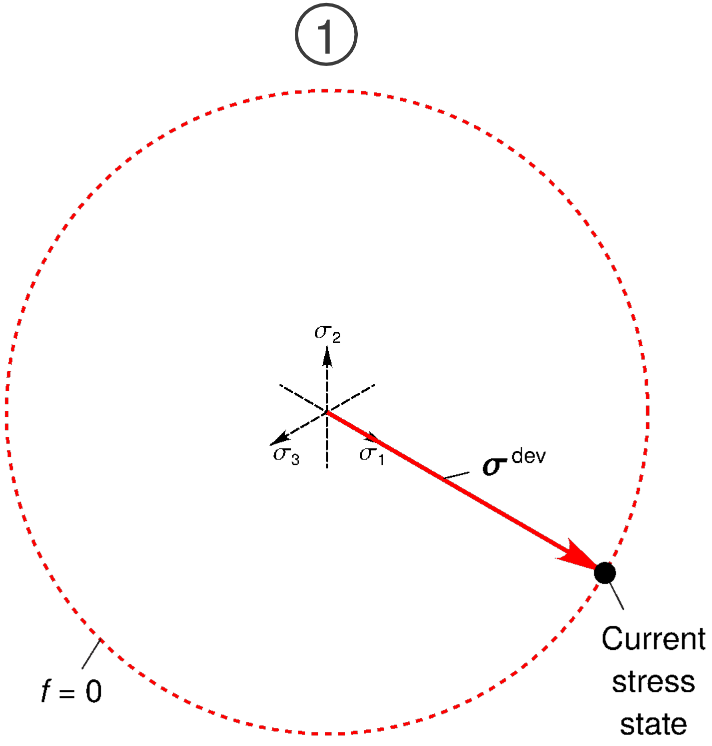

Equivalent Stress

$$\tilde{\sigma} = \sqrt{\frac{3}{2}\, \boldsymbol{\sigma}^{dev} : \boldsymbol{\sigma}^{dev}}$$

Bauschinger Effect: Isotropic Hardening Only

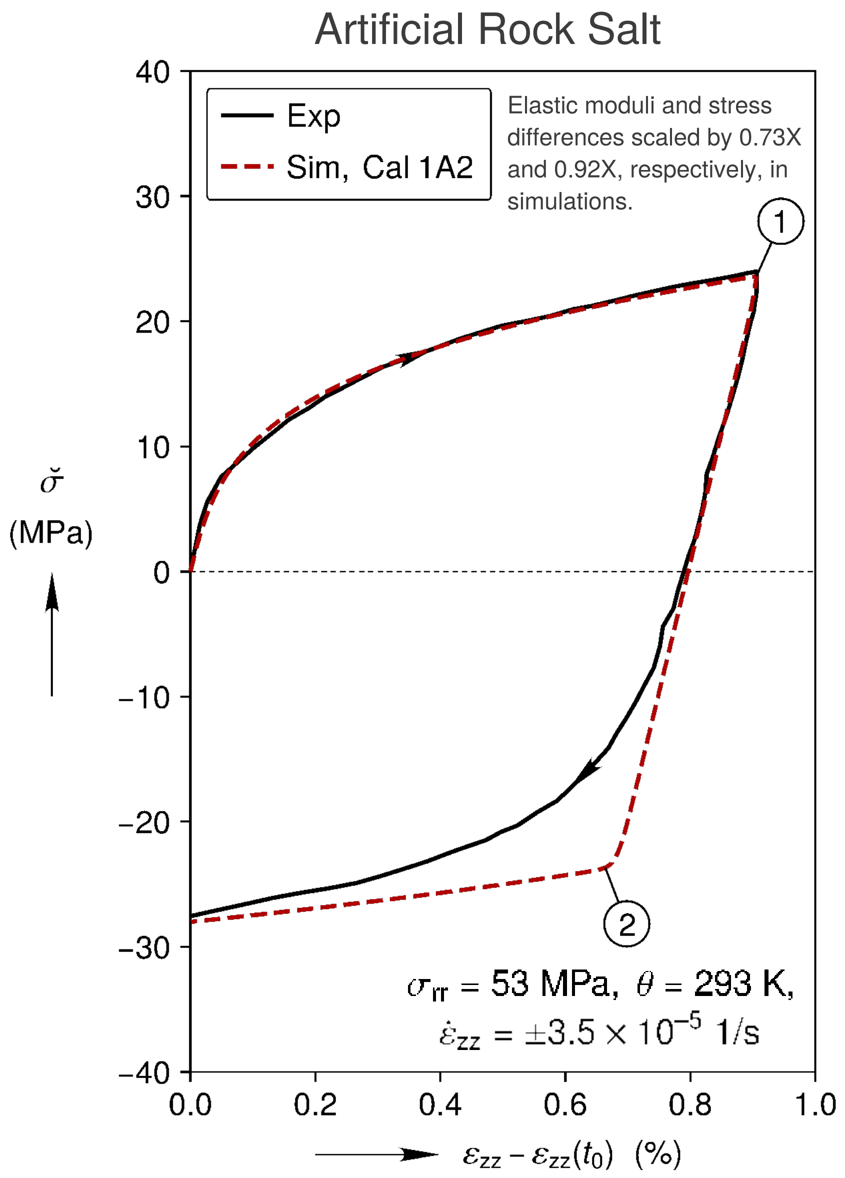

Experimental measurements from Aubertin et al. (1999)

Dynamic Yield Surface

$$f = \tilde{\sigma} - y \sinh^{-1}\left\{\left[\frac{\dot{\varepsilon}^{dg}}{G_1 \exp(-G_2/\theta)}\right]^{1/G_3}\right\} = 0$$

Equivalent Stress

$$\tilde{\sigma} = \sqrt{\frac{3}{2}\boldsymbol{\sigma}^{dev} : \boldsymbol{\sigma}^{dev}}$$

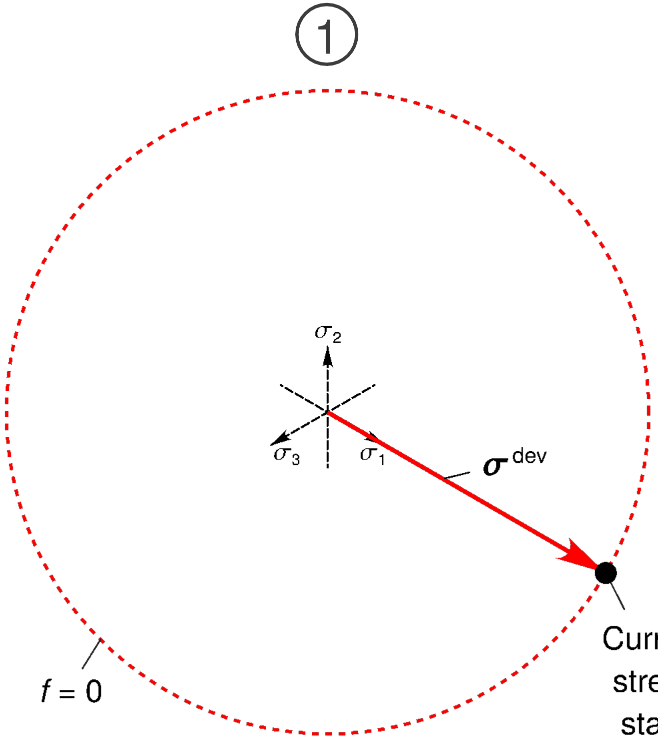

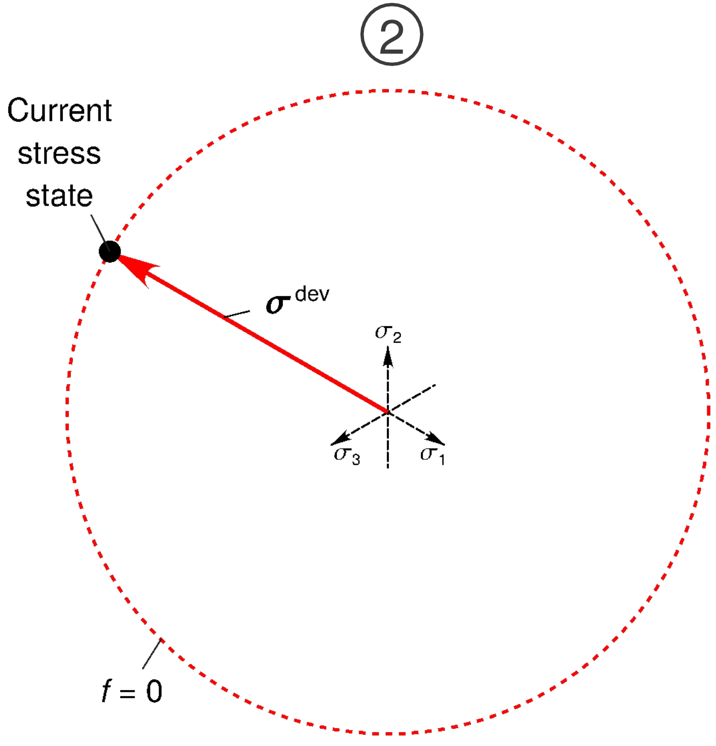

Bauschinger Effect: Isotropic + Kinematic Hardening

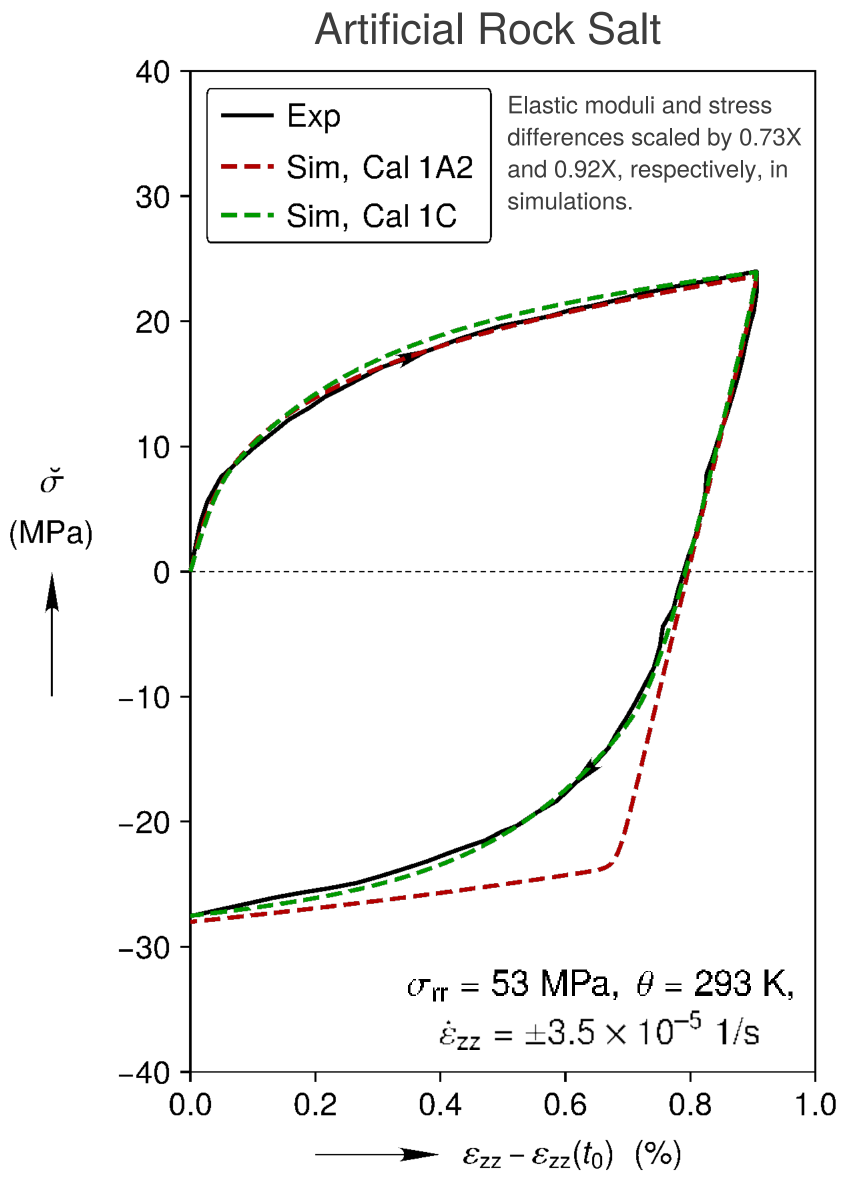

Experimental measurements from Aubertin et al. (1999)

Bauschinger Effect: Isotropic + Kinematic Hardening

Artificial Rock Salt

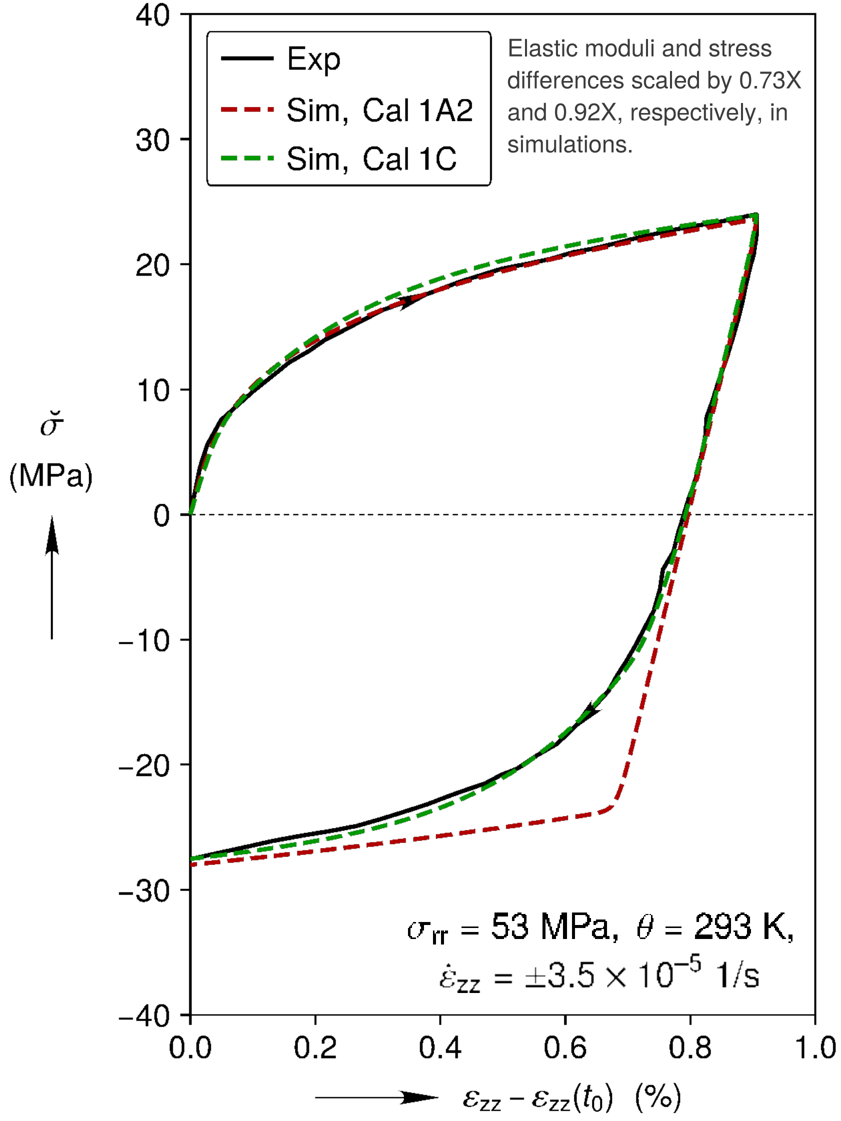

Experimental measurements from Aubertin et al. (1999)

Dynamic Yield Surface

$$f = \tilde{\sigma}^{dg} - y \sinh^{-1} \left\{ \left[\frac{\dot{\bar{\varepsilon}}^{dg}}{G_1 \exp\left(-G_2/\theta\right)} \right]^{1/G_3} \right\} = 0$$

Equivalent Stress

$$\boldsymbol{\sigma}^{dg} = \boldsymbol{\sigma}^{dev} - \boldsymbol{b}$$

$$\tilde{\sigma}^{dg} = \sqrt{\tfrac{3}{2}\boldsymbol{\sigma}^{dg} : \boldsymbol{\sigma}^{dg}}$$

Bauschinger Effect: Isotropic + Kinematic Hardening

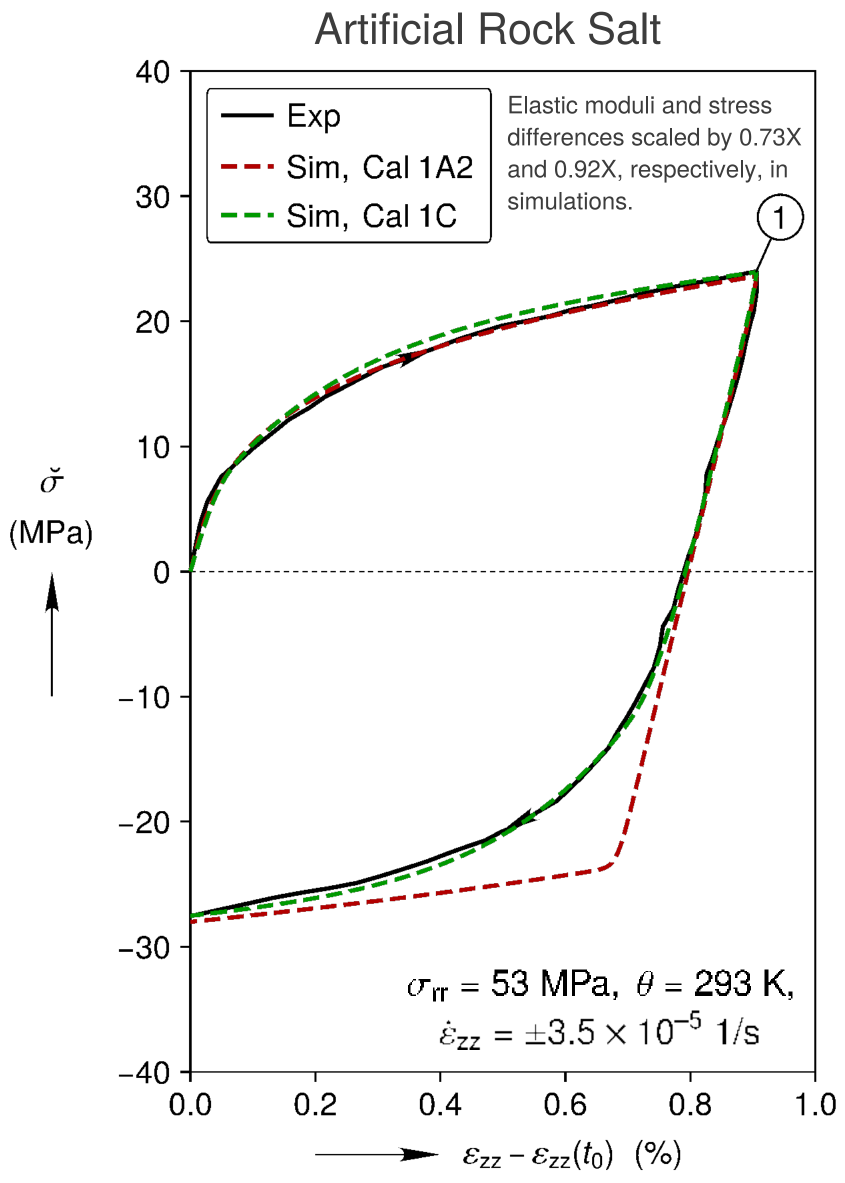

Experimental measurements from Aubertin et al. (1999)

Dynamic Yield Surface

$$f = \tilde{\sigma}^{dg} - y \sinh^{-1}\left\{\left[\frac{\dot{\varepsilon}^{dg}}{G_1 \exp(-G_2/\theta)}\right]^{1/G_3}\right\} = 0$$

Equivalent Stress

$$\boldsymbol{\sigma}^{dg} = \boldsymbol{\sigma}^{dev} - \boldsymbol{b}$$

$$\tilde{\sigma}^{dg} = \sqrt{\frac{3}{2}\boldsymbol{\sigma}^{dg} : \boldsymbol{\sigma}^{dg}}$$

1

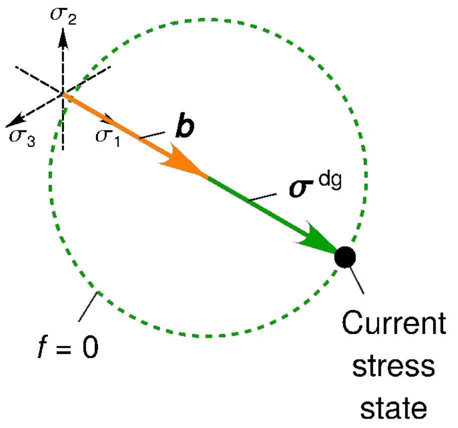

Bauschinger Effect: Isotropic + Kinematic Hardening

Artificial Rock Salt

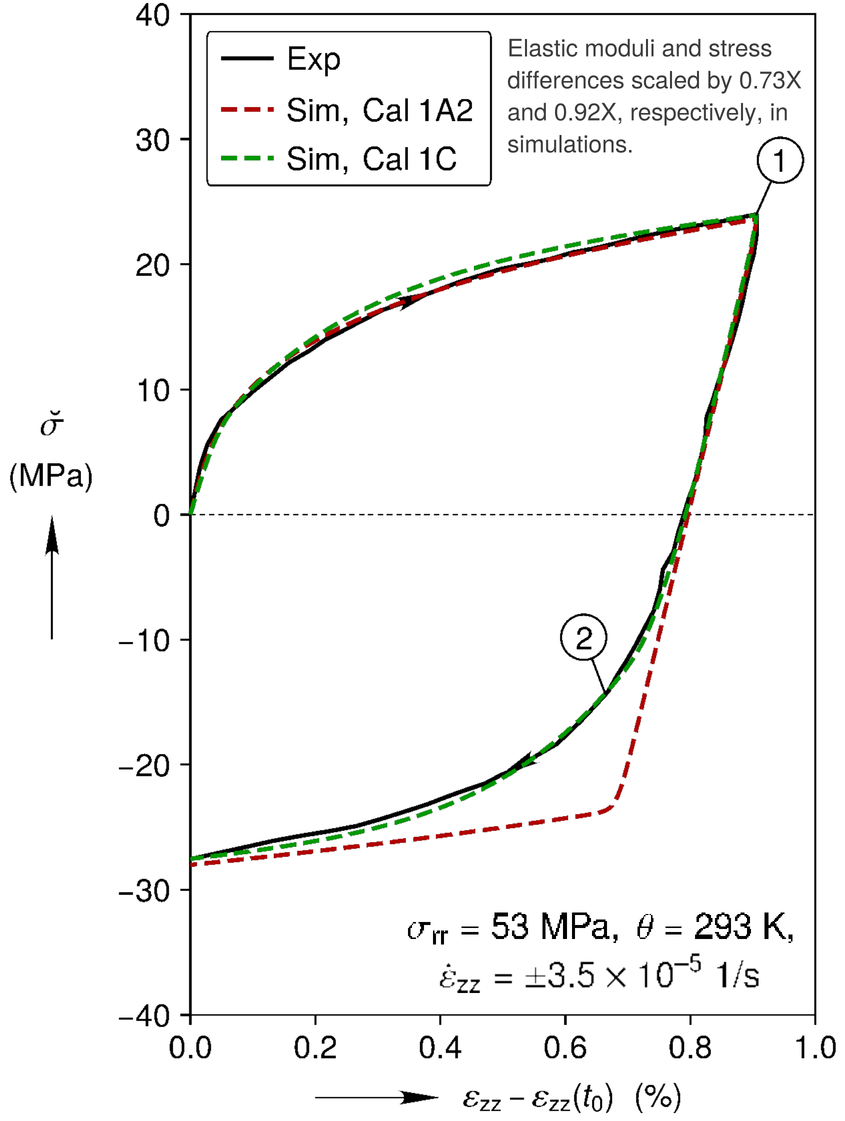

Experimental measurements from Aubertin et al. (1999)

Dynamic Yield Surface

$$f = \tilde{\sigma}^{dg} - y \sinh^{-1}\left\{\left[\frac{\dot{\varepsilon}^{dg}}{G_1 \exp(-G_2/\theta)}\right]^{1/G_3}\right\} = 0$$

Equivalent Stress

$$\boldsymbol{\sigma}^{dg} = \boldsymbol{\sigma}^{dev} - \boldsymbol{b}$$

$$\tilde{\sigma}^{dg} = \sqrt{\frac{3}{2}\boldsymbol{\sigma}^{dg} : \boldsymbol{\sigma}^{dg}}$$

1

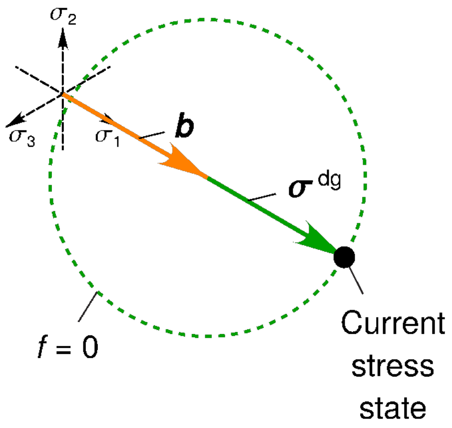

2

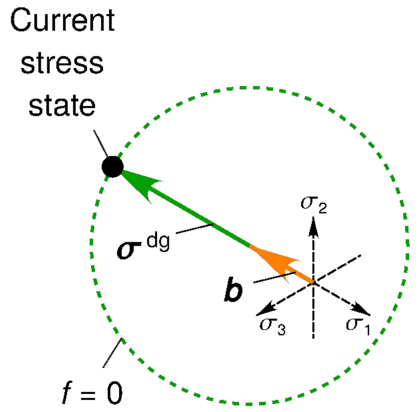

Re-hardening During Non-Monotonic Loading

Asse Salt, Strain Histories

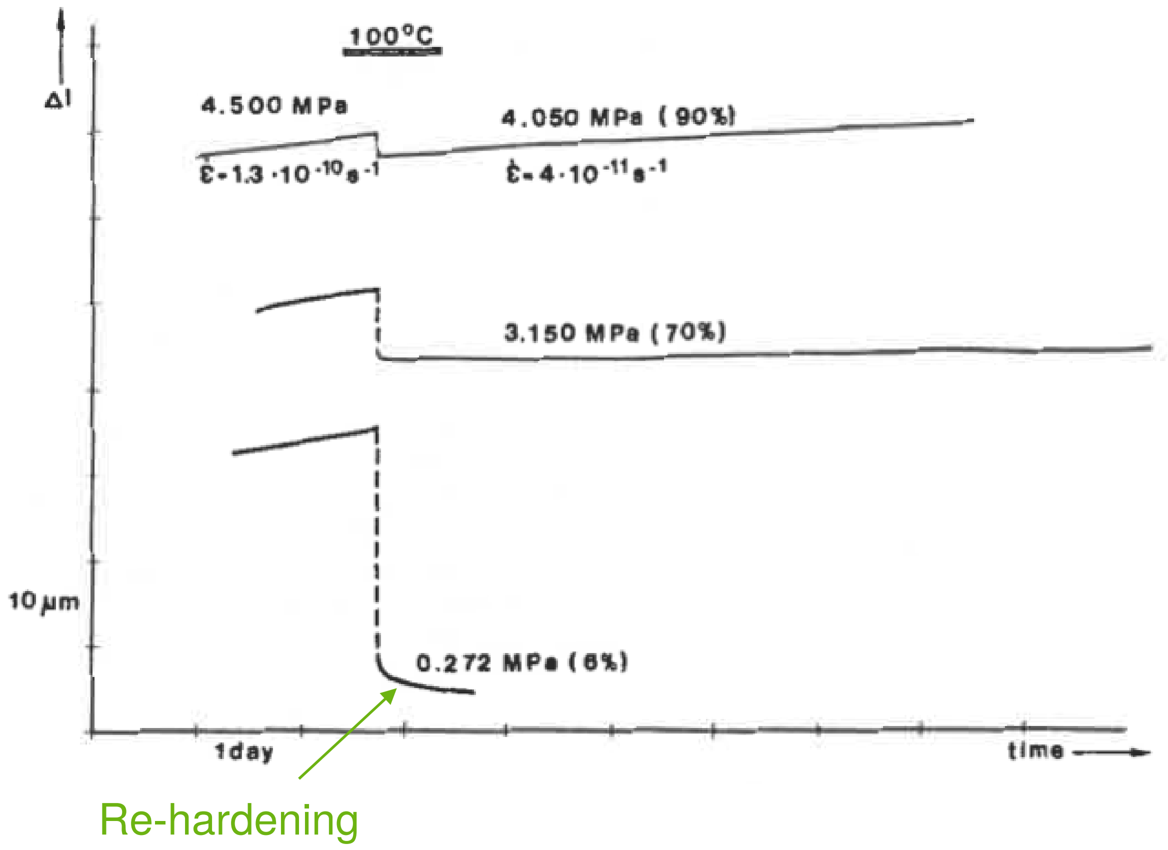

Hunsche, U. 1988. Measurement of creep in rock salt at small strain rates. Proceedings of the 2nd Conference on the Mechanical Behavior of Salt. Pg. 187-196

Wellhead Pressure Before, During, and After a Workover

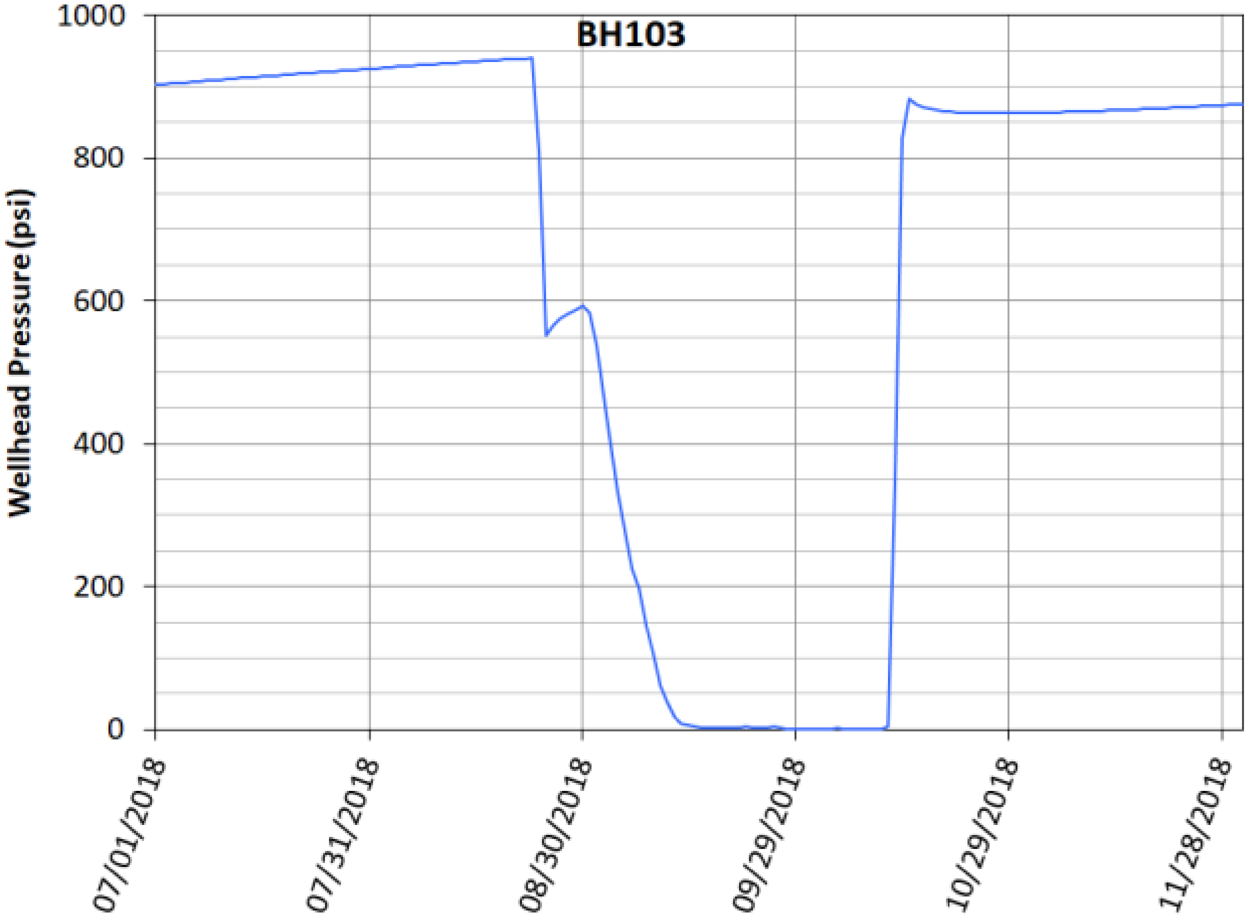

Sobolik, S. 2022. Personal Communication.

Stress Drop Behavior

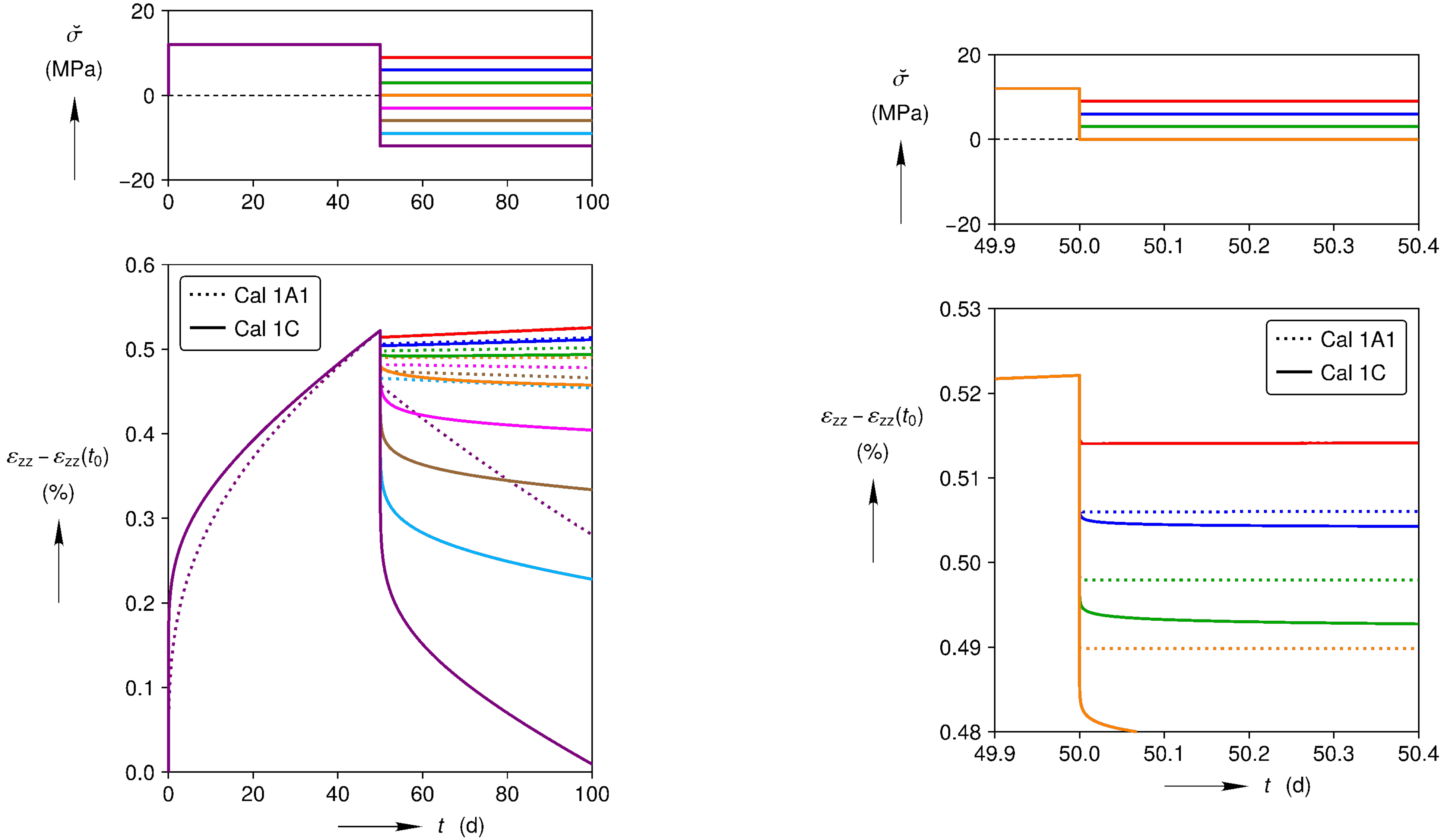

Cal 1A1 strain shifted down by 0.067 % strain.

Gas Storage Cavern Simulation

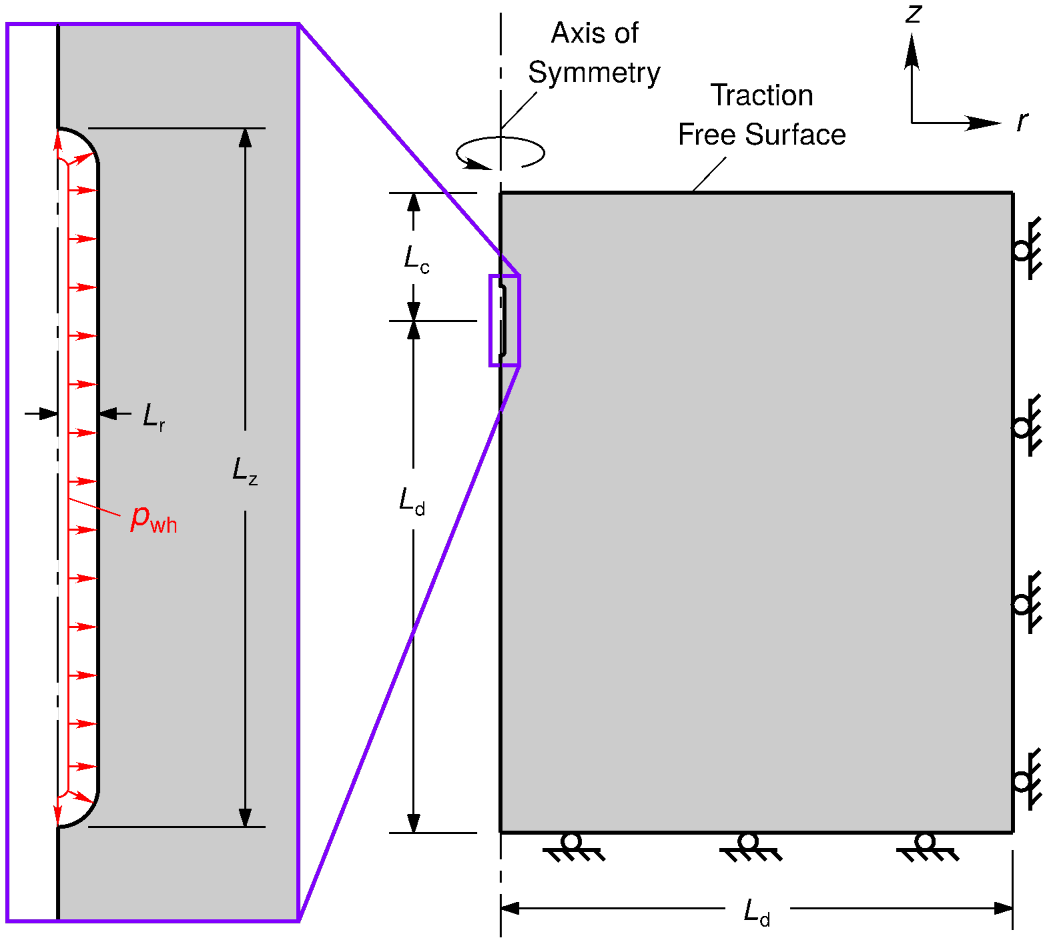

1. Isolated cigar shaped cavern
   1. Axisymmetric analysis
   2. Center of cavern was 1100 m deep
   3. Wellhead pressure held high for 5 years, held low for 3 days, and then cycled 3X.
2. Constitutive model robustness
   1. Model evaluated 2.6 x 10^9 times
   2. Model failed to converge 8 times
3. Constitutive model adaptive time stepping
   1. Initial time step = 10^{-3} s
   2. Time step after 5 years = 10 d

Gas Storage Cavern Simulation Results

von Mises Stress Distributions

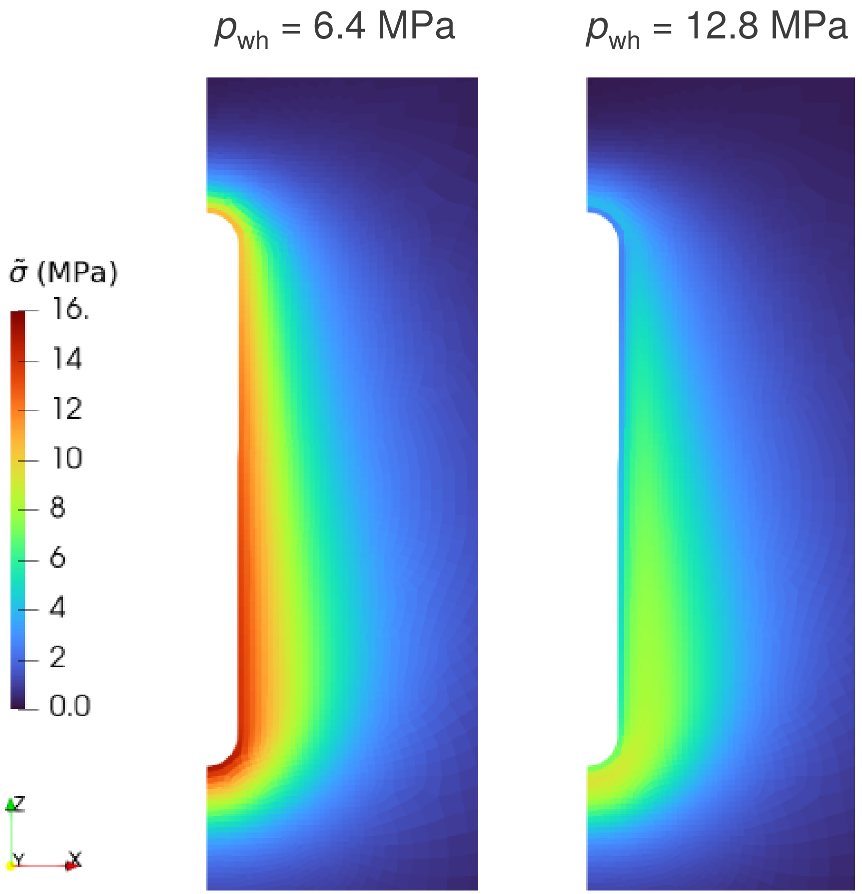

Wellhead Pressure and Cavern Volume Loss Histories